NRL Report 6738

Determination of Electron Temperatures Between 50 eV and 100 keV From X-Ray Continuum Radiation in Plasmas

R. C. Elton

High Temperature Physics Branch
Plasma Physics Division

December 11, 1968

NAVAL RESEARCH LABORATORY
Washington, D.C.

This document has been approved for public release and sale; its distribution is unlimited.

CONTENTS

Abstract	ii
Problem Status	ii
Authorization	ii
INTRODUCTION	1
DESCRIPTION OF CALCULATIONS	1
ABSORPTION COEFFICIENTS USED	2
DISCUSSION	3
ACKNOWLEDGMENT	3
REFERENCES	4

ABSTRACT

Previous calculations of the total integrated bremsstrahlung radiation passing through absorbing foils of beryllium, aluminum, and nickel (as well as aluminum and nickel in combination with carbon (polyethylene)) are included and extended to cover temperatures equivalent to an energy range from 50 eV to 100 keV and to include gold. Such information is necessary in obtaining values for the electron temperature in a plasma from measurements of the soft x-ray continuum emission. The spectral distribution of the transmitted continuum radiation is presented over the entire temperature range, for use in determining the most suitable spectral region.

PROBLEM STATUS

This is a final report on one phase of the problem of electron temperature determination in a plasma.

AUTHORIZATION

NRL Problem H02-24
Project RR 002-09-41-5054

Manuscript submitted April 18, 1968.

DETERMINATION OF ELECTRON TEMPERATURES BETWEEN 50 eV AND 100 keV FROM X-RAY CONTINUUM RADIATION IN PLASMAS

INTRODUCTION

This report presents an extension of previous calculations (1) concerning the transmission of x-ray continuum radiation through thin metallic foils. Such calculations are most useful in determining the electron kinetic temperature in a high-temperature plasma from the wavelength distribution of bremsstrahlung (and recombination) emission (2-6). The previous report on this problem (1) gave the integrated continuum emission (transmitted through thin foils and normalized to zero foil thickness) as a function of foil thickness for electron temperatures ranging from kT = 100 eV ($T = 1.2 \times 10^6$ °K) up to kT = 1.4 keV. This report demonstrated how, by a proper selection of foil material and thickness, the ratio of x-ray flux through two different foils may be used as a sensitive determination of electron temperature. Such results were presented for beryllium, aluminum, and nickel foils as well as for a combination of the latter two with polyethylene (CH_2), used to reduce line radiation at low energies. The wavelength distribution of the specific continuum intensity was also presented for various foil thicknesses and temperatures as an aid in selecting a desirable wavelength region.

The present report includes and extends these calculations to lower (kT = 50 eV) and higher (kT = 100 keV) electron temperatures. The foil thicknesses used are increased accordingly as the x-ray energy increases at the higher temperatures. In addition, gold has been added as a heavier element useful in obtaining more sensitive temperature measurements at higher temperatures. Partly for the sake of completeness, most of the data previously published has been repeated here and presented in a form allowing greater useful precision, particularly in the lower temperature range.

DESCRIPTION OF CALCULATIONS

From Eq. (3) of Ref. 1, the specific intensity (I_λ) at any particular wavelength λ (and energy $E = hc/\lambda$) transmitted through absorbing foils of thickness D_j with an absorption coefficient K_j is given by the product of the bremsstrahlung emission and the foil transmission as

$$I_\lambda \propto \lambda^{-2} (kT)^{-1/2} \exp\left[-E/kT - \sum_j K_j(E) D_j\right] , \tag{1}$$

where the subscript j refers to the various foil materials.*

Values of Eq. (1) have been computed for various foil materials and thicknesses in mg/cm^2 and for various electron temperatures in eV. A graph useful in converting foil thickness expressed in mg/cm^2 into inches is given for values relevant to this report in Fig. 1, where specific gravities were obtained from Ref. 7 and a value of unity was assumed for polyethylene.

*As discussed in Ref. 1, the Gaunt factors have been assumed to be a constant in the calculations, which is not expected to greatly affect the temperatures deduced, since they will always appear as approximately equal quantities in ratio.

The values of Eq. (1) were plotted automatically versus wavelength, and the results are shown in Figs. 2 through 23. Such graphs are useful in determining the wavelength region observed, thereby assuring the avoidance of regions of characteristic line radiation and recombination edges. Combining polyethylene (CH_2) with aluminum and nickel foils has been found useful in suppressing O VII and O VIII radiation between 16 and 22 Å, as seen from Figs. 10 through 12 and 17 through 19.

A numerical integration of Eq. (1) was performed on the NRL CDC 3870 computer over a photon energy range E of 0.1 keV to 1000 keV,* with a fine mesh near the absorption edges. The normalized total transmission, given by the integral of Eq. (1) divided by the integral over the incident bremsstrahlung radiation ($D_j = 0$), is plotted versus foil thickness for various temperatures in Figs. 24 through 39. It is the ratios of such transmissions for various foils that are useful for determining electron temperatures when plotted versus temperature as in Figs. 28 and 29 of Ref. 1.

For most cases the data can be read from Figs. 24 through 39 with sufficient accuracy, particularly when compared to experimental uncertainties involved in measuring the relative continuum emission. Therefore, an extensive tabulation of numerical results has not been included. Numerical results will be made available upon request, however, if required.

ABSORPTION COEFFICIENTS USED

Numerical values for the absorption coefficients $K_j(E)$ used were obtained as follows:

1. Beryllium

For energies E greater than 400 eV, the beryllium absorption coefficients recommended by Gilmore (8), which also agree very well with recent measurements of Cooke and Stewardson (9), were used. In the present calculations, values for energies less than 400 eV were obtained from the recent listing by Henke (10) rather than from the recommendation of Gilmore, which follows the experimental values of Johnston and Tomboulian (11). This change has not resulted in a significant variation from the previous results (1).

2. Aluminum

In the previous calculations (1) for aluminum, absorption coefficients for photon energies between 100 eV and 100 keV were obtained from the compilation of Gilmore (8) using the measured values obtained from Tomboulian and Pell (12) at low energies (less than 800 eV). It has been pointed out recently (9, 10, 13, 14) that these values are too low, as is somewhat the case for the values between 800 eV and 3 keV (7, 15, 16) also quoted by Gilmore. Therefore, in the present calculations on aluminum, absorption coefficients between 100 eV and 6 keV have been obtained from Henke (10), which are in close agreement with measurements of Cooke and Stewardson (9), Fomichev and Lukirskii (13), and Singer (17) at low energies and fit smoothly to the data compiled by Allen (7) at higher energies. The latter have been used up to the new limit of 1000 keV, including the additional "effective" absorption due to scattering at energies greater than 40 keV.

*An upper limit of 100 keV was used previously (1) for lower temperatures. The 10 keV quoted on page 2 of this reference is a misprint.

3. Nickel

As previously reported (1), nickel absorption coefficients were obtained from Allen (7) for energies above the L edge. For lower energies, values were obtained from those measured for copper (9) by multiplying by 0.91.

4. Gold

For gold, absorption coefficients for wavelengths shorter than 1.93 Å were obtained from Allen (7) and between 1.5 Å and 8.3 Å from Andrews (18). An extrapolation toward shorter wavelengths was then made and forced through the value at 44.6 Å given by Allen, with an allowance made for the N_5 edge near 40 Å as shown by Gilmore (8). The large uncertainty in the present results at wavelengths longer than 10 Å caused by this extrapolation of absorption coefficients is indicated in Fig. 37 by the dashed portions.

DISCUSSION

For measurements at the lower temperature range, the lighter materials such as beryllium and aluminum are generally most convenient, since they may be used in greater thicknesses. For temperatures over 300 eV, nickel foils of reasonable thickness may be used. These have the additional advantage of blocking stray radiation of longer wavelengths, which could be transmitted through the lighter foils.

In using the data in Figs. 24 through 39, it may be noticed that the most sensitive temperature measurement is obtained with two foils of material and thickness such that the change in slope with temperature is high over the temperature range expected. For any particular material, it will be seen from these graphs that such a change in slope with temperature decreases toward higher temperatures. At such a temperature where the measurement becomes insensitive, it may also be seen that the sensitivity again improves with the use of foils of heavier elements. It is for this reason that the computations were extended to include gold at the higher temperatures. Again, the calculations for gold are not expected to be particularly reliable at lower temperatures and thicknesses, as indicated by the dashed portions in Fig. 37.

Thus, it is often possible to improve the sensitivity of the temperature determination by using foils of different material. Again, the variation in the slope (with temperature) of the curves presented in Figs. 24 through 39 for the temperature range expected may serve as an immediate indication of the sensitivity for the material chosen.

Finally, as discussed in Ref. 1, the additional continuum emission caused by recombination should not create any difficulties in using this technique for temperature determination, since Eq. (1) continues to be valid between recombination edges corresponding to the discrete bound states involved. Where a large step in the continuum spectrum is expected, it is of course necessary to select (using Figs. 2 through 23) suitable foil materials and thicknesses to avoid this region.

ACKNOWLEDGMENT

The assistance of R. L. Babcock in the formulation of a plotter program used to generate Figs. 2 through 23 is gratefully acknowledged.

REFERENCES

1. Elton, R.C., and Anderson, A.D., "Calculations Useful in the Determination of Electron Temperature from X-Ray Continuum Radiation Emitted from High Temperature Plasmas," NRL Report 6541, Mar. 1967. See also Roth, N.V. and Elton, R.C., Appl. Optics 6:2071 (1967) for a synopsis.

2. Jahoda, F.C., Little, E.M., Quinn, W.E., Sawyer, G.A., and Stratton, T.F., Phys. Rev. 119:843 (1960)

3. Griem, H.R., Kolb, A.C., Lupton, W.H., and Phillips, D.T., Nuclear Fusion Supplement, Vienna: International Atomic Energy Agency, Part 2, p. 543 (1962)

4. Griem, H.R., "Plasma Spectroscopy," New York: McGraw-Hill, 1964

5. Peacock, N.J., United Kingdom Atomic Energy Authority, Culham Laboratory Report CLM-M-39, 1964

6. Elton, R.C., Hintz, E., and Swartz, M., "Proceedings Seventh International Conference on Phenomena in Ionized Gases," Vol. 3, Belgrade: Gradevinska Knjiga Publ. House, p. 190, 1966

7. Allen, S.J.M., "Handbook of Chemistry and Physics," 45th edition 1964-1965, Cleveland: Chemical Rubber Co., pp. 69E-70E (1964)

8. Gilmore, F.R., "Graphs of X-Ray Absorption Coefficients for Fourteen Substances," Research Memorandum, RM-2367-AEC, The Rand Corp., Santa Monica, Calif. Apr. 10, 1959

9. Cooke, B.A., and Stewardson, E.A., Brit. J. Appl. Phys. 15:1315 (1964)

10. Henke, B.L., Elgin, R.L., Lent, R.E. and Ledingham, R.B., "X-Ray Absorption in the 2-to-200 Å Region," Norelco Reporter XIV (No. 3-4):112, July-Dec. 1967

11. Johnston, R.W., and Tomboulian, D.H., Phys. Rev. 94:1585 (1954)

12. Tomboulian, D.H., and Pell, E.M., Phys. Rev. 83:1196 (1951)

13. Fomichev, V.A., and Lukirskii, A.P., Opt. Spectros. 22:432 (1967)

14. Ershov, O.A., Opt. Spectros. 22:252 (1967)

15. Victoreen, J.A., J. App. Phys. 20:1141 (1949)

16. Henke, B.L., White, R. and Lundberg, B., J. Appl. Physics, 28:98 (1957)

17. Singer, S., J. Appl. Phys. 38:2897 (1967)

18. Andrews, C.L., Phys. Rev. 54:994 (1938)

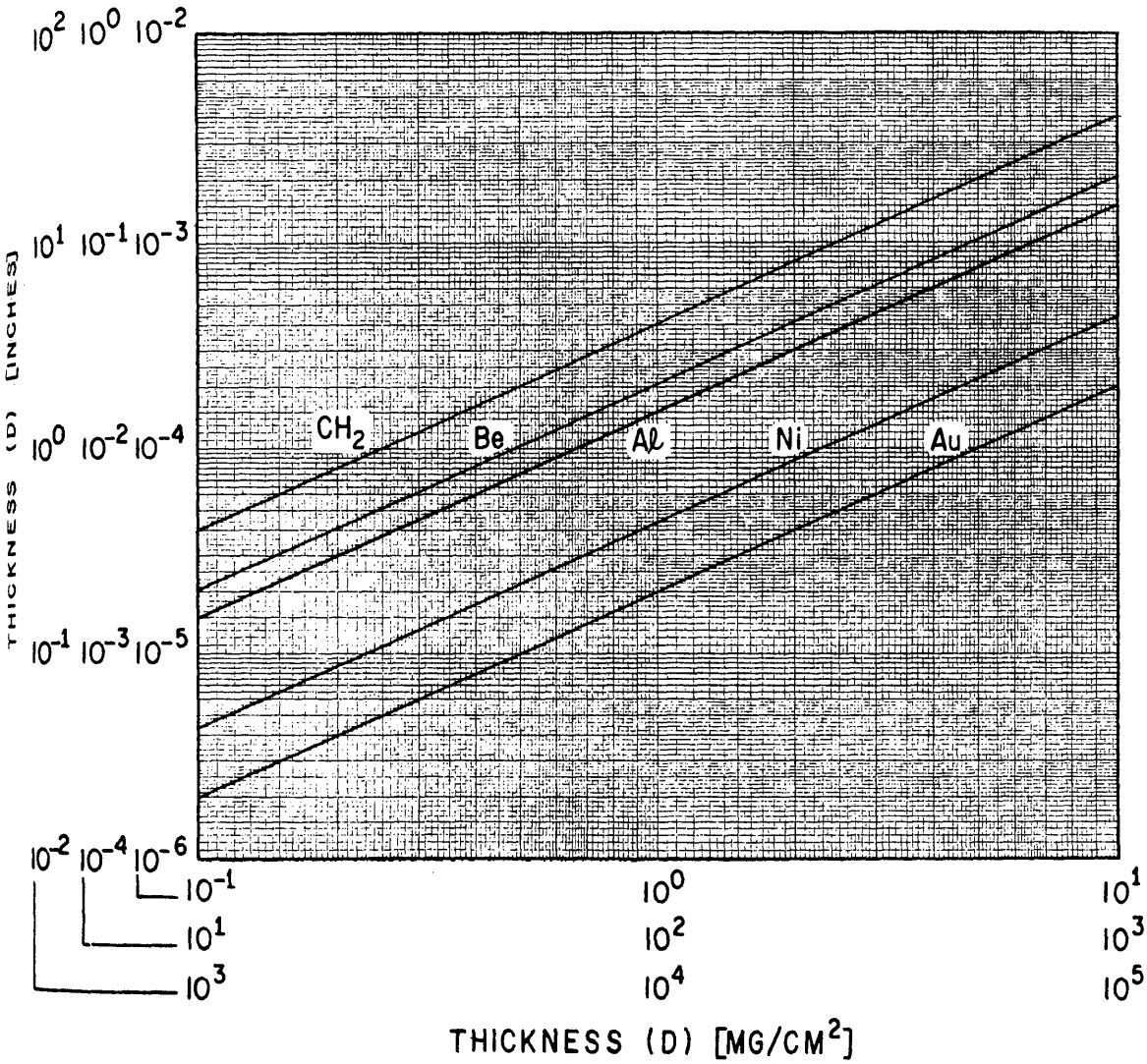

Fig. 1 - Graph for converting foil thicknesses expressed in mg/cm^2 into inches for various foil materials

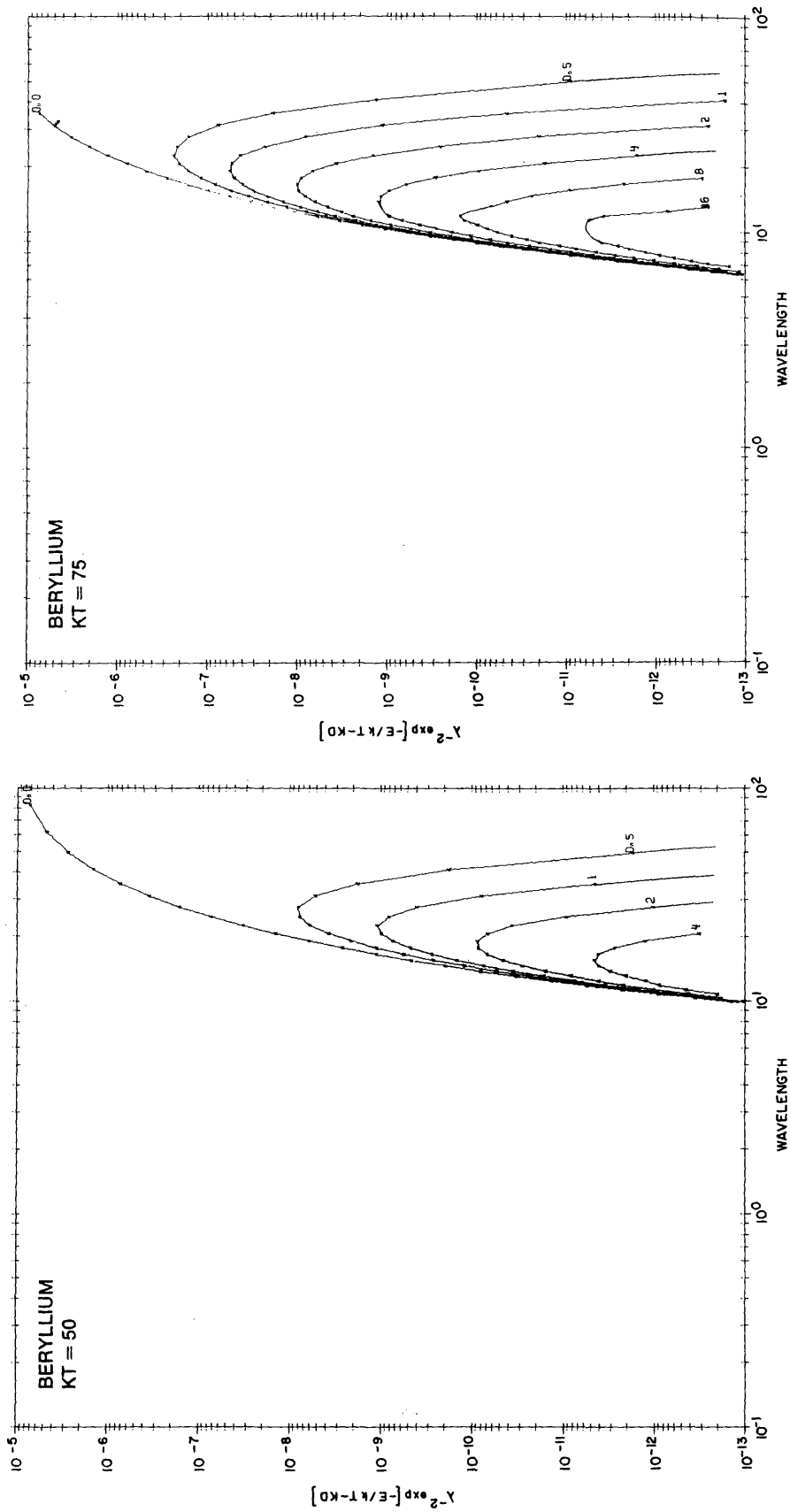

Fig. 2 - Relative bremsstrahlung emission at a temperature kT (in electron volts) transmitted through absorbing foils of thickness D (in mg/cm^2) versus wavelength (in Å).

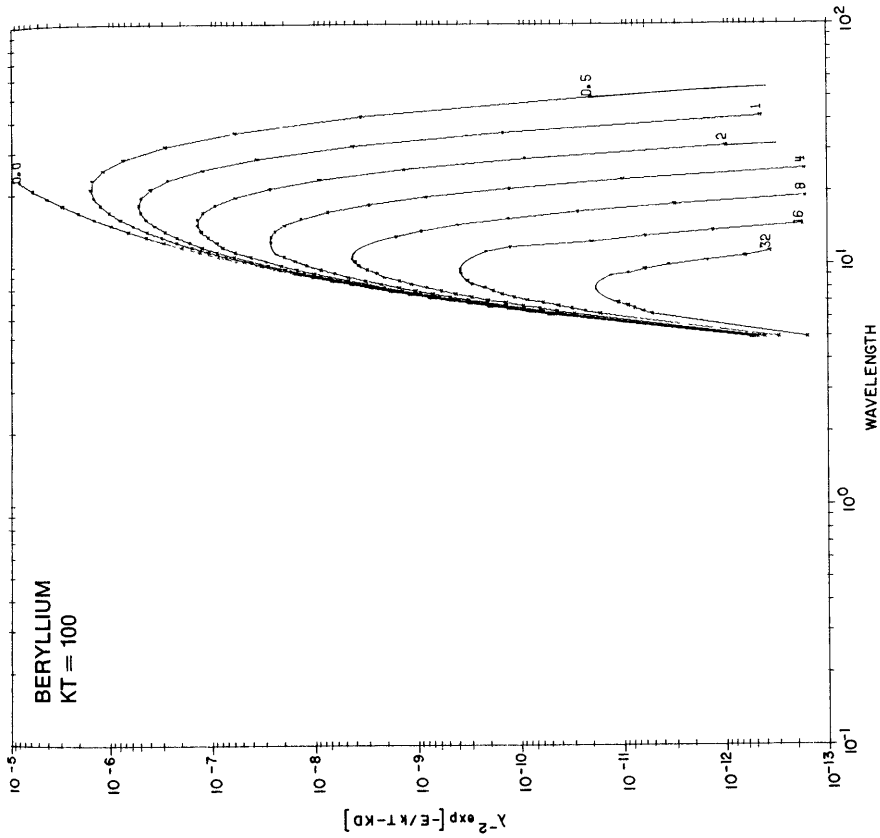

Fig. 2 - Relative bremsstrahlung emission at a temperature kT (in electron volts) transmitted through absorbing foils of thickness D (in mg/cm^2) versus wavelength (in Å) (Continued).

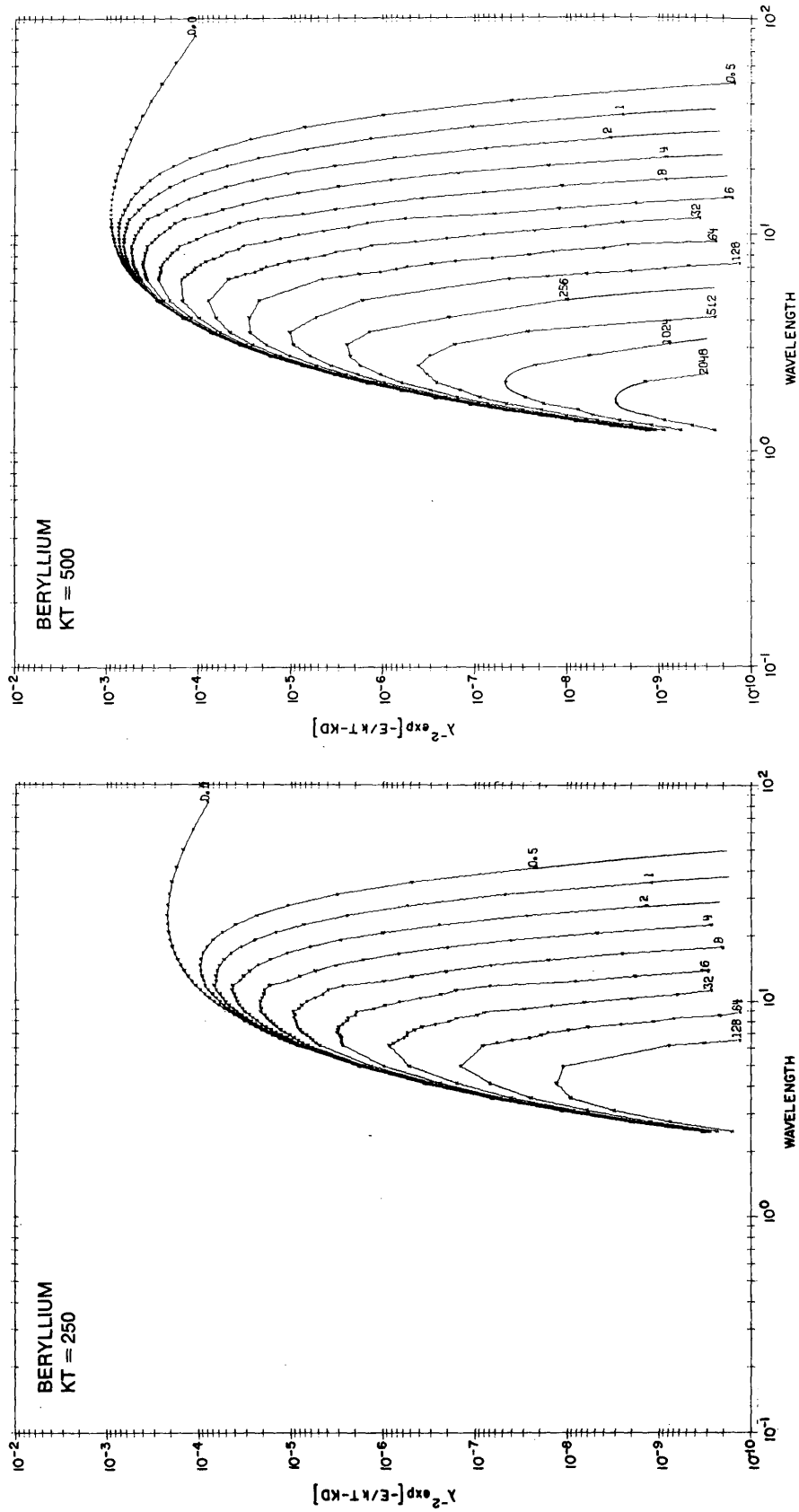

Fig. 3 - Relative bremsstrahlung emission at a temperature kT (in electron volts) transmitted through absorbing foils of thickness D (in mg/cm^2) versus wavelength (in Å).

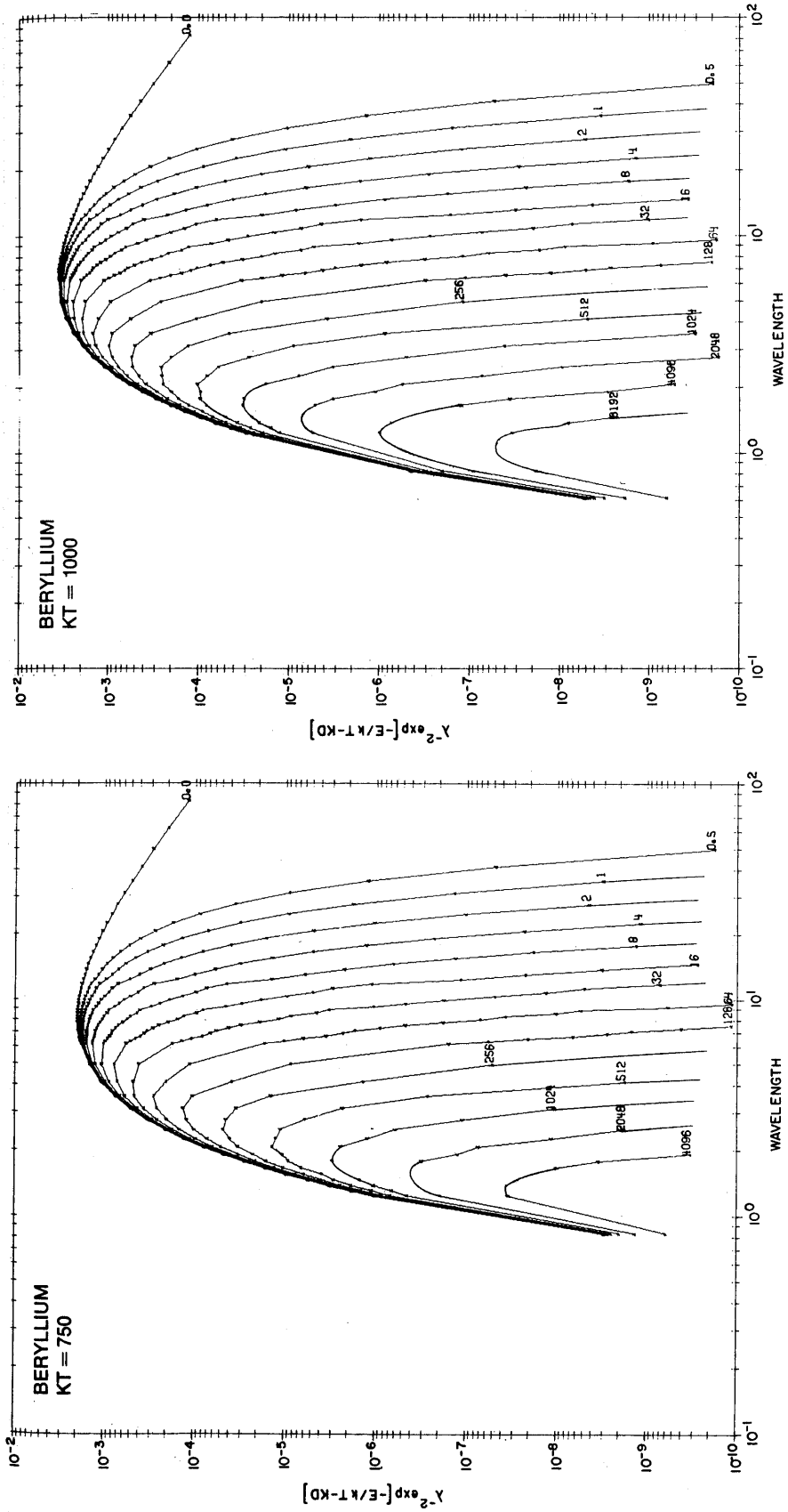

Fig. 3 - Relative bremsstrahlung emission at a temperature kT (in electron volts) transmitted through absorbing foils of thickness D (in mg/cm^2) versus wavelength (in Å) (Continued).

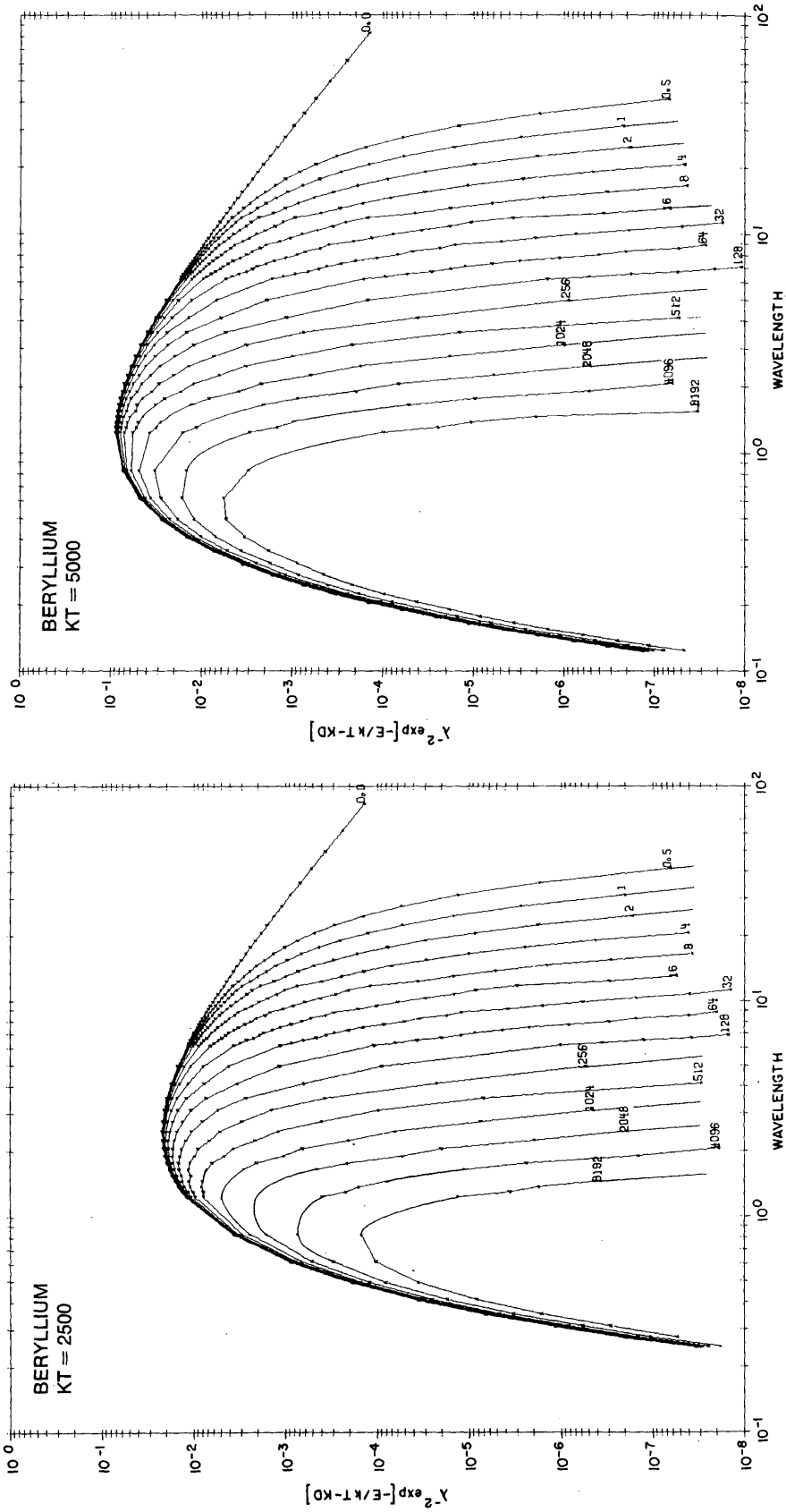

Fig. 4 - Relative bremsstrahlung emission at a temperature kT (in electron volts) transmitted through absorbing foils of thickness D (in mg/cm^2) versus wavelength (in Å).

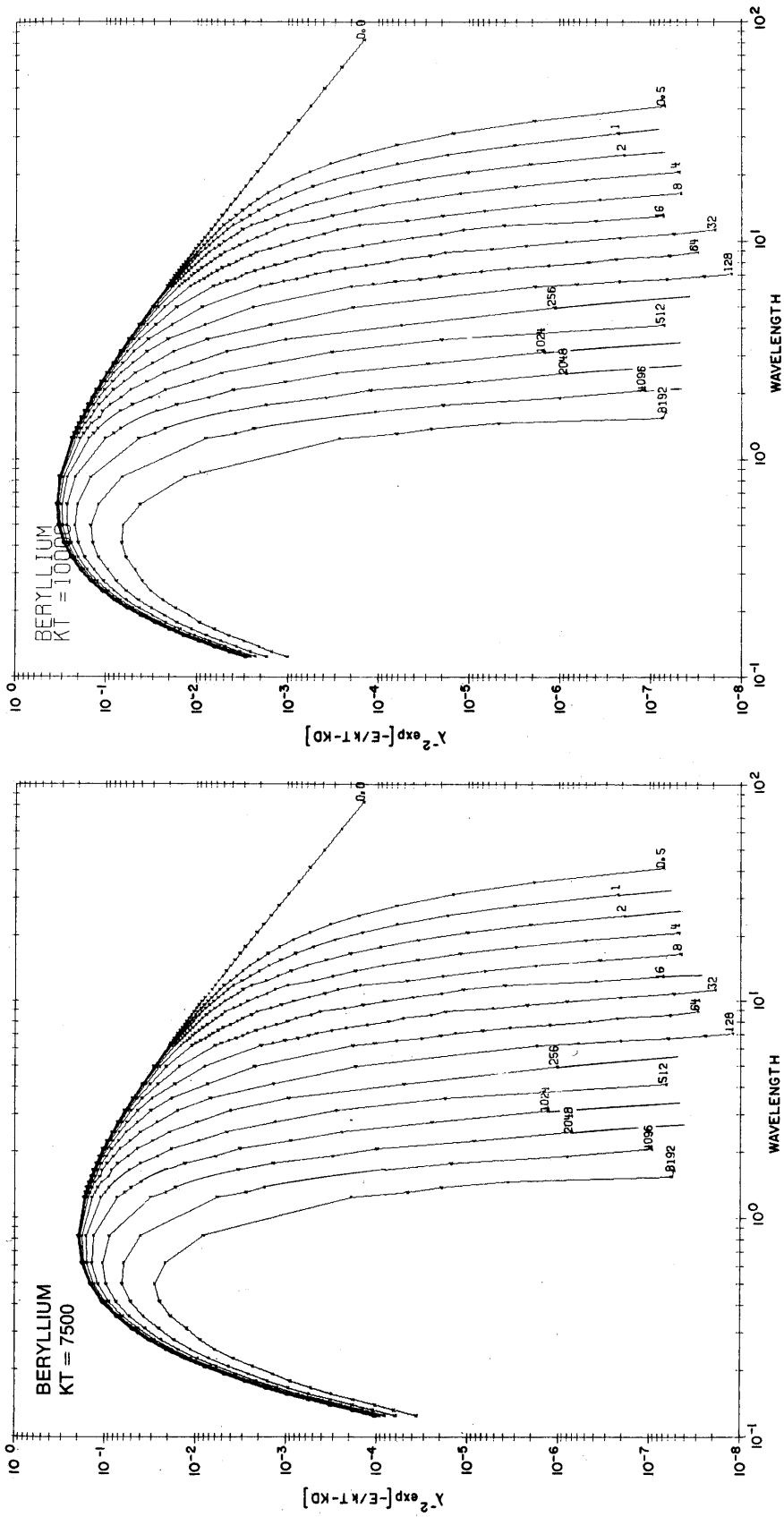

Fig. 4 - Relative bremsstrahlung emission at a temperature kT (in electron volts) transmitted through absorbing foils of thickness D (in mg/cm^2) versus wavelength (in Å) (Continued).

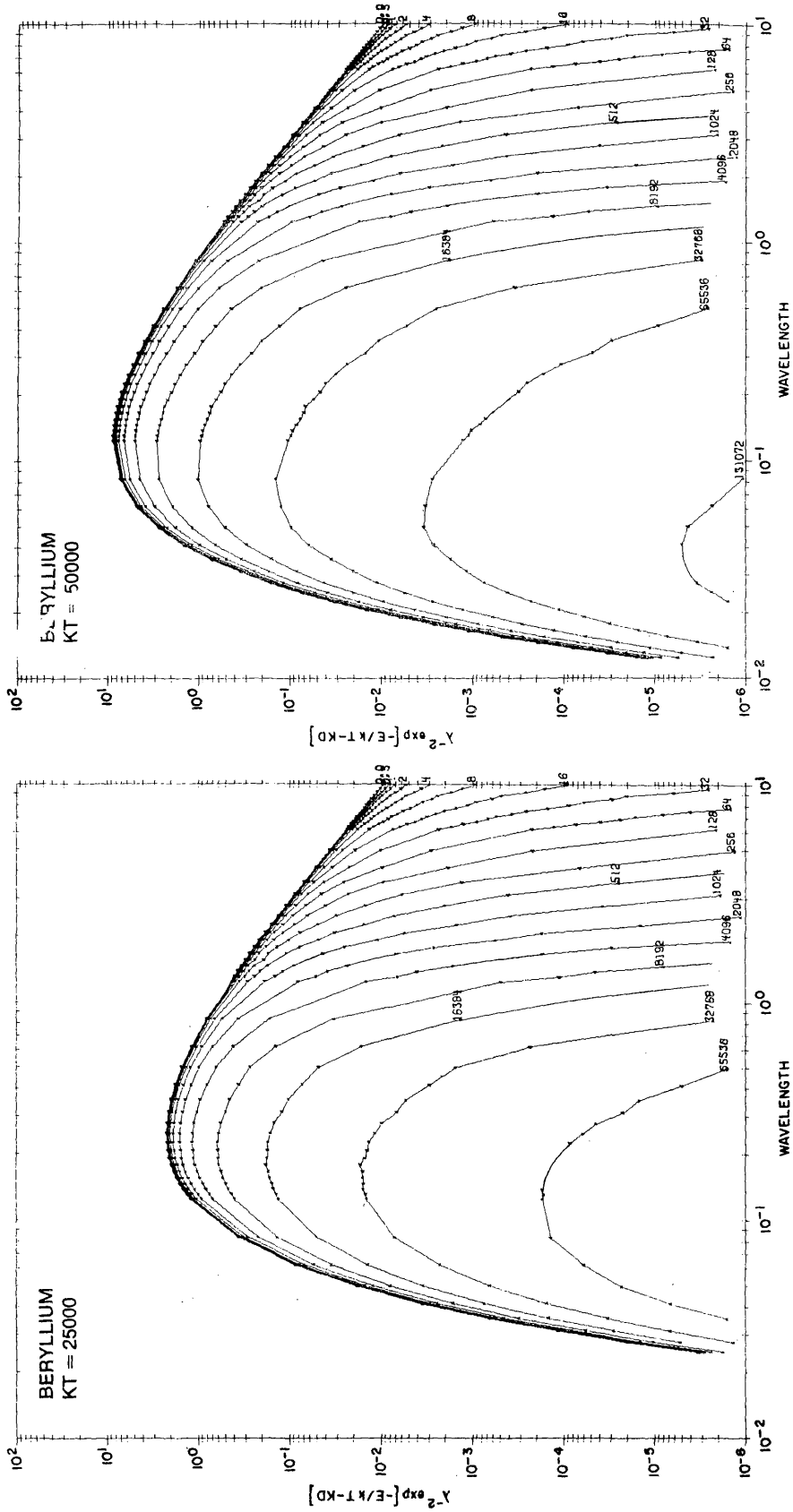

Fig. 5 - Relative bremsstrahlung emission at a temperature kT (in electron volts) transmitted through absorbing foils of thickness D (in mg/cm^2) versus wavelength (in Å).

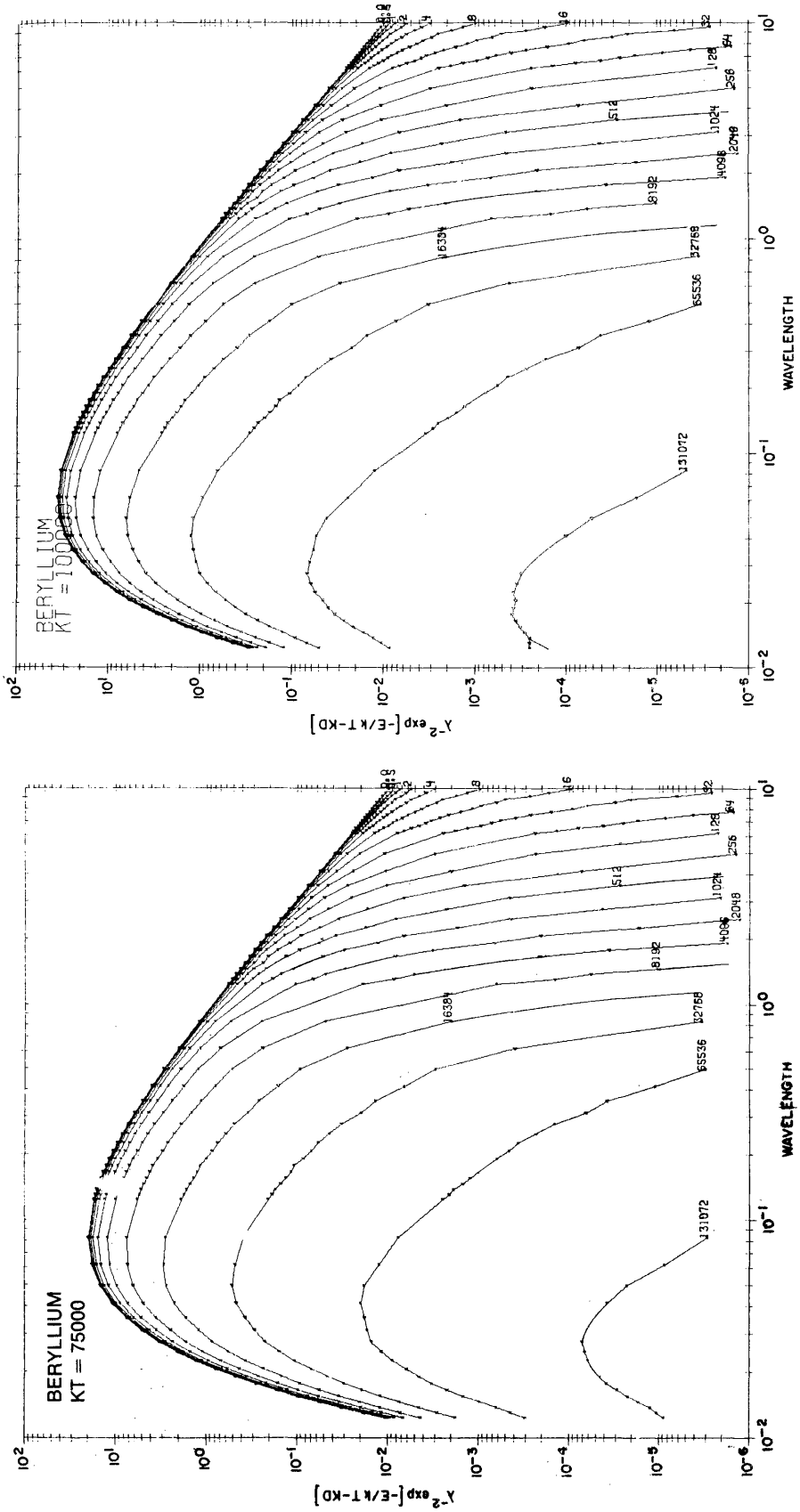

Fig. 5 - Relative bremsstrahlung emission at a temperature kT (in electron volts) transmitted through absorbing foils of thickness D (in mg/cm^2) versus wavelength (in Å) (Continued).

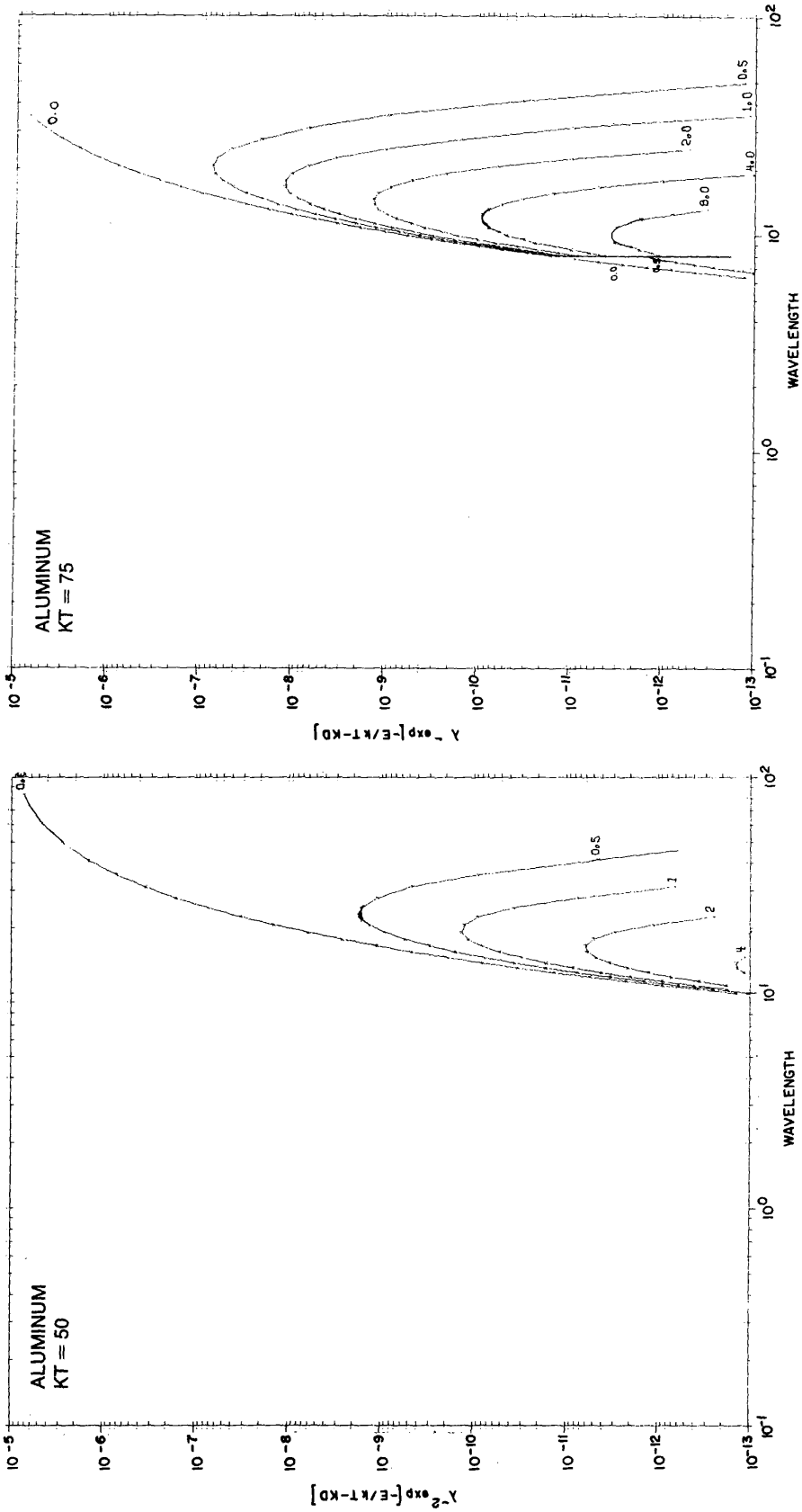

Fig. 6 - Relative bremsstrahlung emission at a temperature kT (in electron volts) transmitted through absorbing foils of thickness D (in mg/cm²) versus wavelength (in Å).

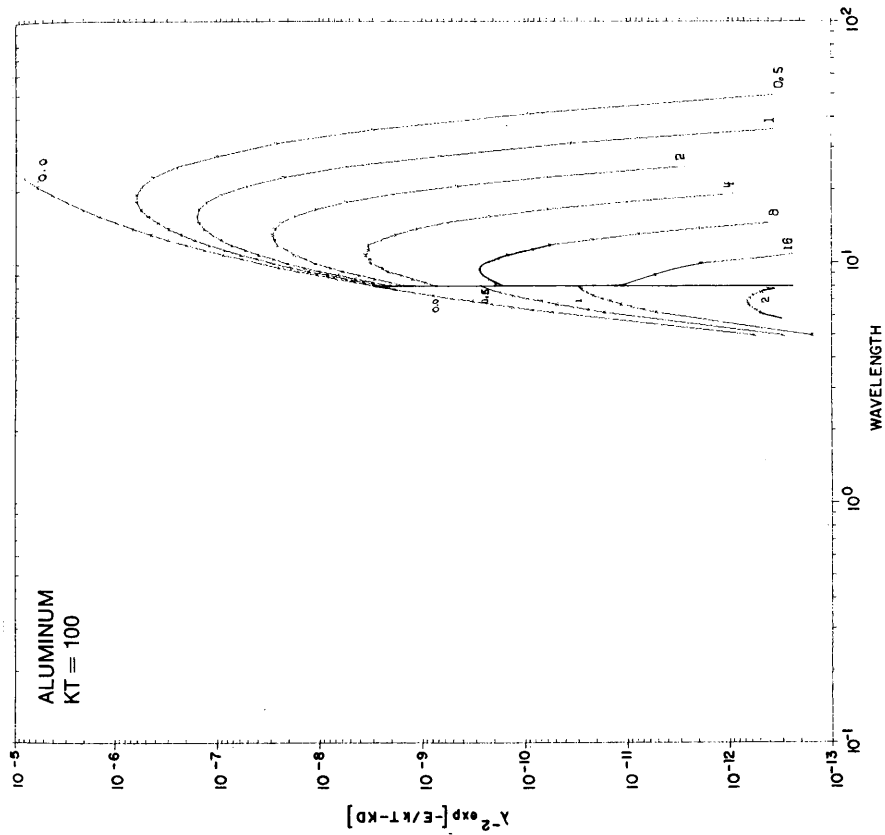

Fig. 6 - Relative bremsstrahlung emission at a temperature kT (in electron volts) transmitted through absorbing foils of thickness D (in mg/cm^2) versus wavelength (in Å) (Continued).

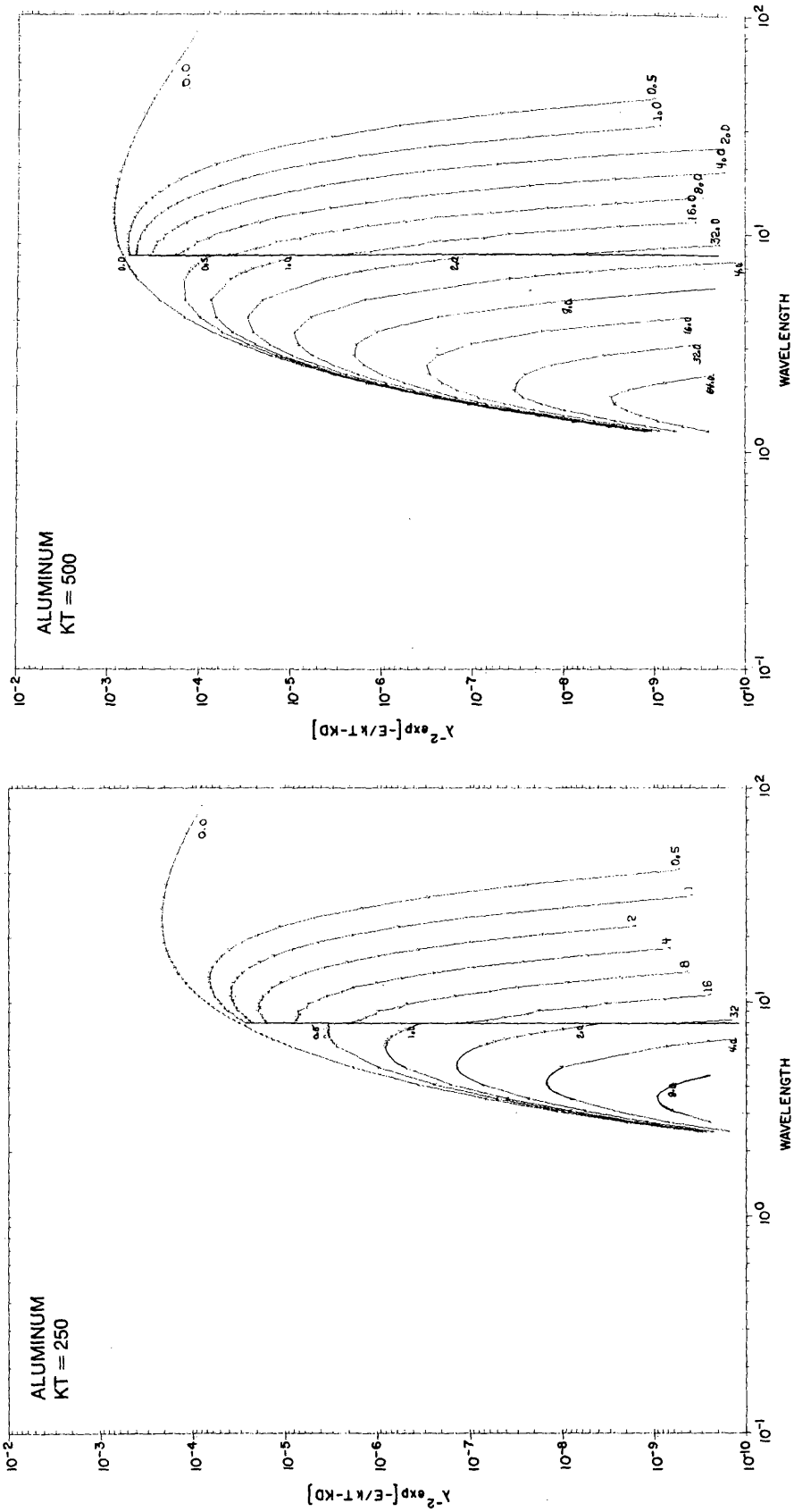

Fig. 7 - Relative bremsstrahlung emission at a temperature kT (in electron volts) transmitted through absorbing foils of thickness D (in mg/cm^2) versus wavelength (in Å).

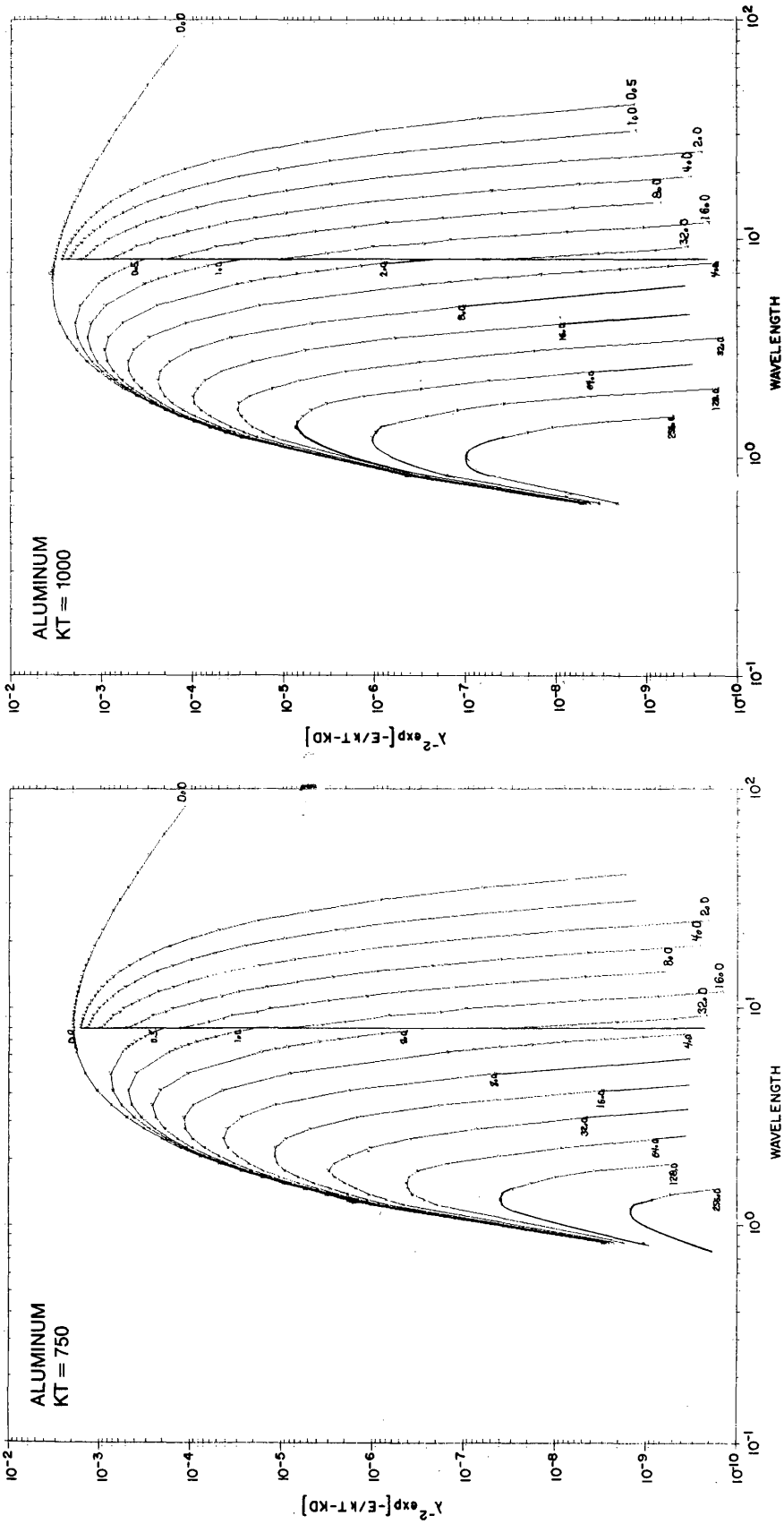

Fig. 7 - Relative bremsstrahlung emission at a temperature kT (in electron volts) transmitted through absorbing foils of thickness D (in mg/cm^2) versus wavelength (in Å) (Continued).

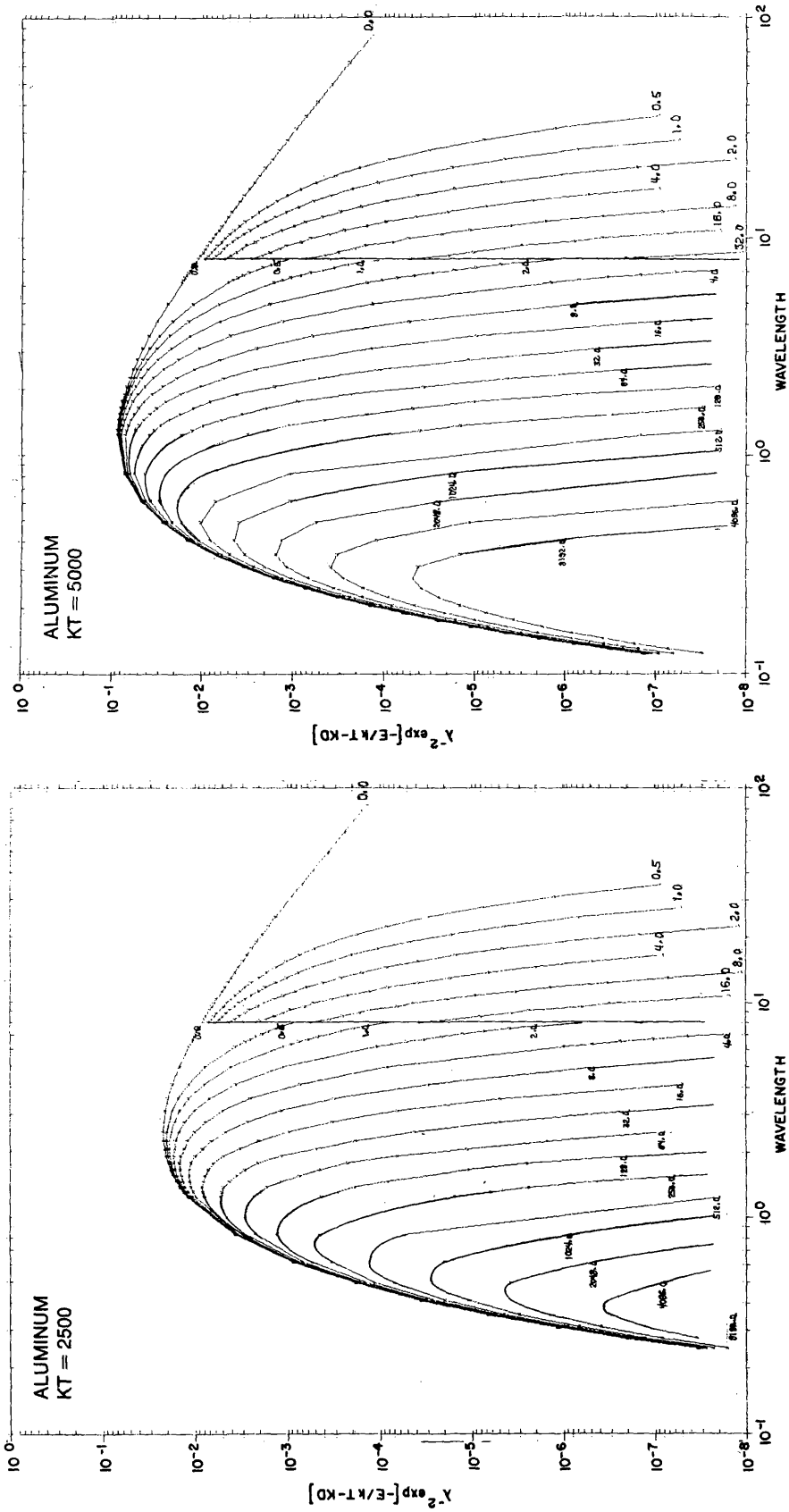

Fig. 8 - Relative bremsstrahlung emission at a temperature kT (in electron volts) transmitted through absorbing foils of thickness D (in mg/cm^2) versus wavelength (in Å).

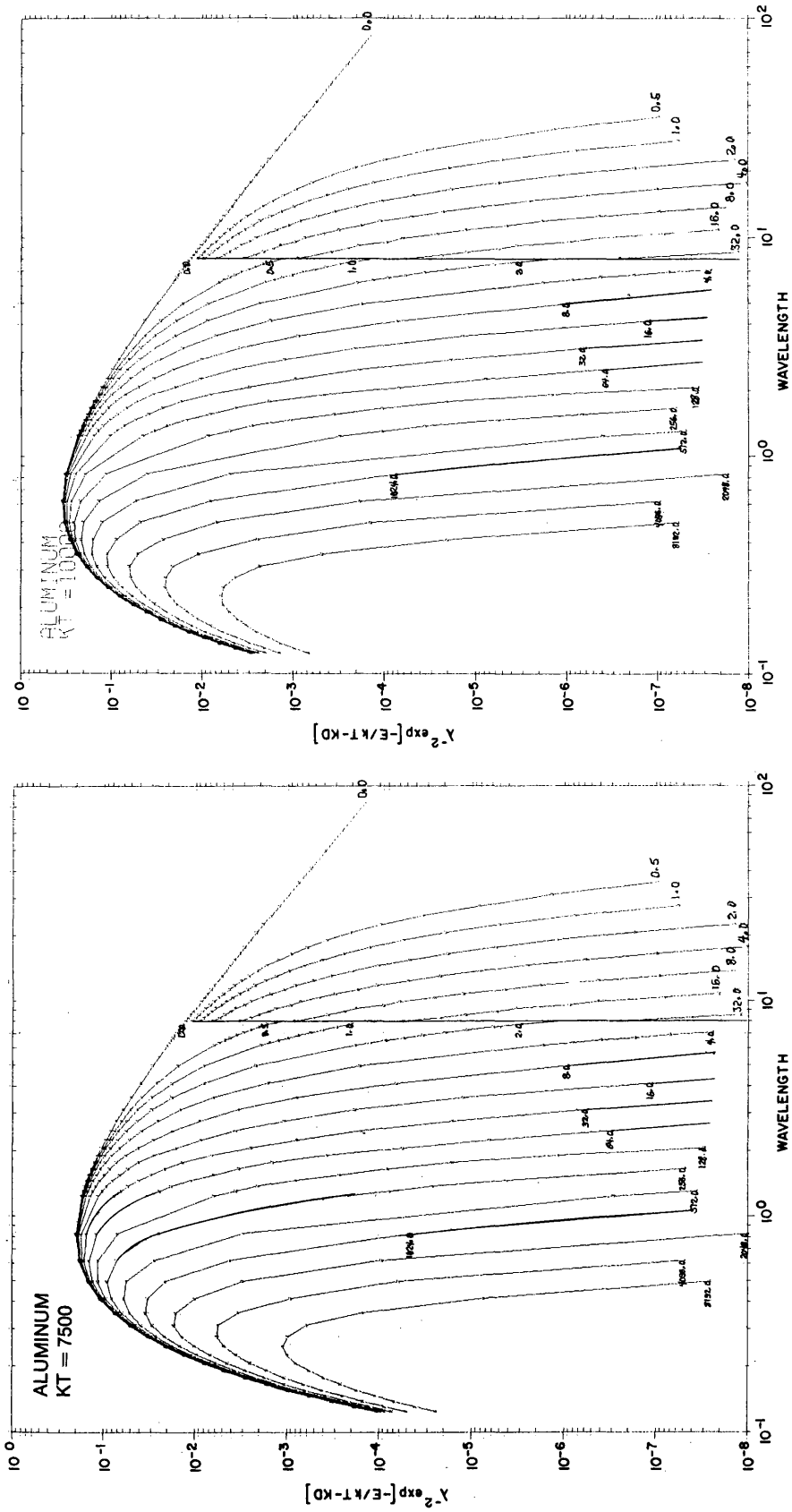

Fig. 8 - Relative bremsstrahlung emission at a temperature kT (in electron volts) transmitted through absorbing foils of thickness D (in mg/cm^2) versus wavelength (in Å) (Continued).

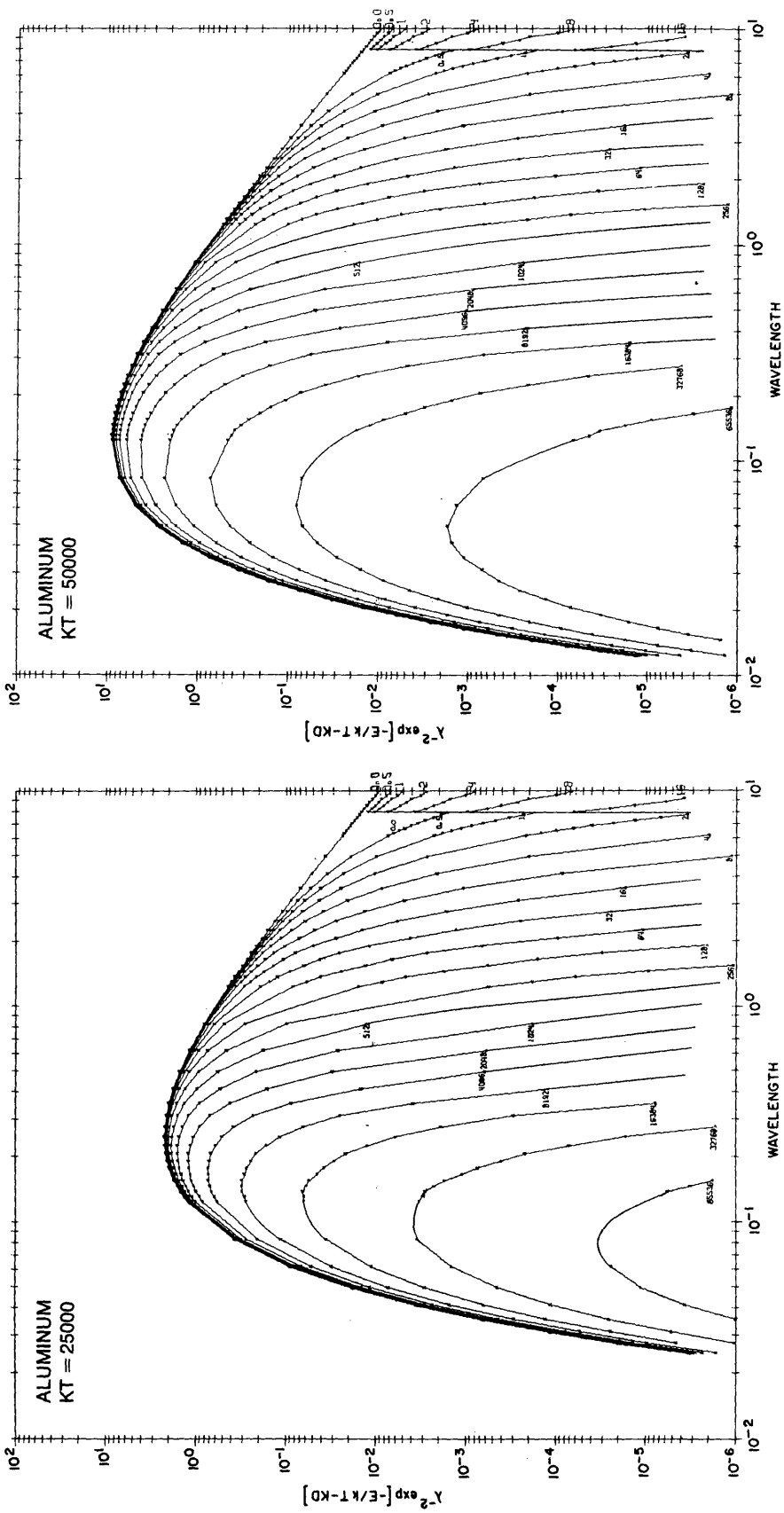

Fig. 9 - Relative bremsstrahlung emission at a temperature kT (in electron volts) transmitted through absorbing foils of thickness D (in mg/cm^2) versus wavelength (in Å).

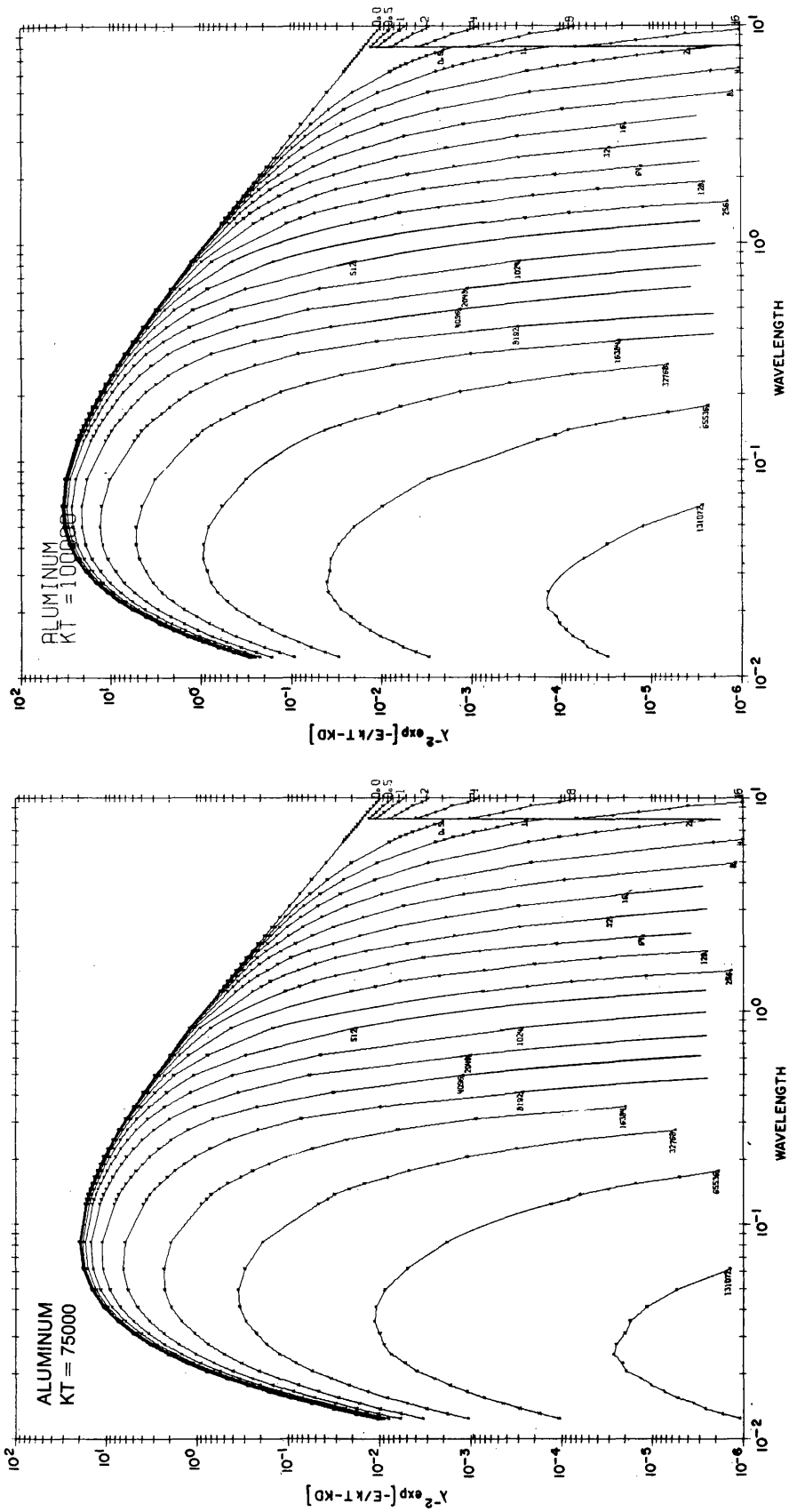

Fig. 9 - Relative bremsstrahlung emission at a temperature kT (in electron volts) transmitted through absorbing foils of thickness D (in mg/cm^2) versus wavelength (in Å) (Continued).

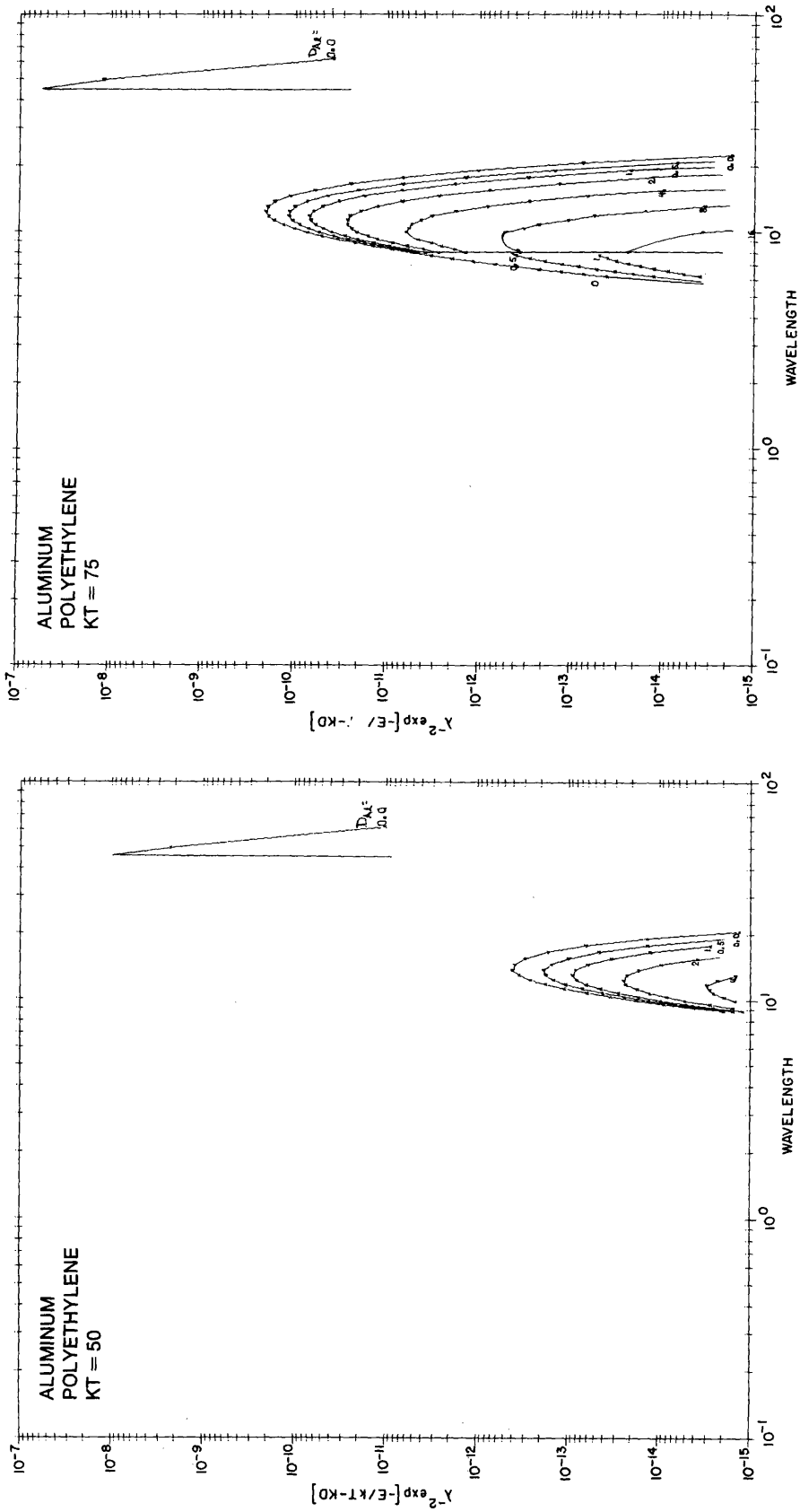

Fig. 10 - Relative bremsstrahlung emission at a temperature kT (in electron volts) transmitted through absorbing foils of thickness D (in mg/cm^2) versus wavelength (in Å). Polyethylene thickness 0.001 inches (2.3 mg/cm^2).

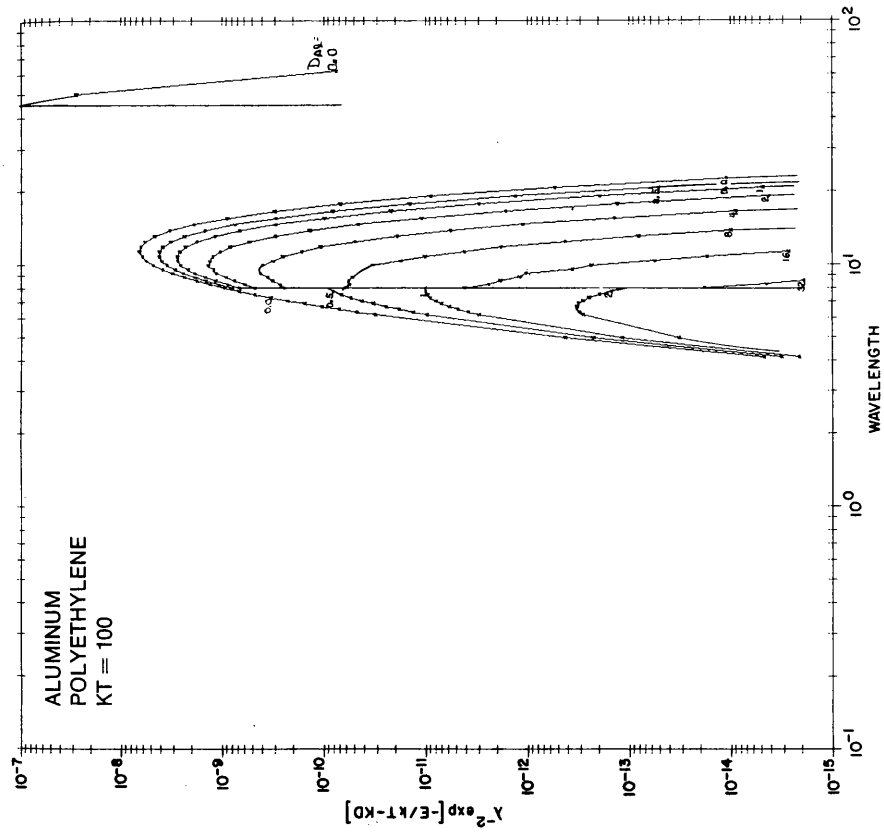

Fig. 10 - Relative bremsstrahlung emission at a temperature kT (in electron volts) transmitted through absorbing foils of thickness D (in mg/cm^2) versus wavelength (in Å) (Continued). Polyethylene thickness 0.001 inches (2.3 mg/cm^2).

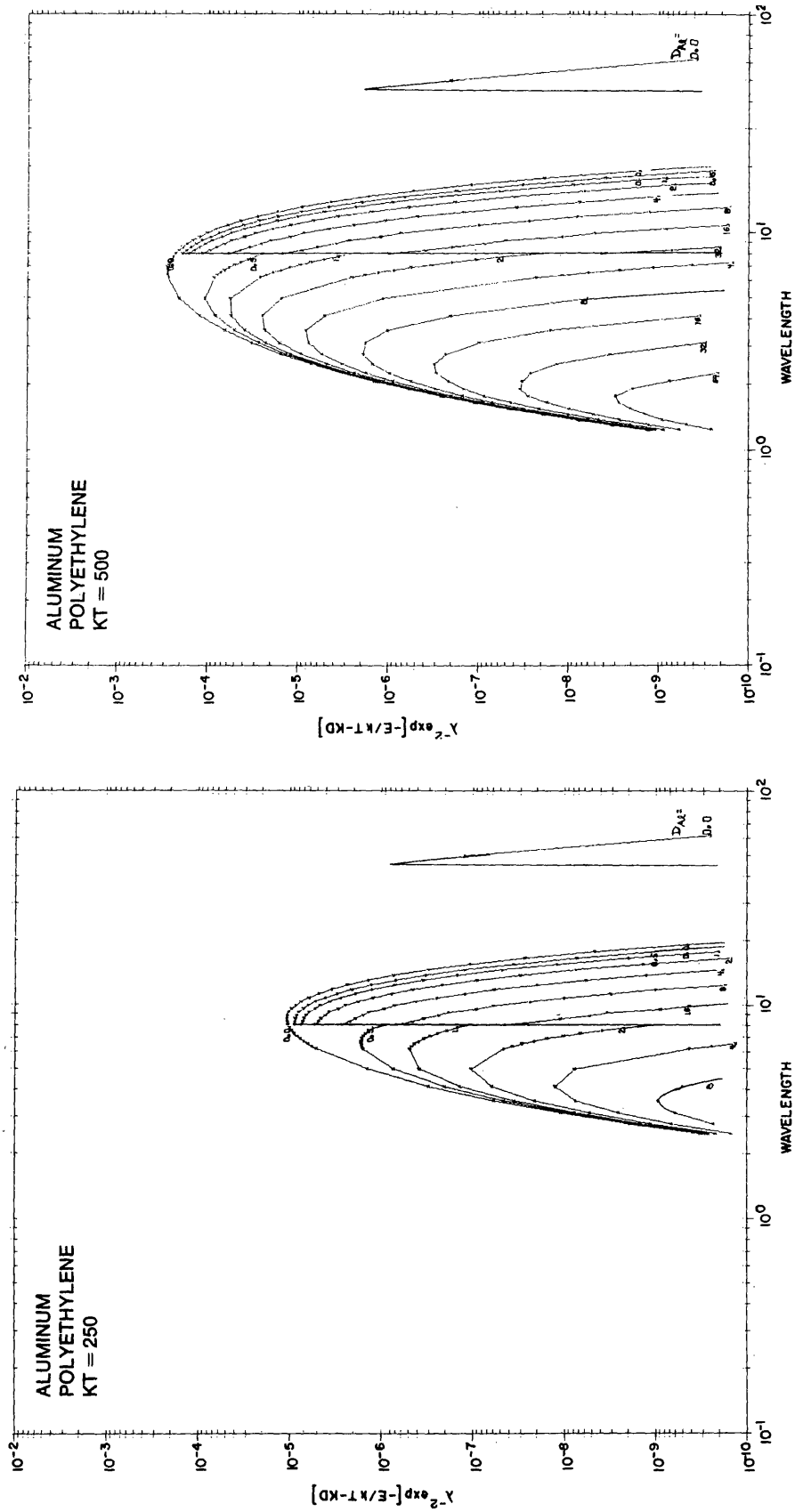

Fig. 11 - Relative bremsstrahlung emission at a temperature kT (in electron volts) transmitted through absorbing foils of thickness D (in mg/cm²) versus wavelength (in Å). Polyethylene thickness 0.001 inches (2.3 mg/cm²).

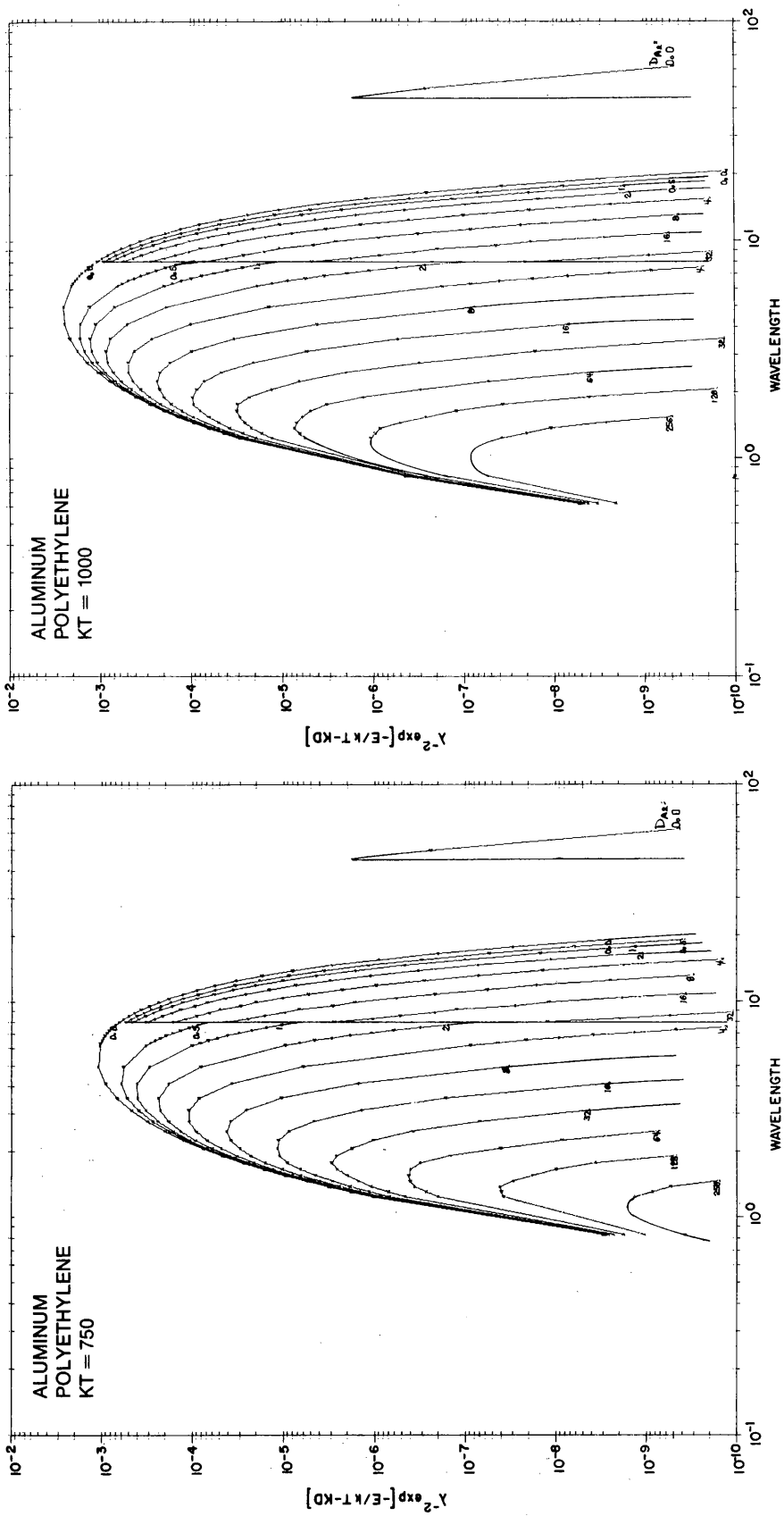

Fig. 11 - Relative bremsstrahlung emission at a temperature kT (in electron volts) transmitted through absorbing foils of thickness D (in mg/cm^2) versus wavelength (in Å) (Continued). Polyethylene thickness 0.001 inches (2.3 mg/cm^2).

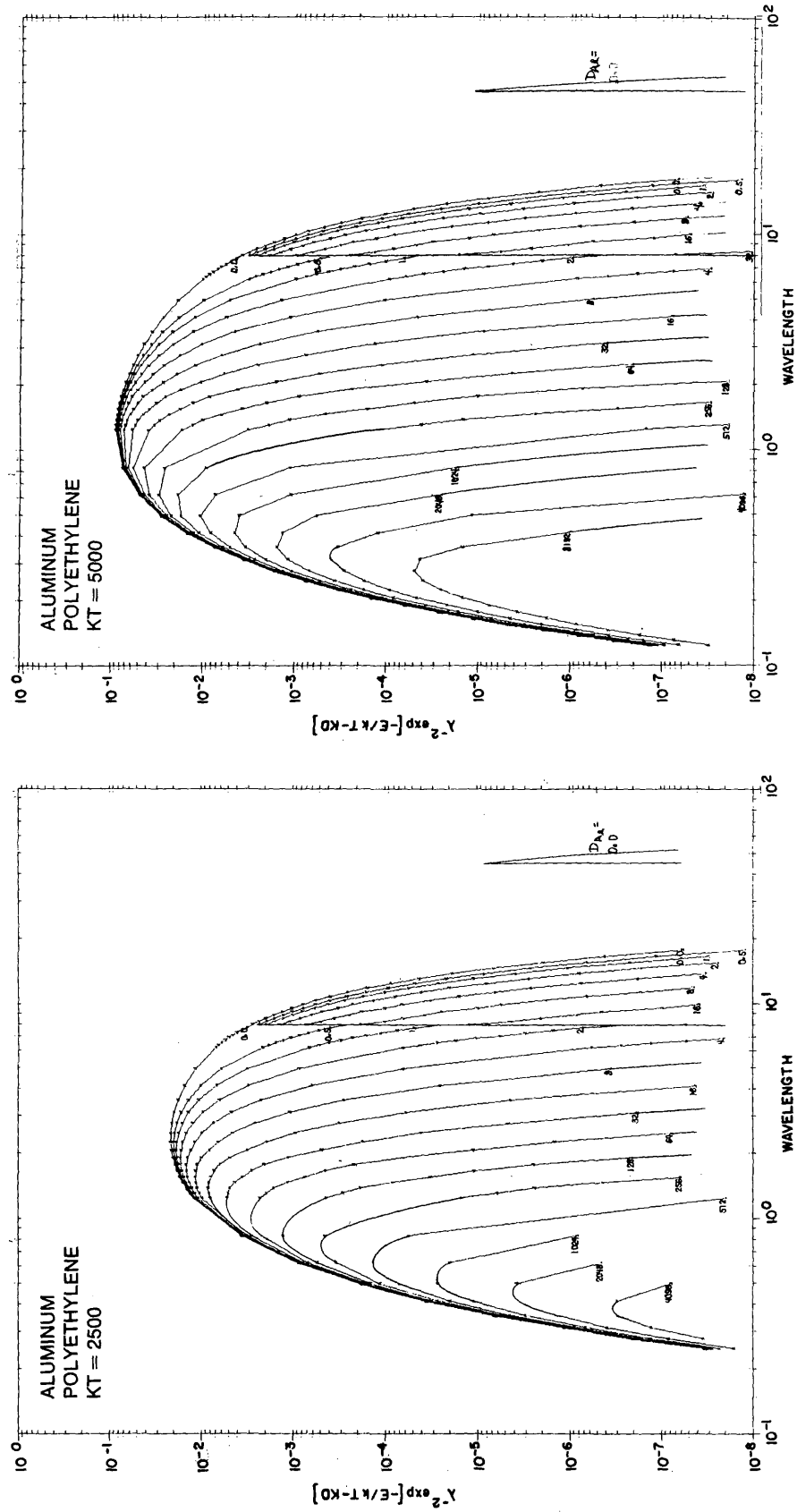

Fig. 12 - Relative bremsstrahlung emission at a temperature kT (in electron volts) transmitted through absorbing foils of thickness D (in mg/cm^2) versus wavelength (in Å). Polyethylene thickness 0.001 inches (2.3 mg/cm^2).

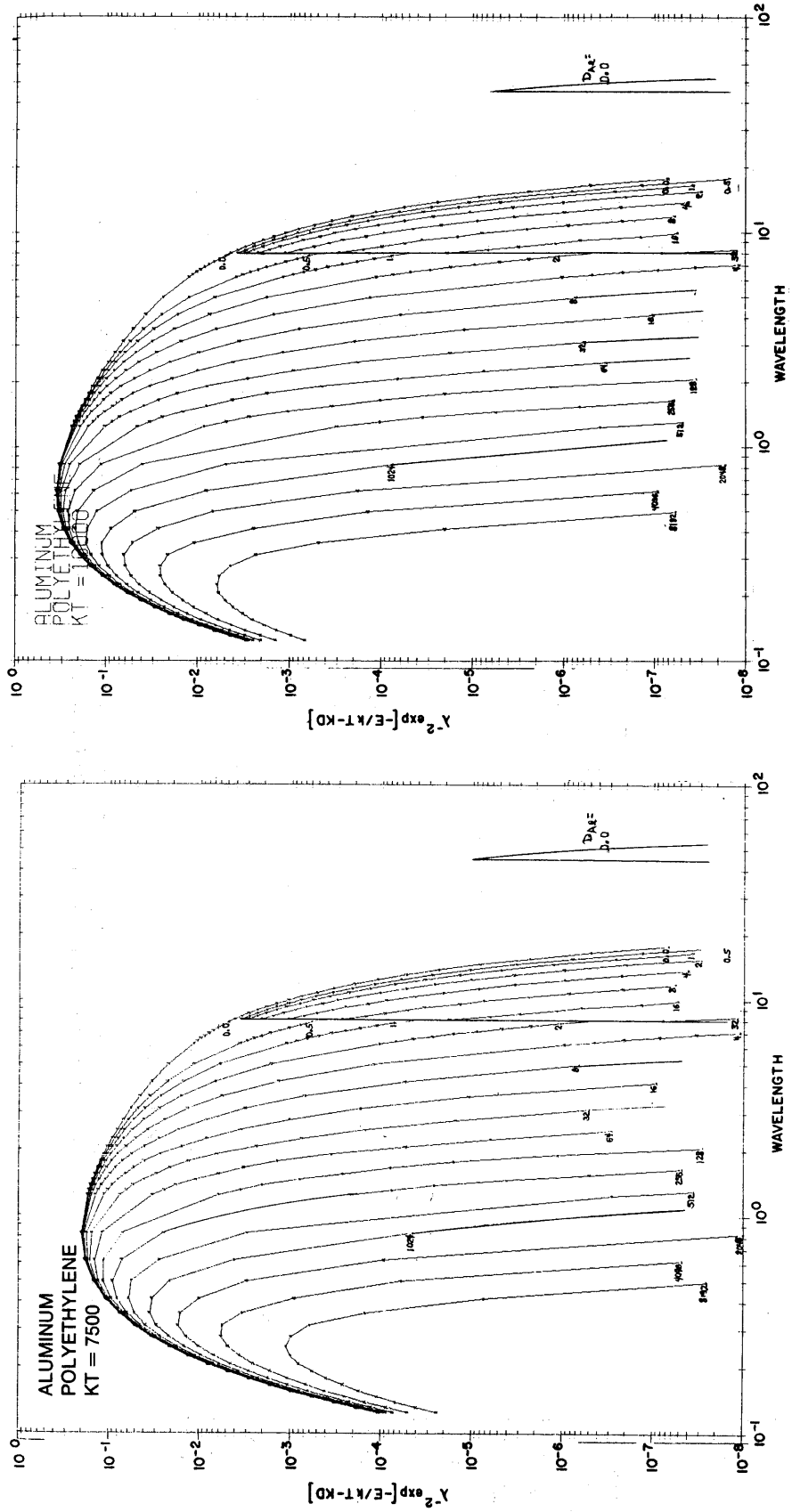

Fig. 12 - Relative bremsstrahlung emission at a temperature kT (in electron volts) transmitted through absorbing foils of thickness D (in mg/cm^2) versus wavelength (in Å) (Continued). Polyethylene thickness 0.001 inches (2.3 mg/cm^2).

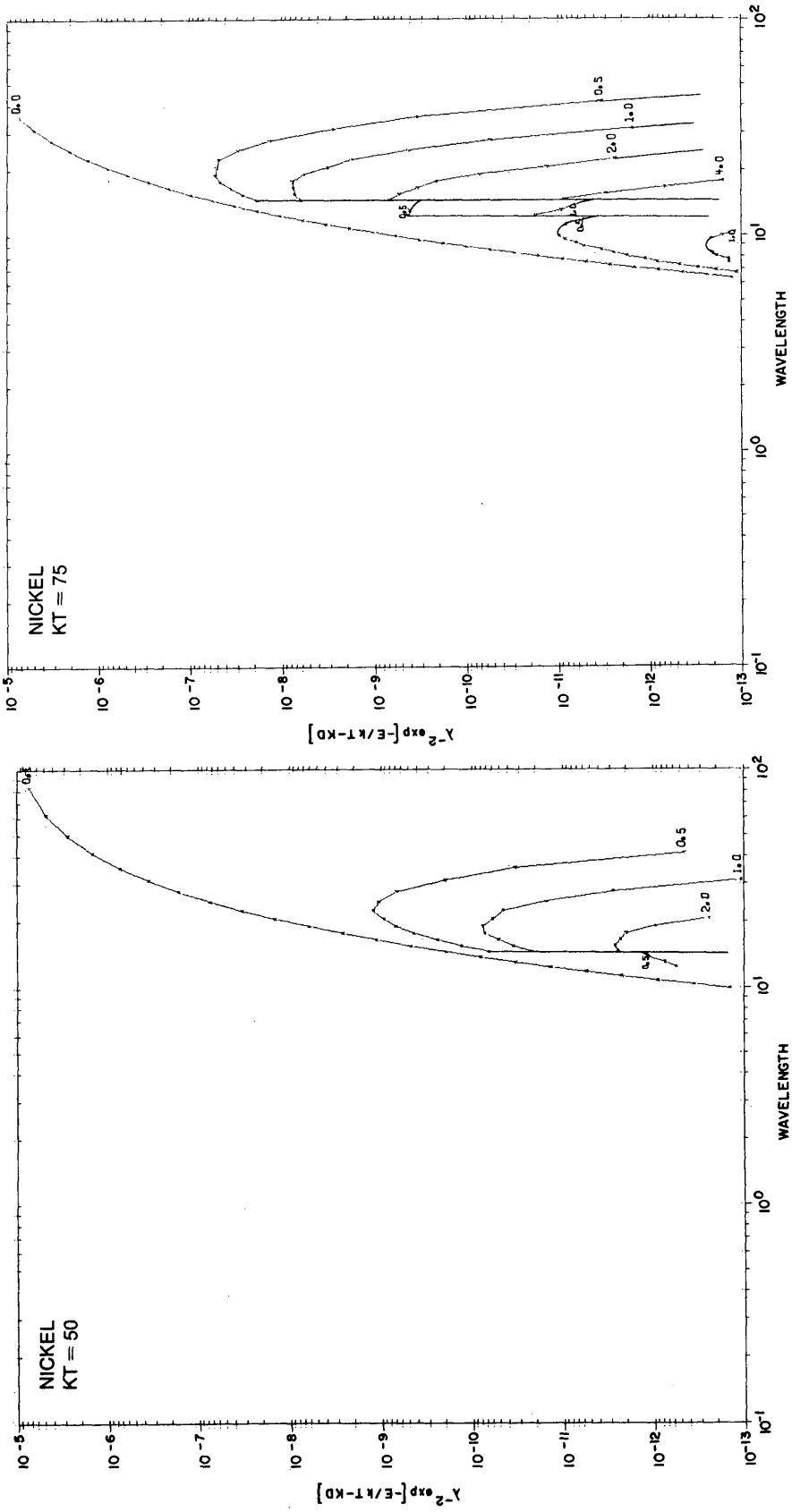

Fig. 13 - Relative bremsstrahlung emission at a temperature kT (in electron volts) transmitted through absorbing foils of thickness D (in mg/cm^2) versus wavelength (in Å).

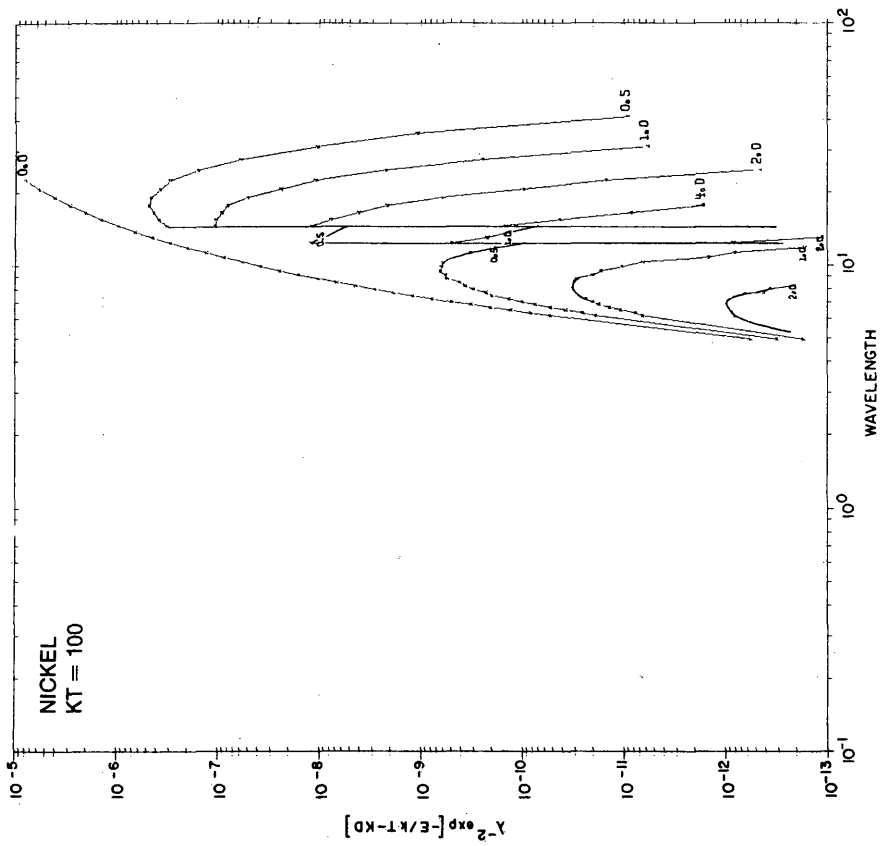

Fig. 13 - Relative bremsstrahlung emission at a temperature kT (in electron volts) transmitted through absorbing foils of thickness D (in mg/cm^2) versus wavelength (in Å) (Continued).

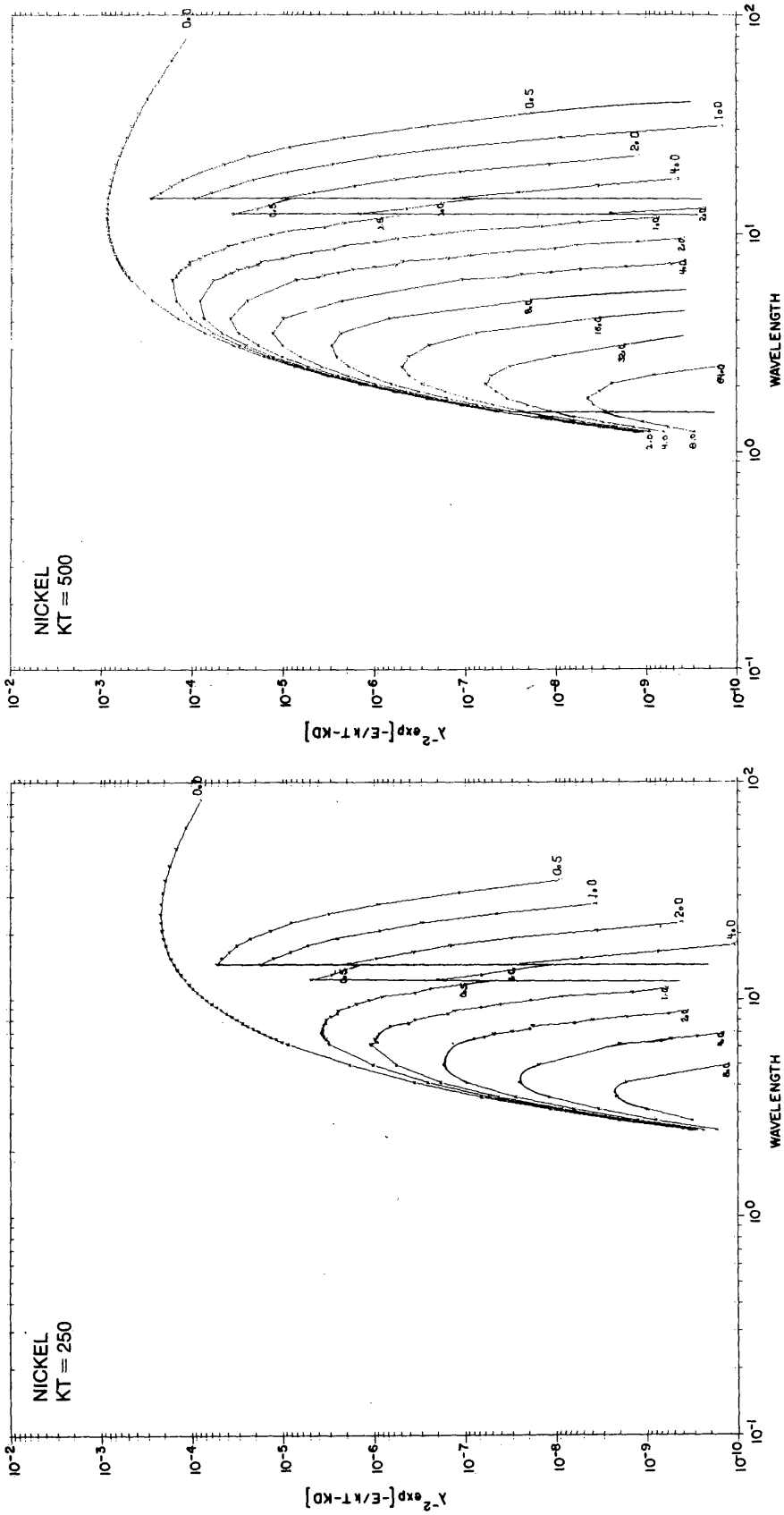

Fig. 14 - Relative bremsstrahlung emission at a temperature kT (in electron volts) transmitted through absorbing foils of thickness D (in mg/cm^2) versus wavelength (in Å).

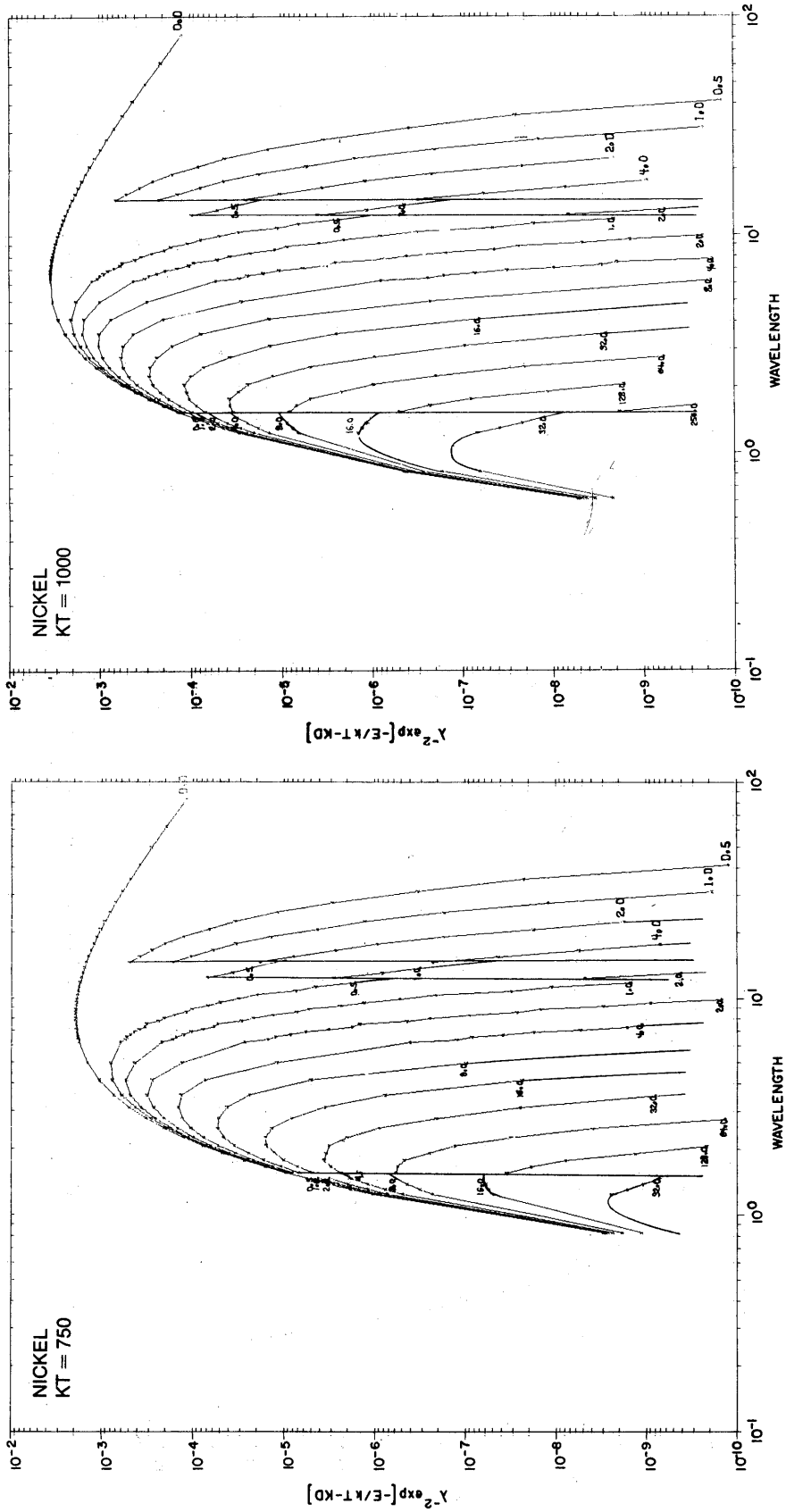

Fig. 14 - Relative bremsstrahlung emission at a temperature kT (in electron volts) transmitted through absorbing foils of thickness D (in mg/cm^2) versus wavelength (in Å) (Continued).

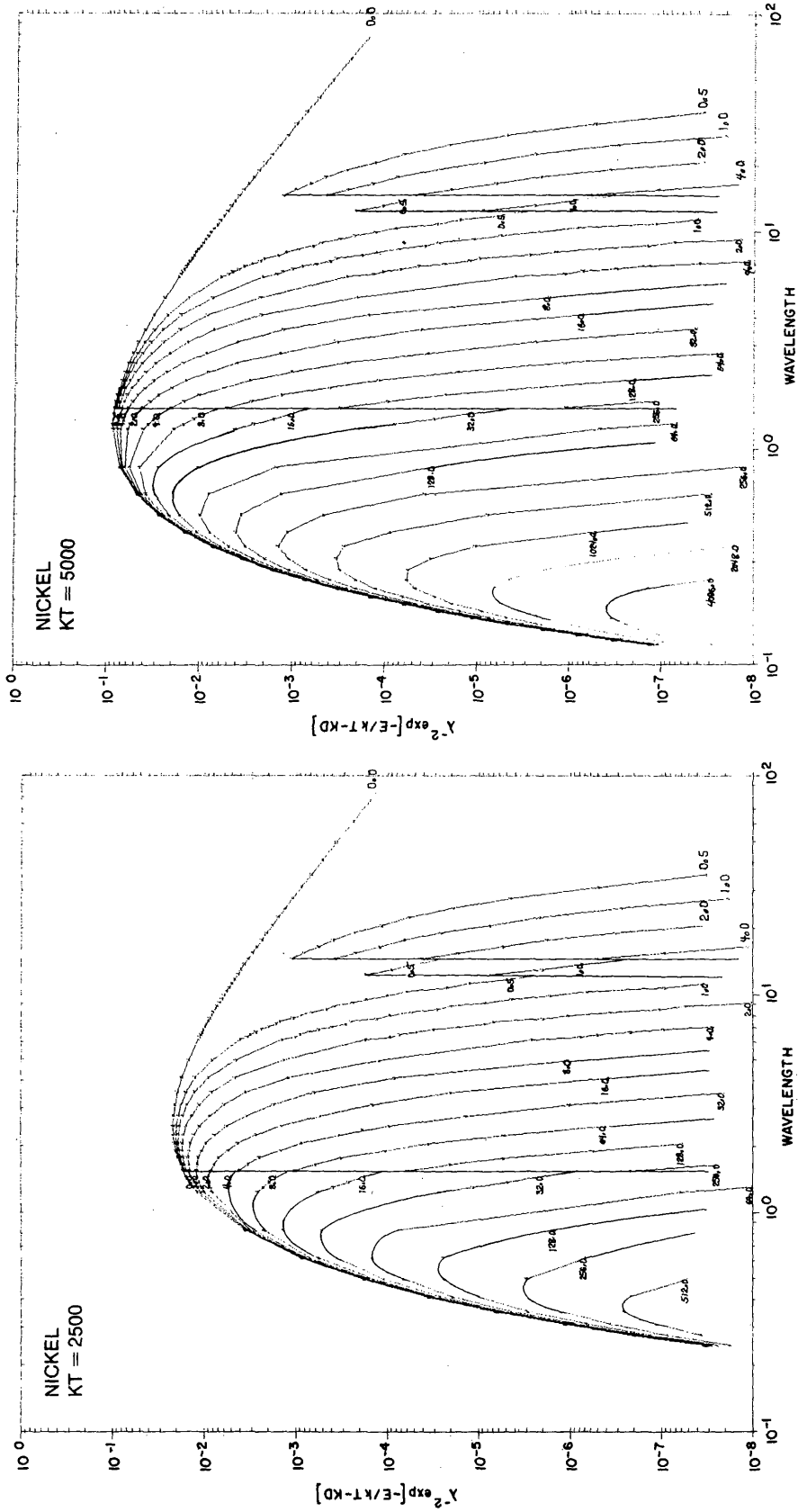

Fig. 15 - Relative bremsstrahlung emission at a temperature kT (in electron volts) transmitted through absorbing foils of thickness D (in mg/cm^2) versus wavelength (in Å).

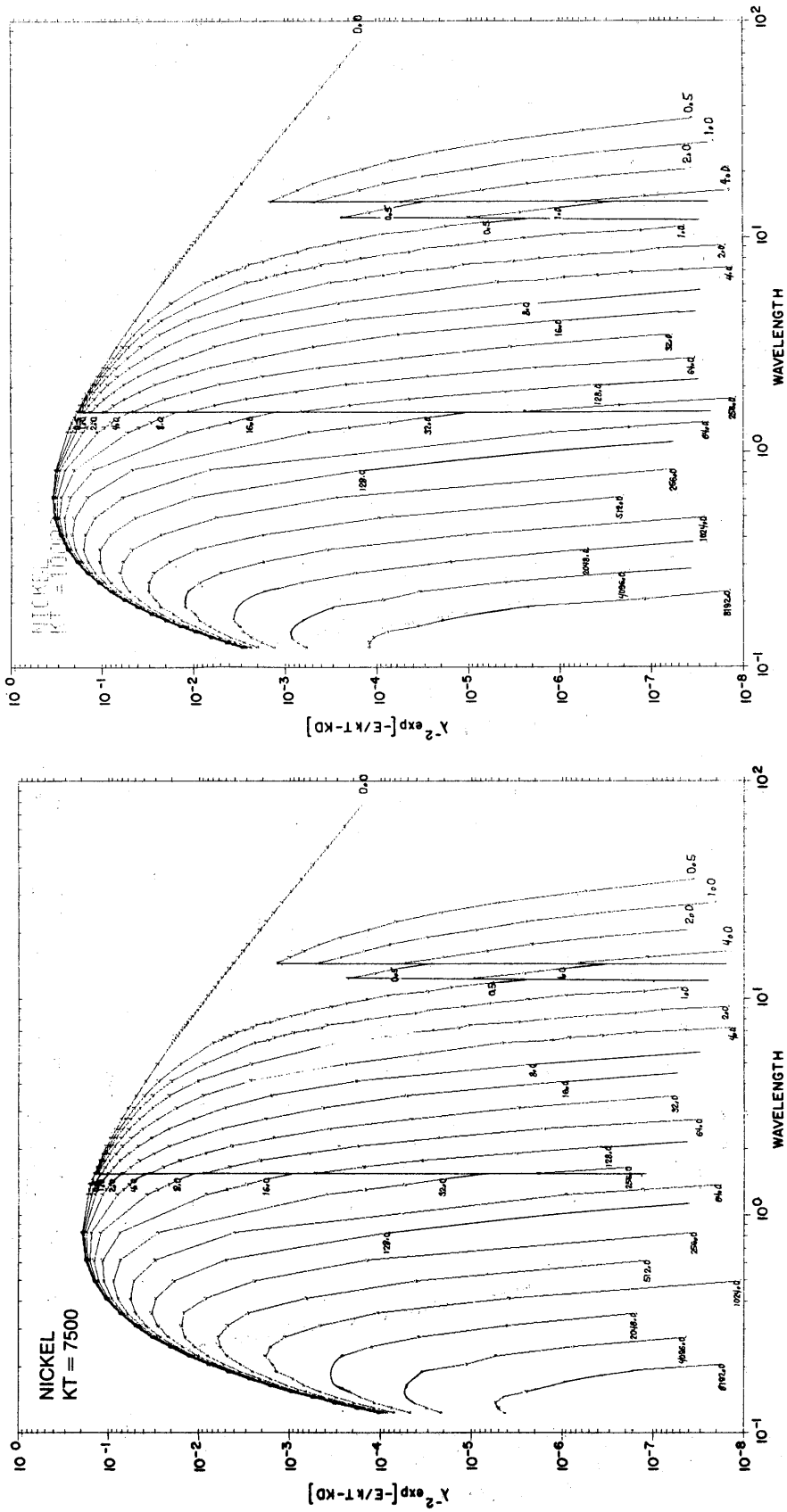

Fig. 15 - Relative bremsstrahlung emission at a temperature kT (in electron volts) transmitted through absorbing foils of thickness D (in mg/cm^2) versus wavelength (in Å) (Continued).

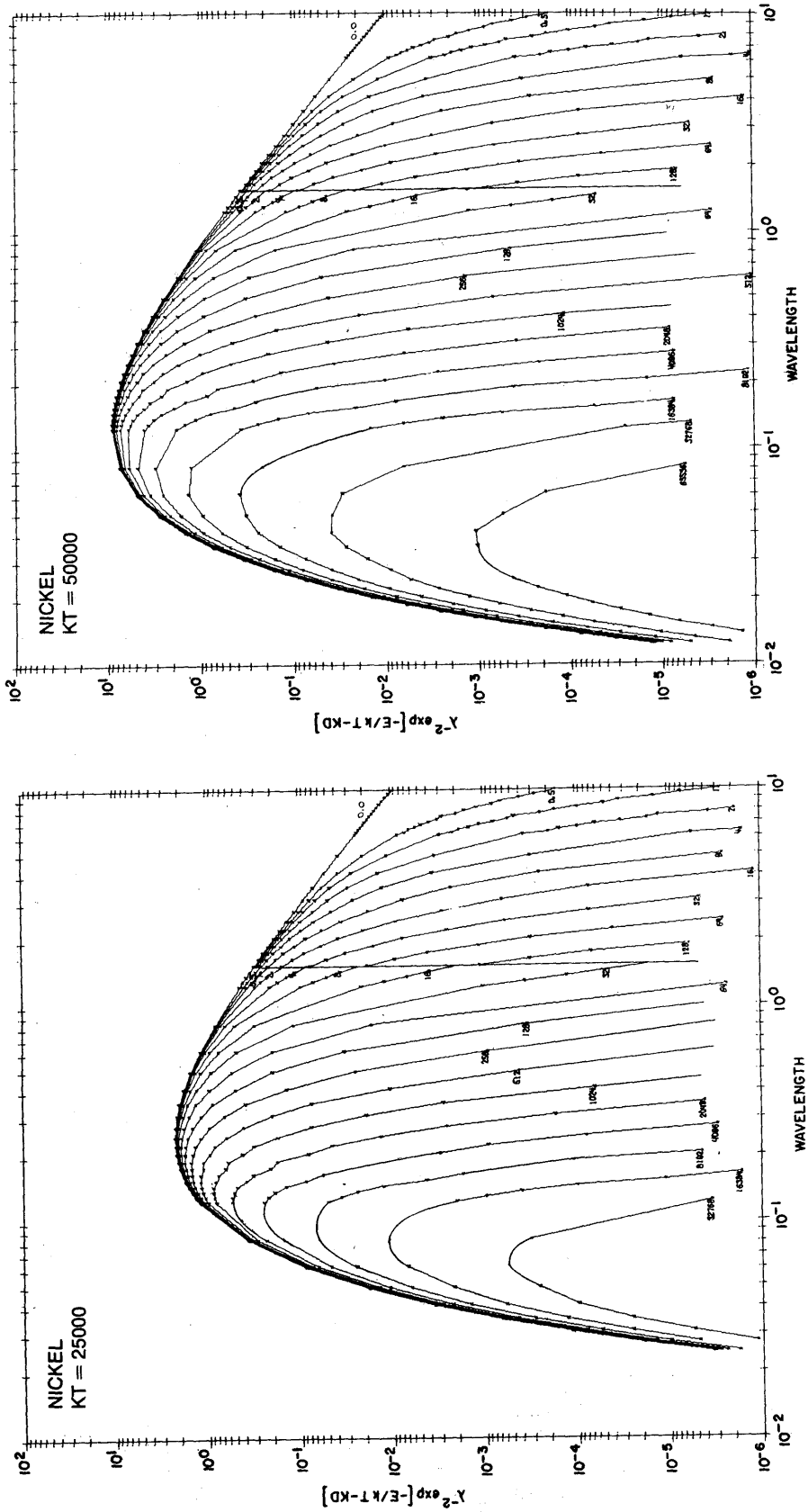

Fig. 16 - Relative bremsstrahlung emission at a temperature kT (in electron volts) transmitted through absorbing foils of thickness D (in mg/cm^2) versus wavelength (in Å).

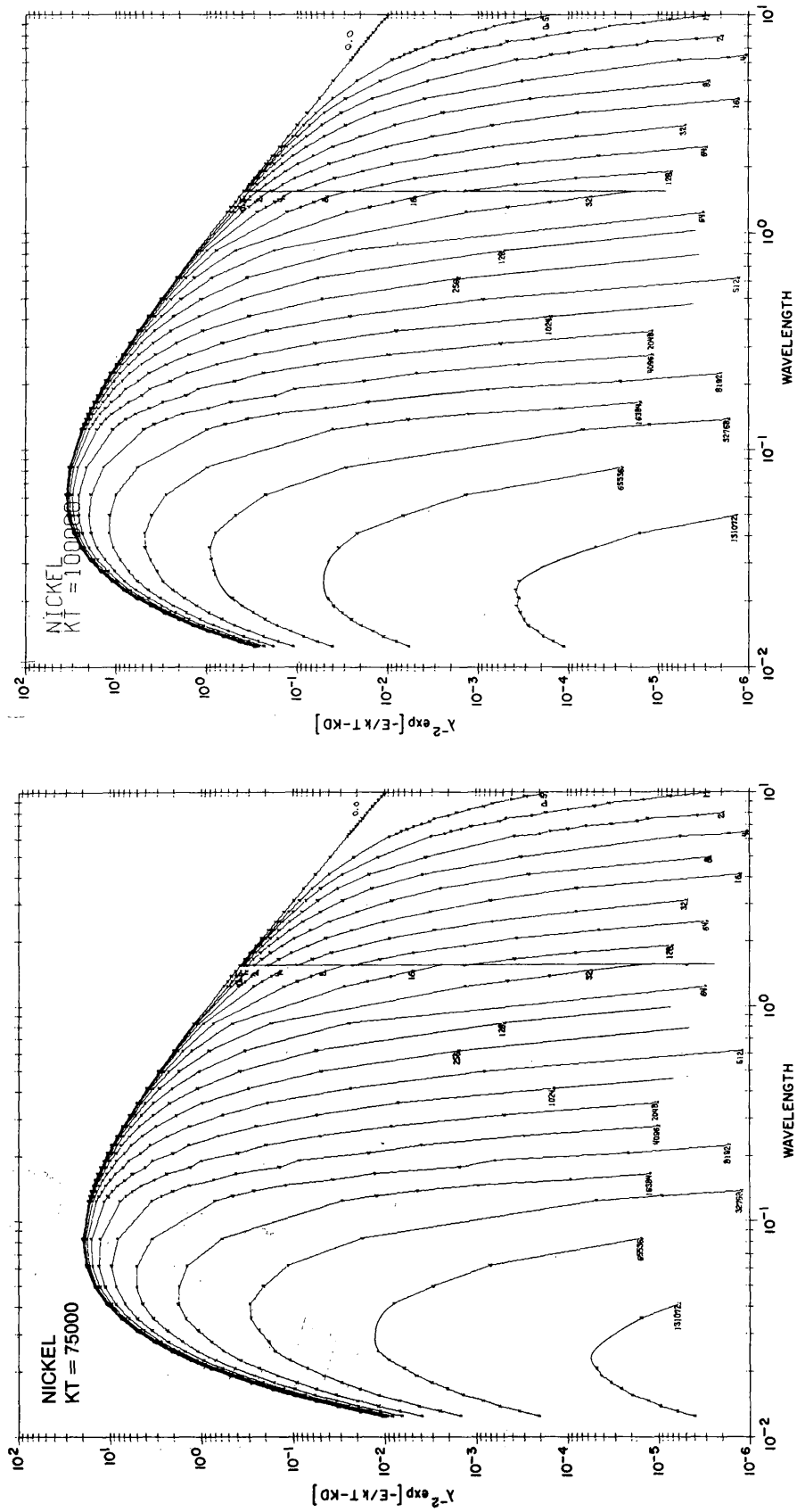

Fig. 16 - Relative bremsstrahlung emission at a temperature kT (in electron volts) transmitted through absorbing foils of thickness D (in mg/cm^2) versus wavelength (in Å) (Continued).

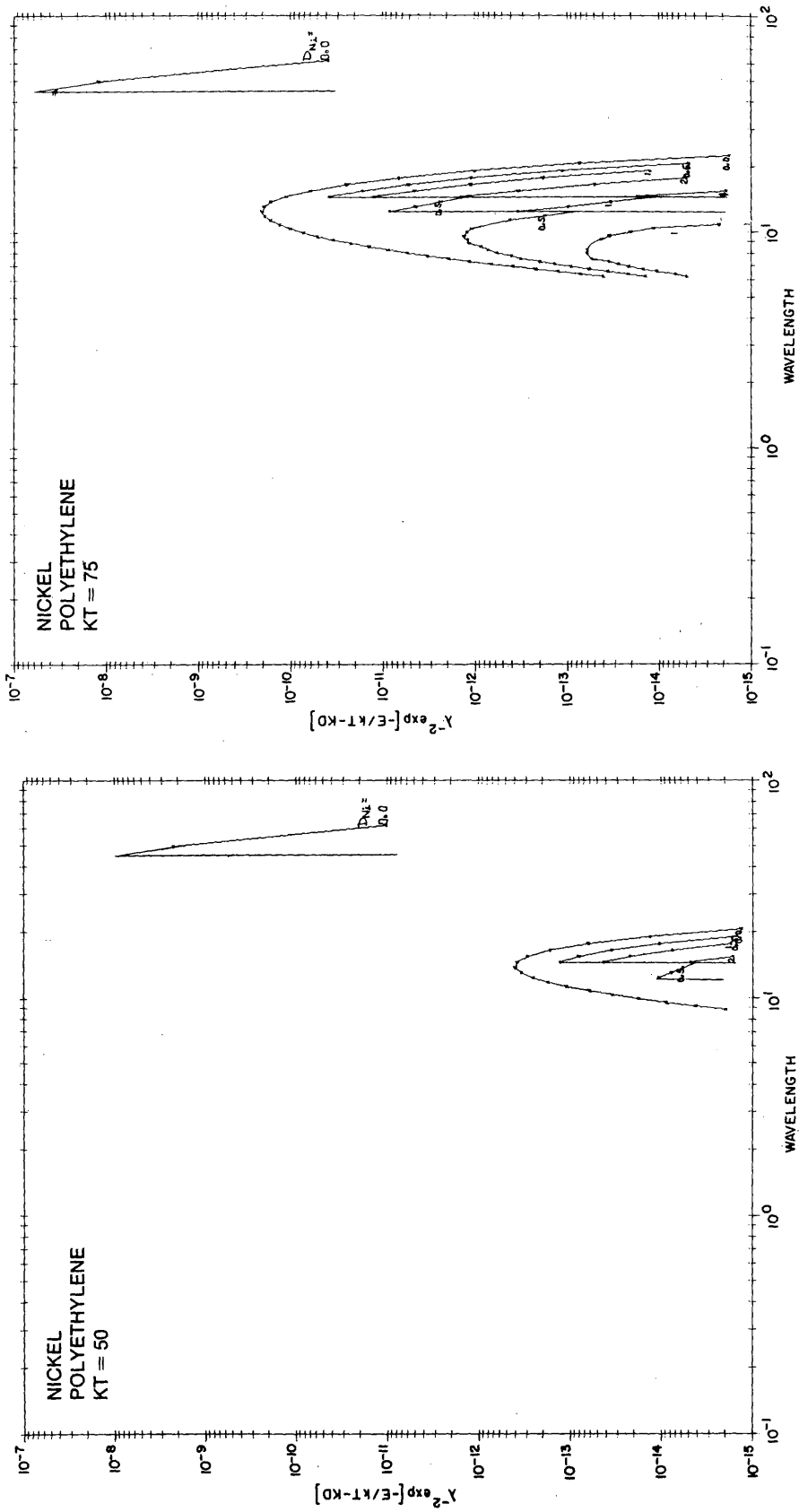

Fig. 17 - Relative bremsstrahlung emission at a temperature kT (in electron volts) transmitted through absorbing foils of thickness D (in mg/cm^2) versus wavelength (in Å). Polyethylene thickness 0.001 inches (2.3 mg/cm^2).

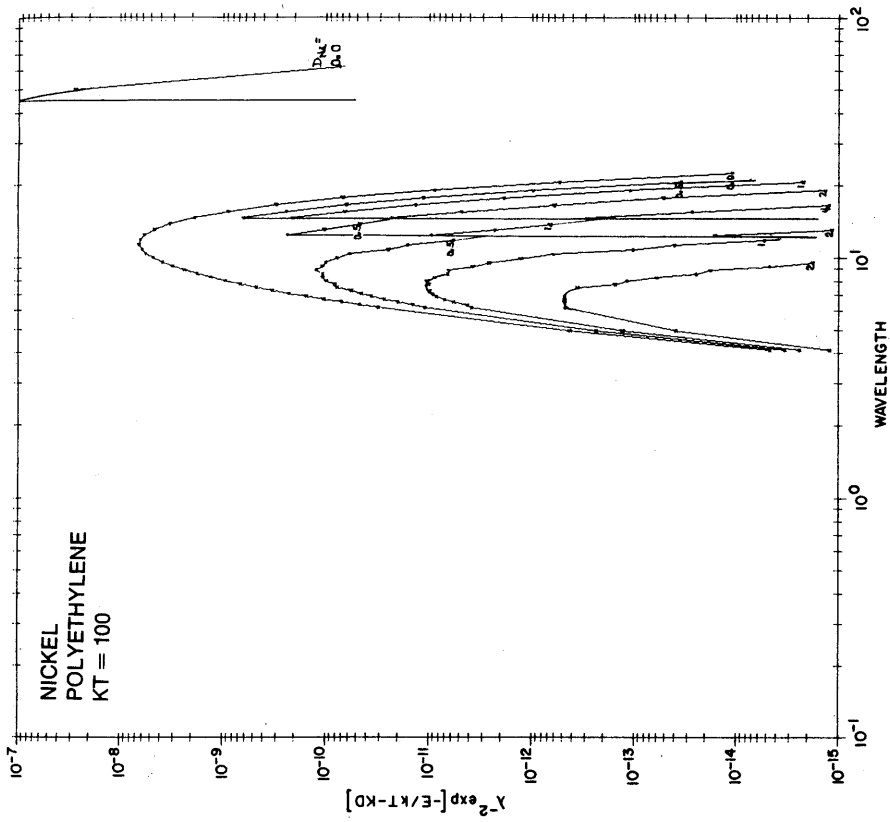

Fig. 17 - Relative bremsstrahlung emission at a temperature kT (in electron volts) transmitted through absorbing foils of thickness D (in mg/cm^2) versus wavelength (in Å) (Continued). Polyethylene thickness 0.001 inches (2.3 mg/cm^2).

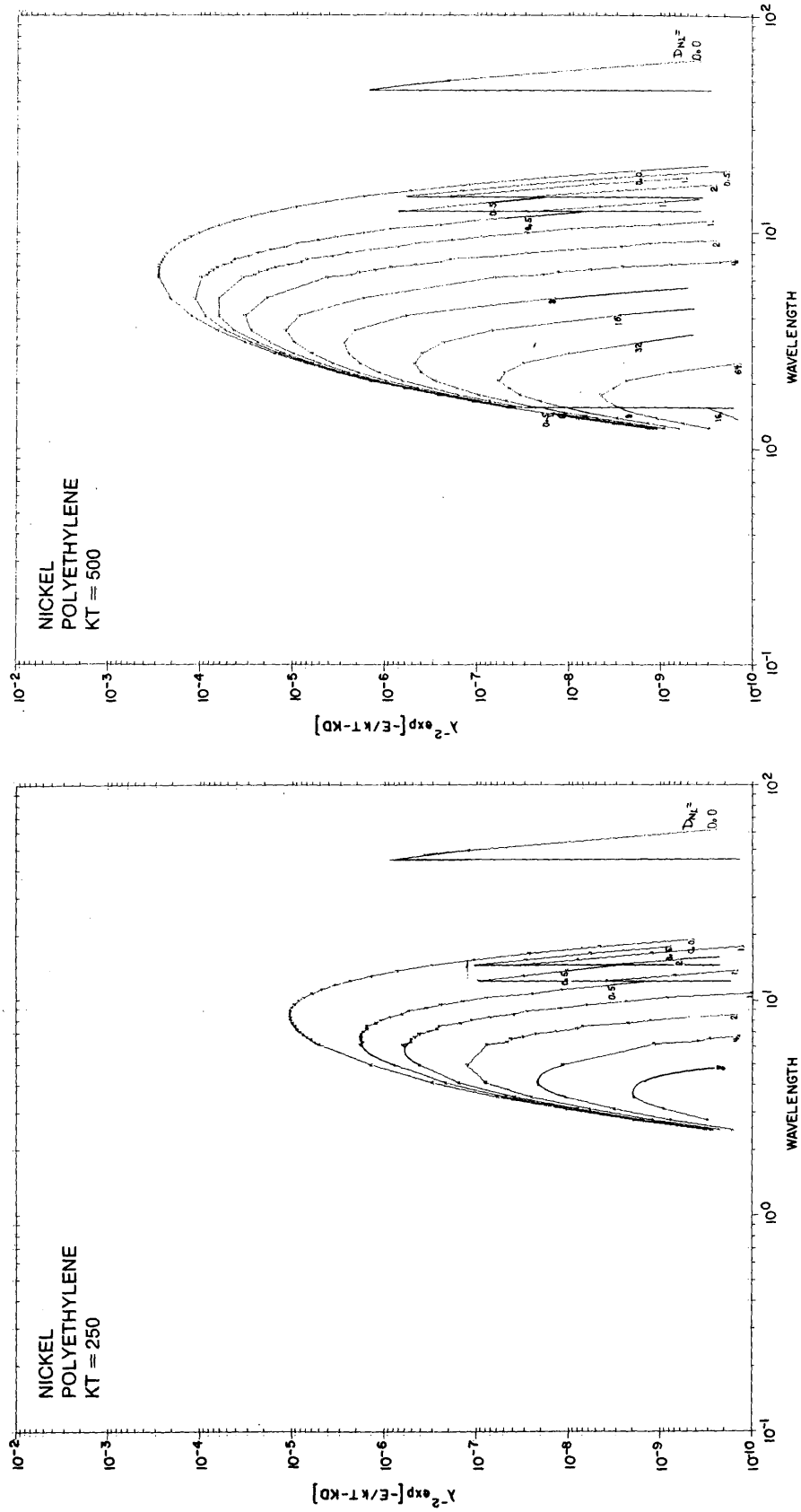

Fig. 18 - Relative bremsstrahlung emission at a temperature kT (in electron volts) transmitted through absorbing foils of thickness D (in mg/cm^2) versus wavelength (in Å). Polyethylene thickness 0.001 inches (2.3 mg/cm^2).

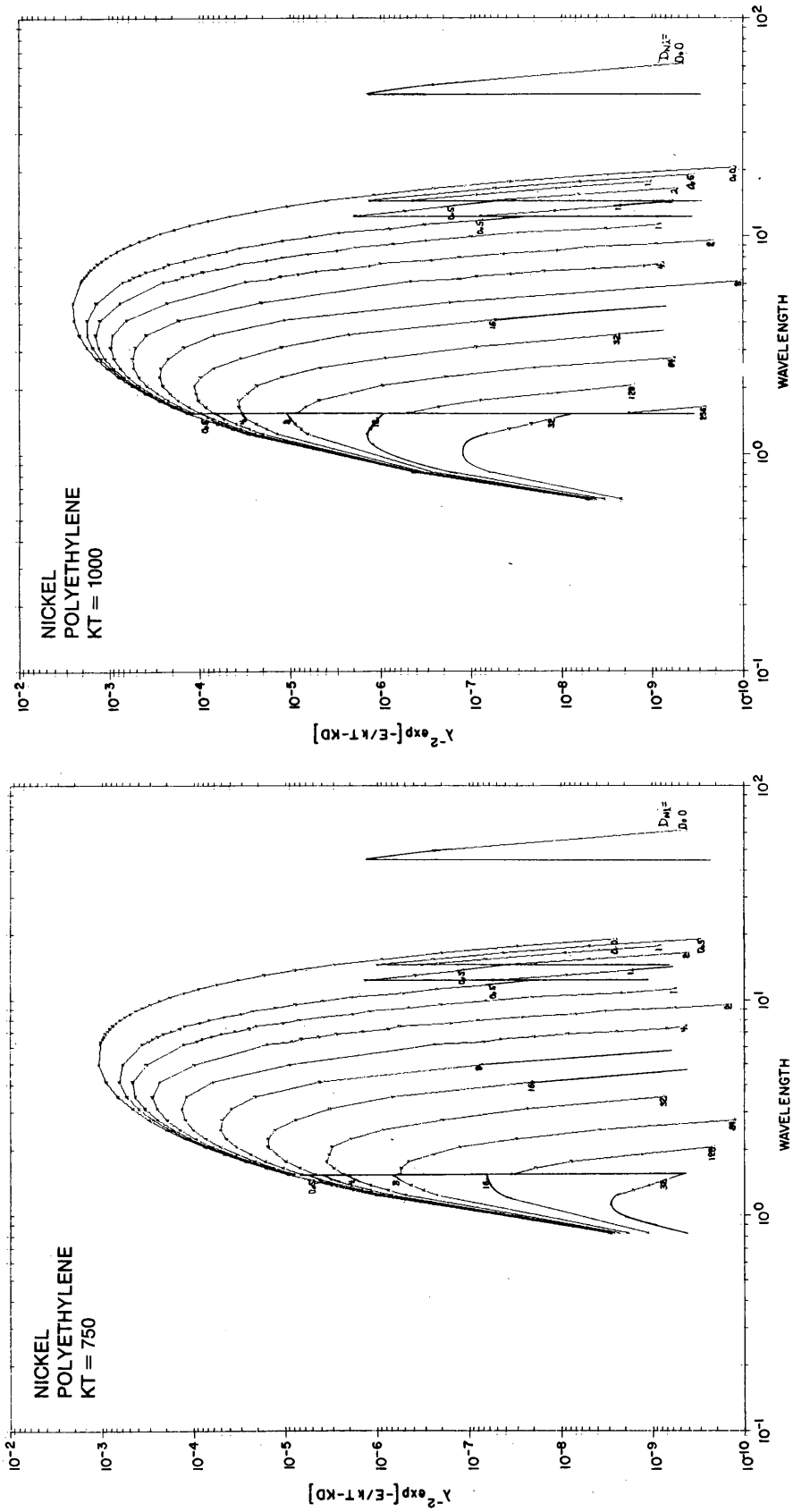

Fig. 18 - Relative bremsstrahlung emission at a temperature kT (in electron volts) transmitted through absorbing foils of thickness D (in mg/cm^2) versus wavelength (in Å) (Continued). Polyethylene thickness 0.001 inches (2.3 mg/cm^2).

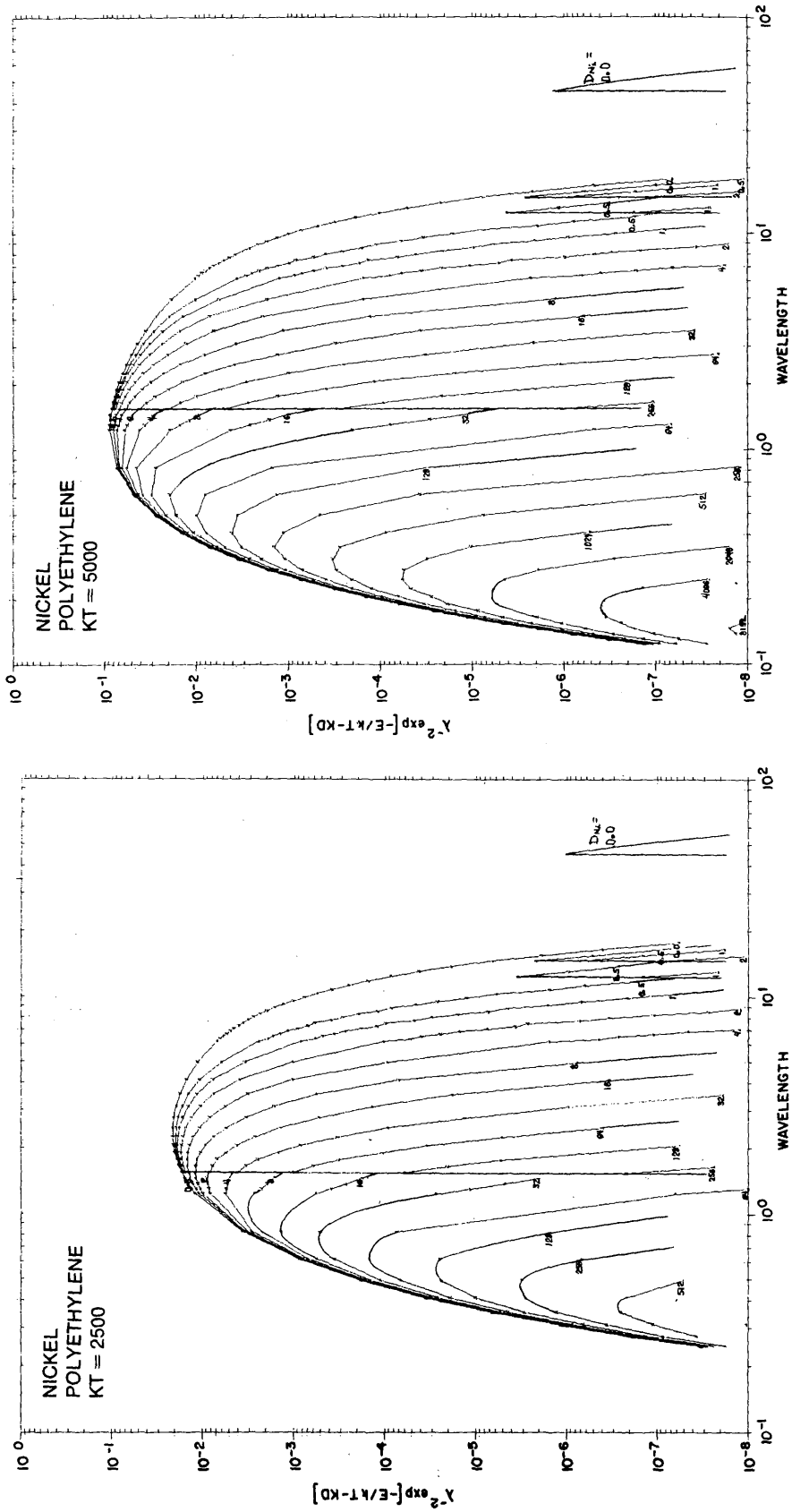

Fig. 19 - Relative bremsstrahlung emission at a temperature kT (in electron volts) transmitted through absorbing foils of thickness D (in mg/cm^2) versus wavelength (in Å). Polyethylene thickness 0.001 inches (2.3 mg/cm^2).

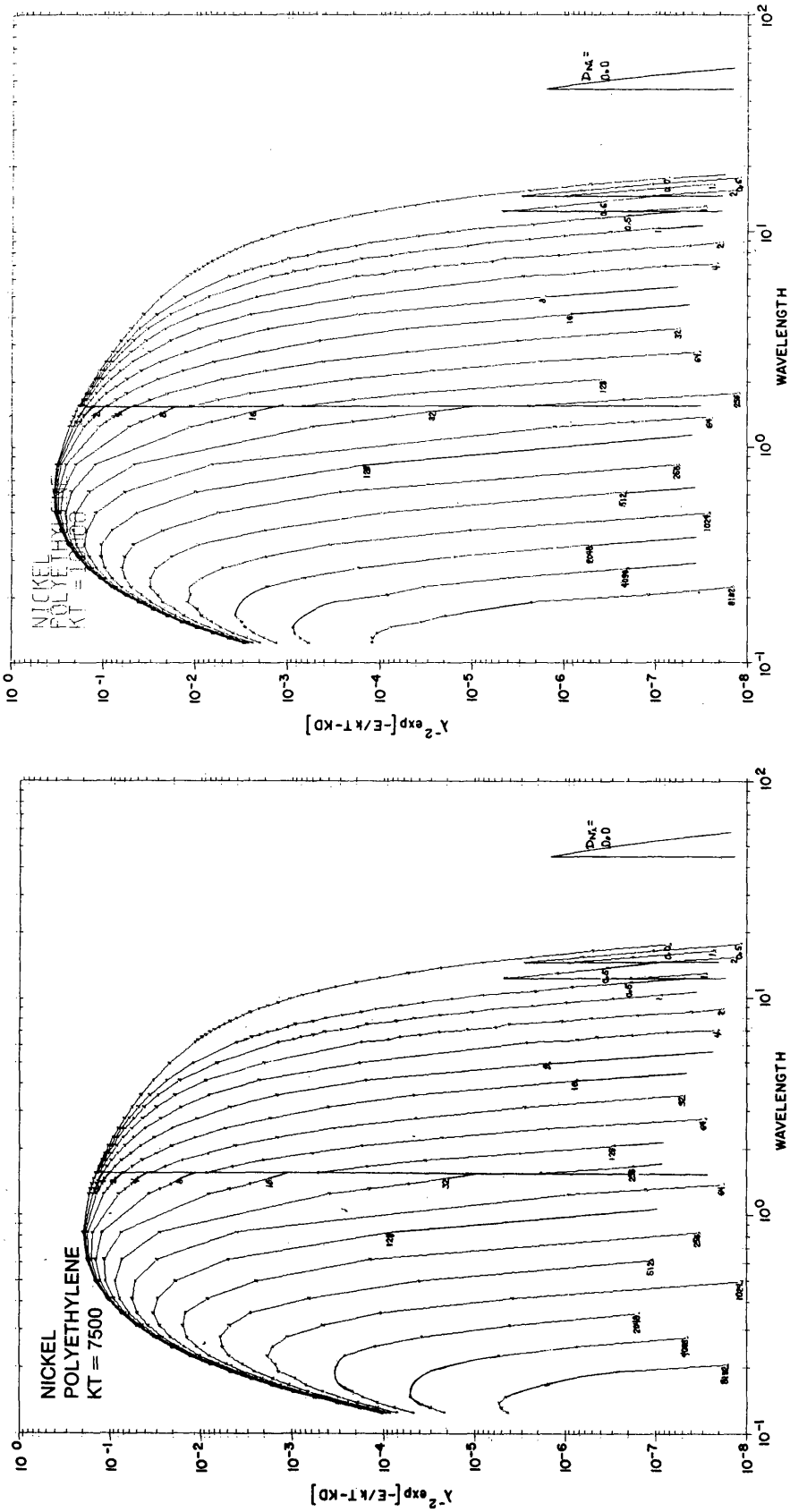

Fig. 19 - Relative bremsstrahlung emission at a temperature kT (in electron volts) transmitted through absorbing foils of thickness D (in mg/cm^2) versus wavelength (in Å) (Continued). Polyethylene thickness 0.001 inches (2.3 mg/cm^2).

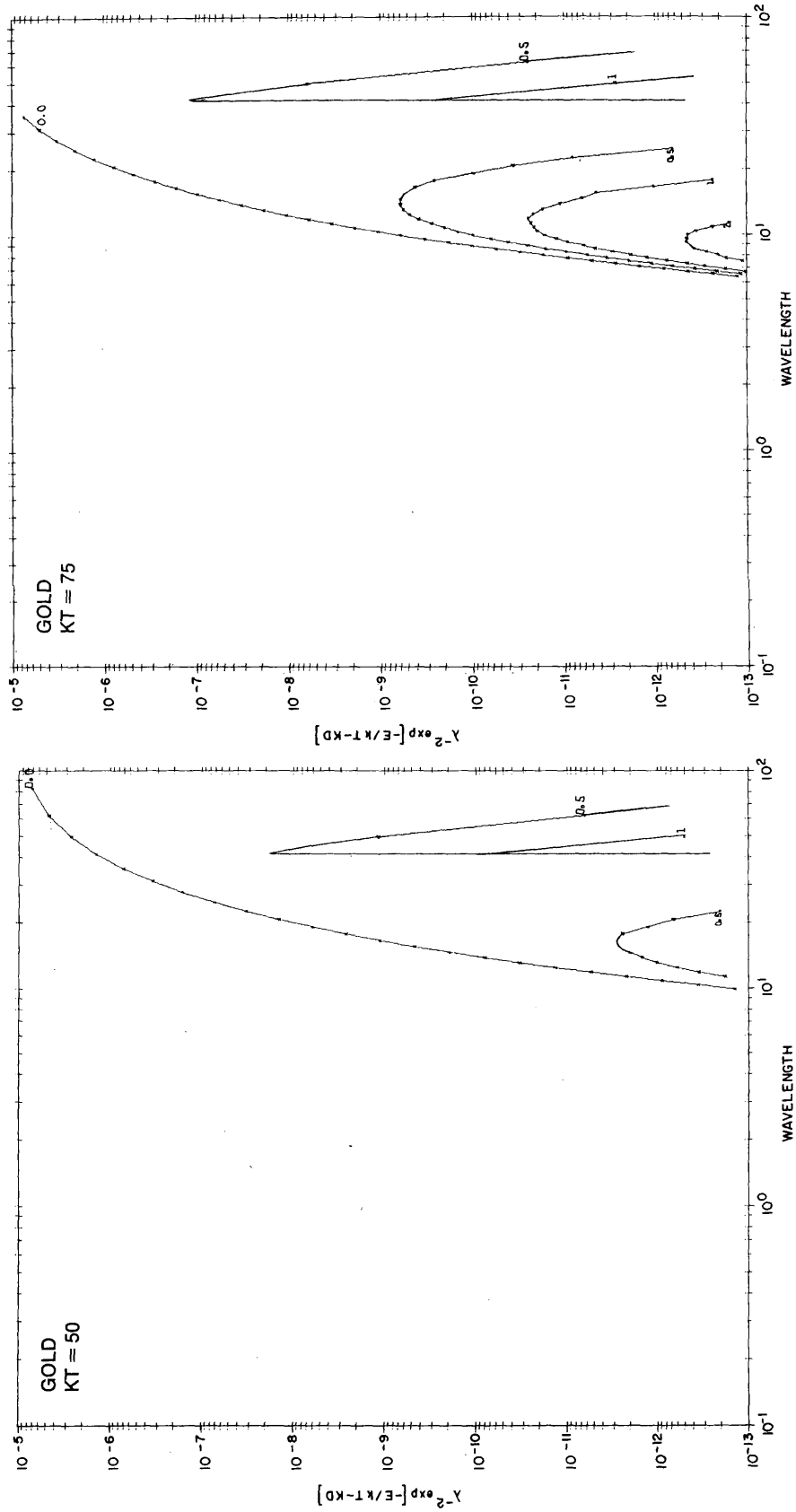

Fig. 20 - Relative bremsstrahlung emission at a temperature kT (in electron volts) transmitted through absorbing foils of thickness D (in mg/cm^2) versus wavelength (in Å).

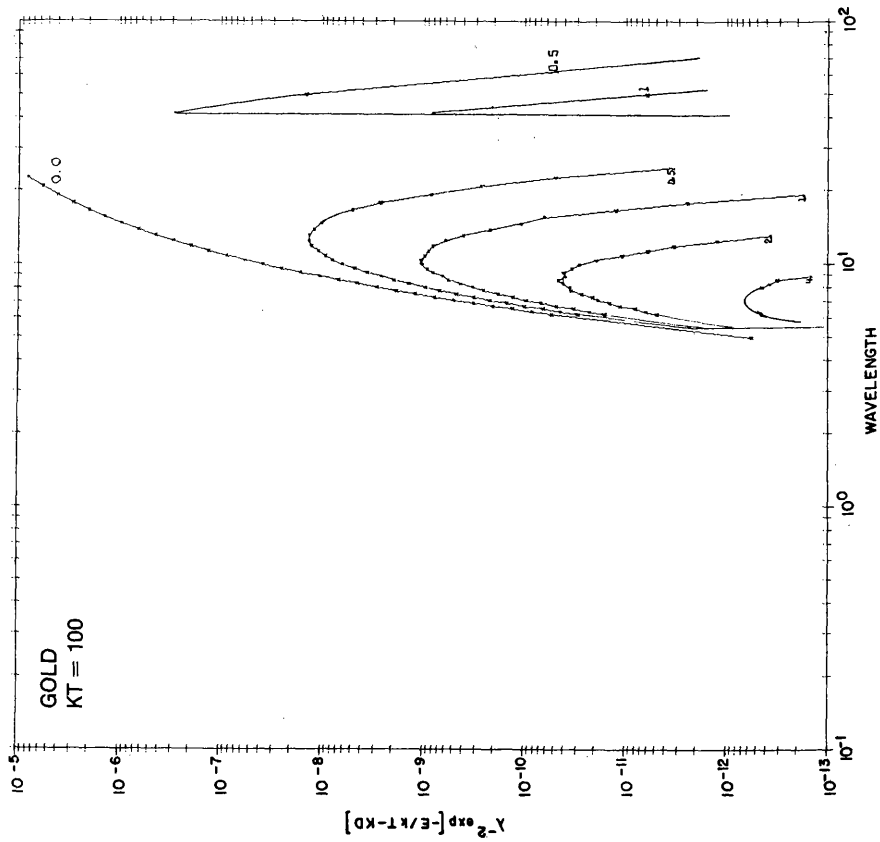

Fig. 20 - Relative bremsstrahlung emission at a temperature kT (in electron volts) transmitted through absorbing foils of thickness D (in mg/cm^2) versus wavelength (in Å) (Continued).

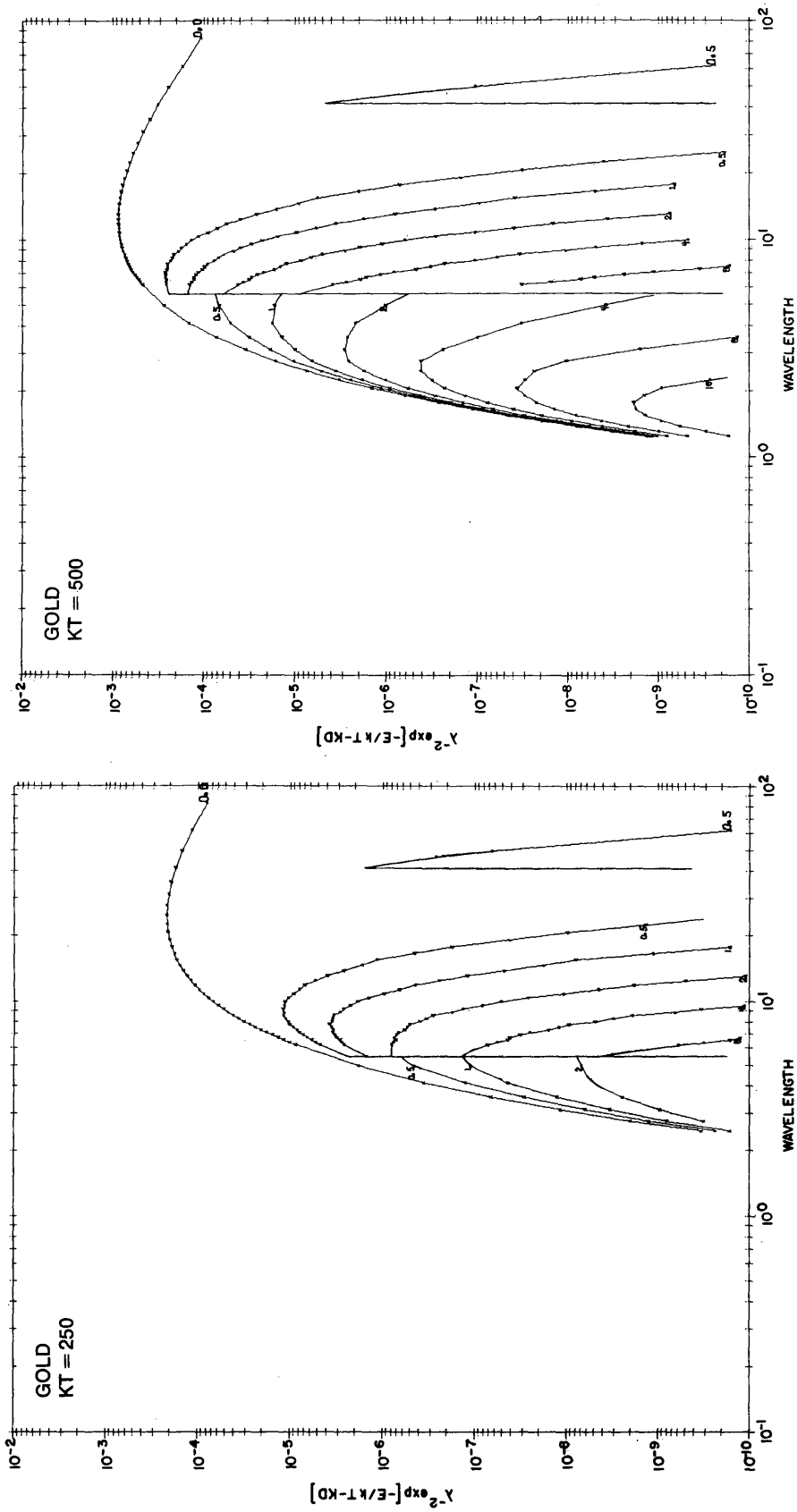

Fig. 21 - Relative bremsstrahlung emission at a temperature kT (in electron volts) transmitted through absorbing foils of thickness D (in mg/cm^2) versus wavelength (in Å).

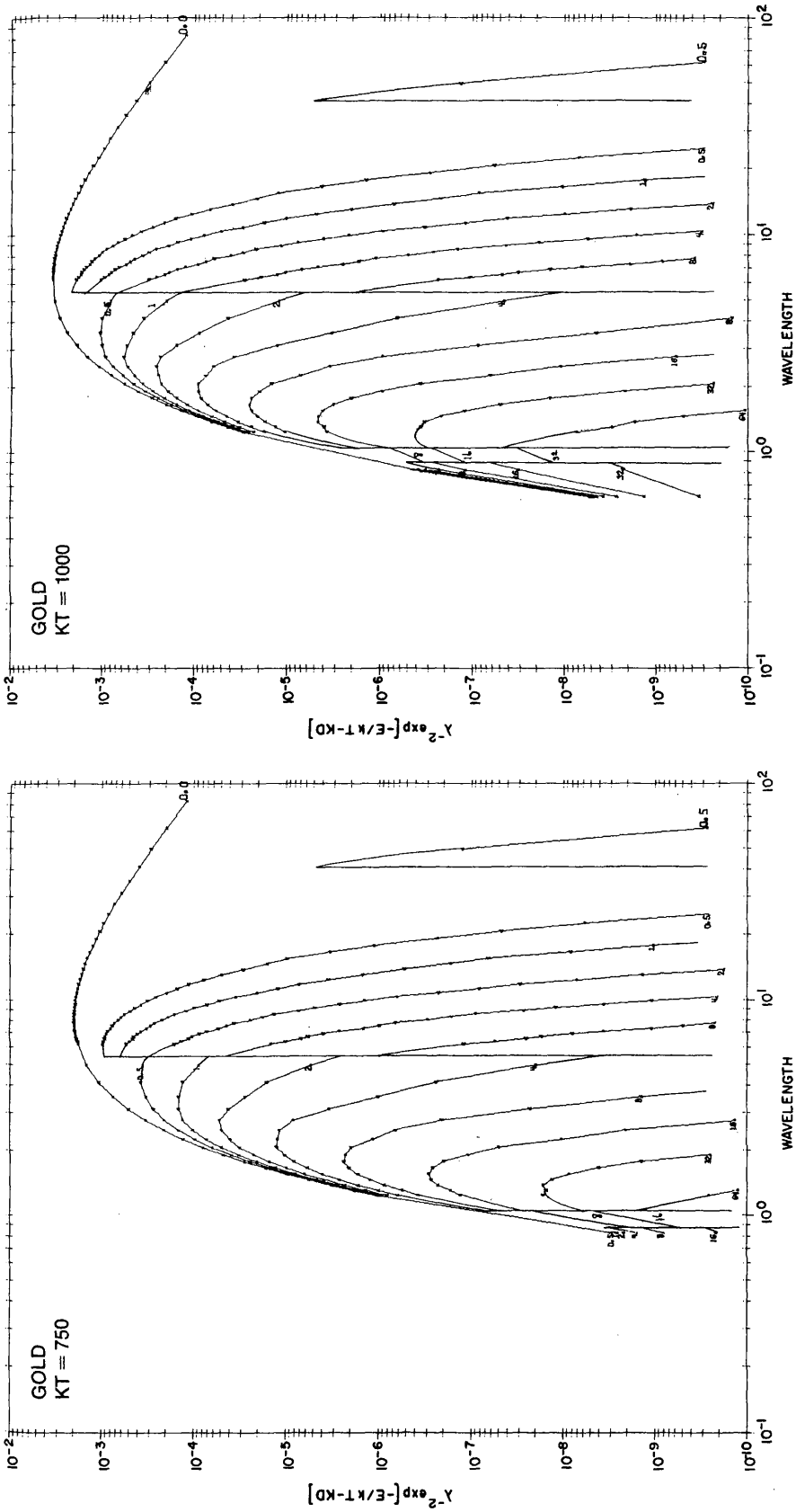

Fig. 21 - Relative bremsstrahlung emission at a temperature kT (in electron volts) transmitted through absorbing foils of thickness D (in mg/cm^2) versus wavelength (in Å) (Continued).

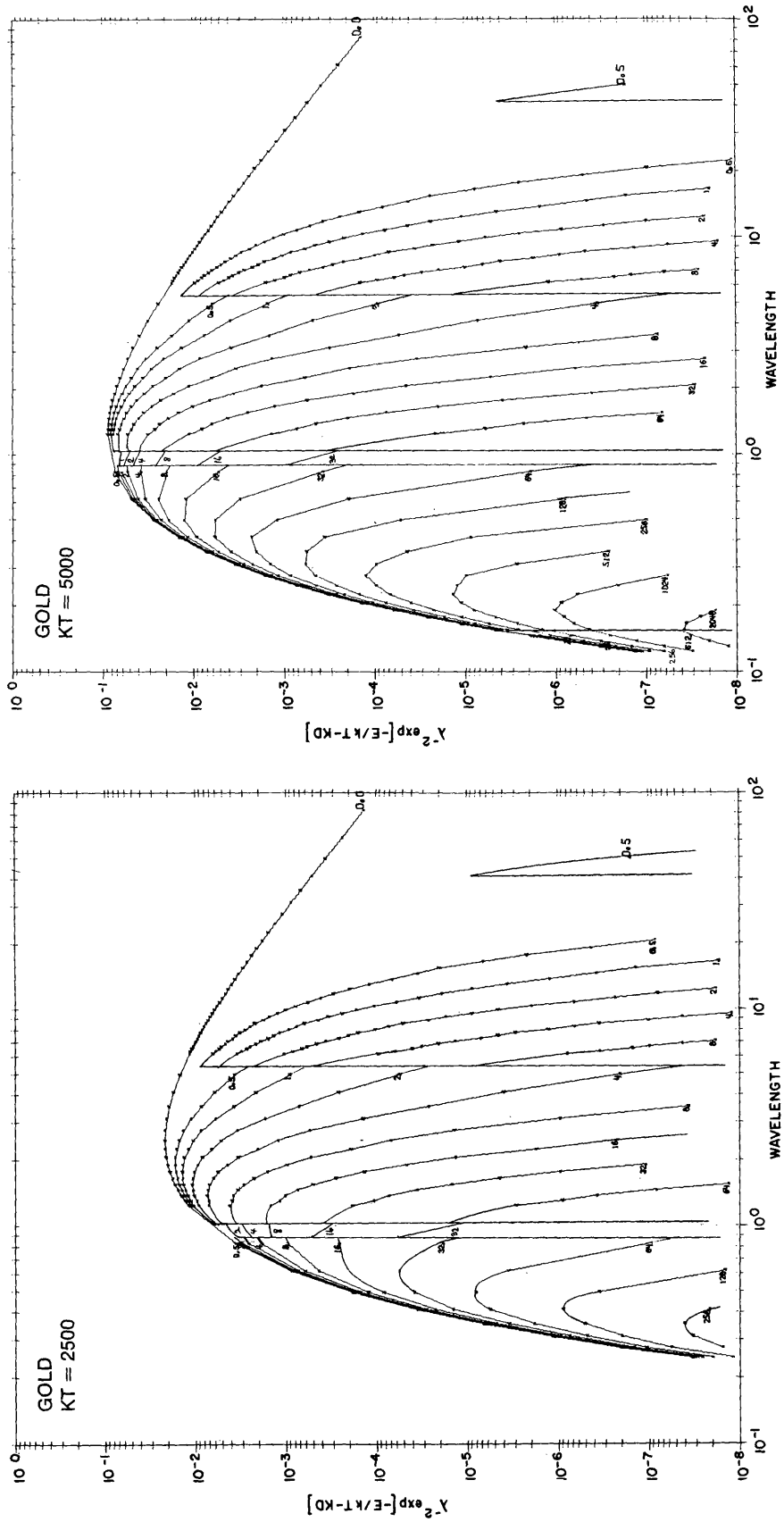

Fig. 22 - Relative bremsstrahlung emission at a temperature kT (in electron volts) transmitted through absorbing foils of thickness D (in mg/cm^2) versus wavelength (in Å).

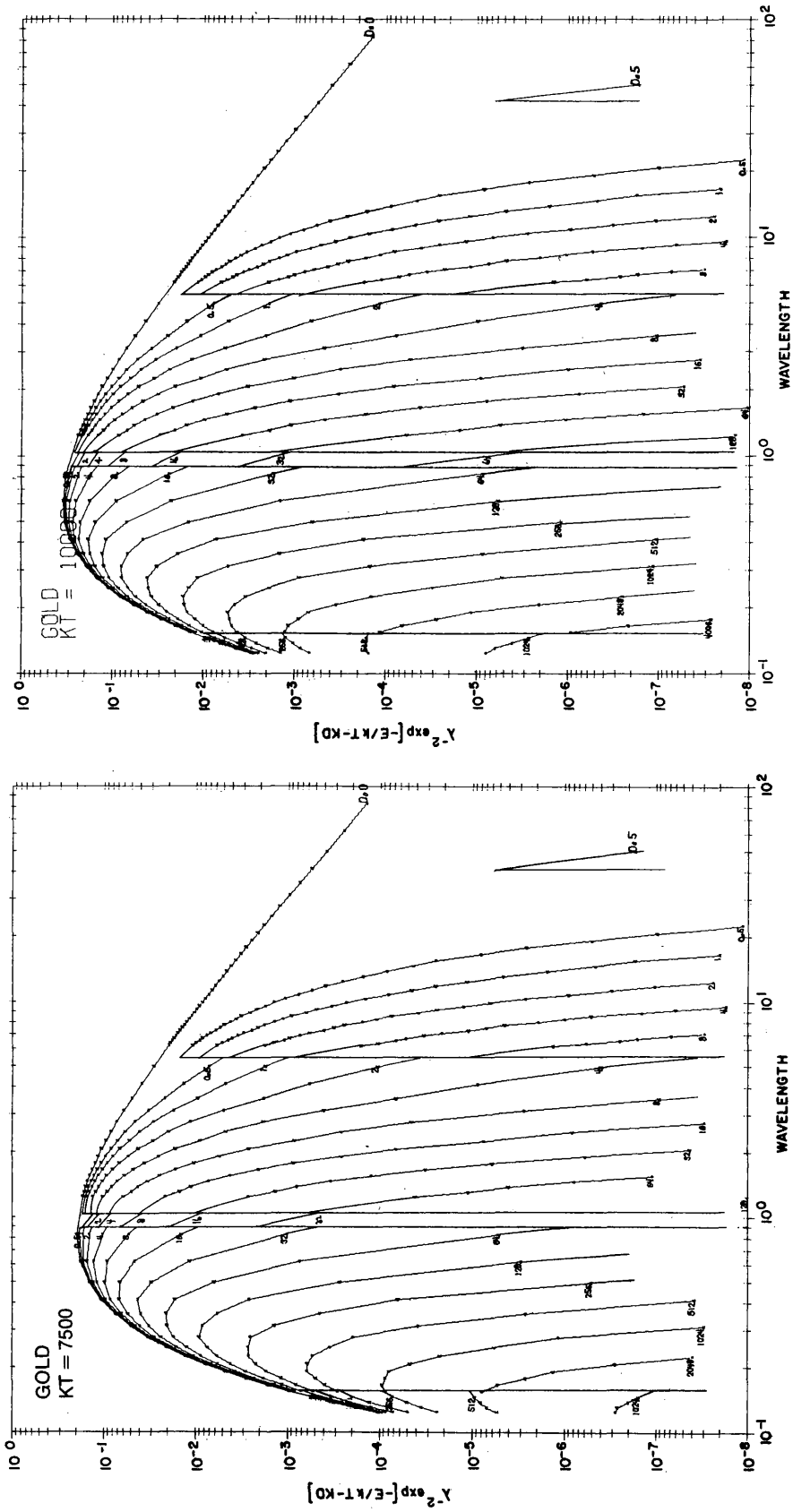

Fig. 22 - Relative bremsstrahlung emission at a temperature kT (in electron volts) transmitted through absorbing foils of thickness D (in mg/cm^2) versus wavelength (in Å) (Continued).

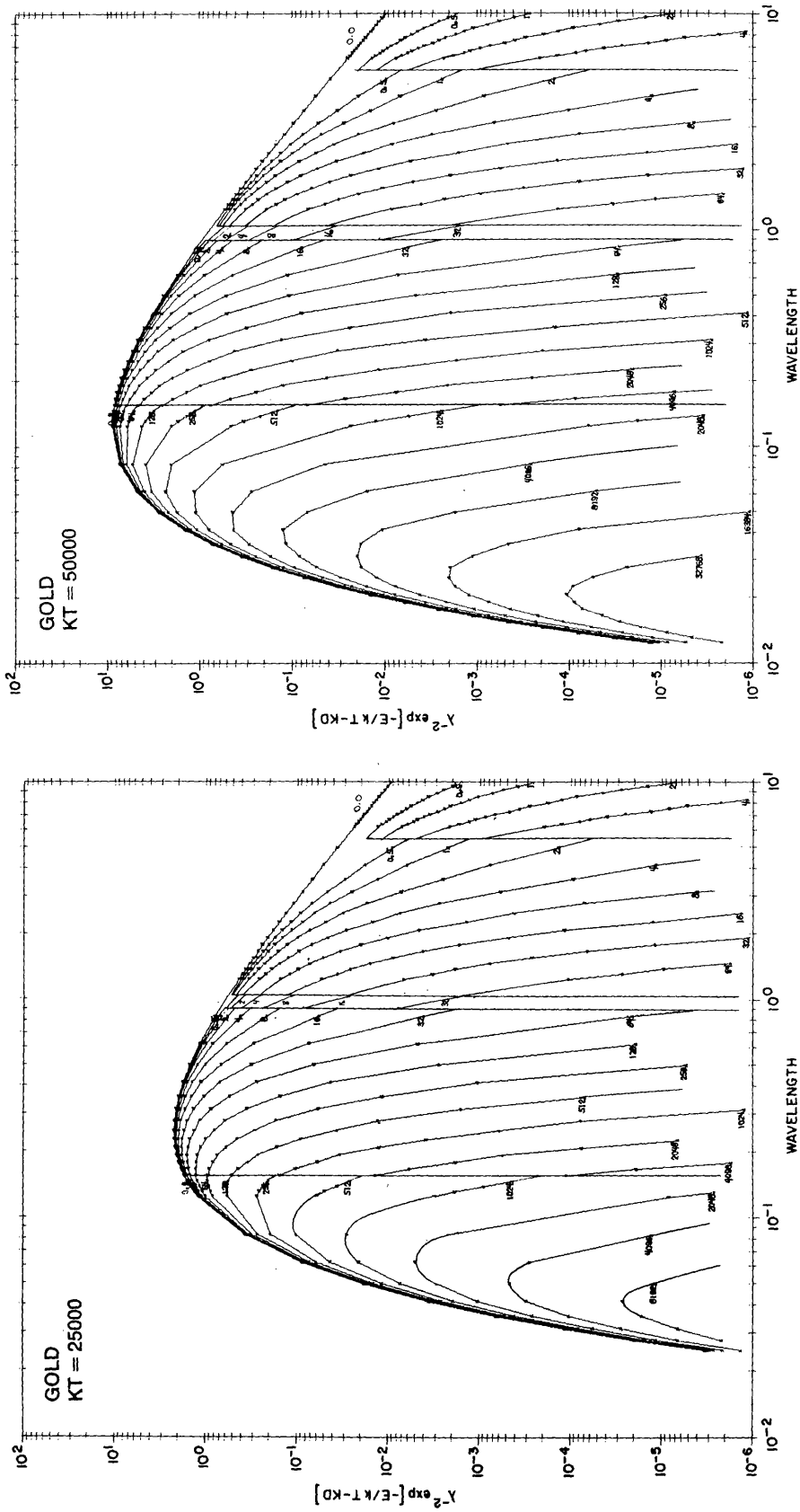

Fig. 23 - Relative bremsstrahlung emission at a temperature kT (in electron volts) transmitted through absorbing foils of thickness D (in mg/cm^2) versus wavelength (in Å).

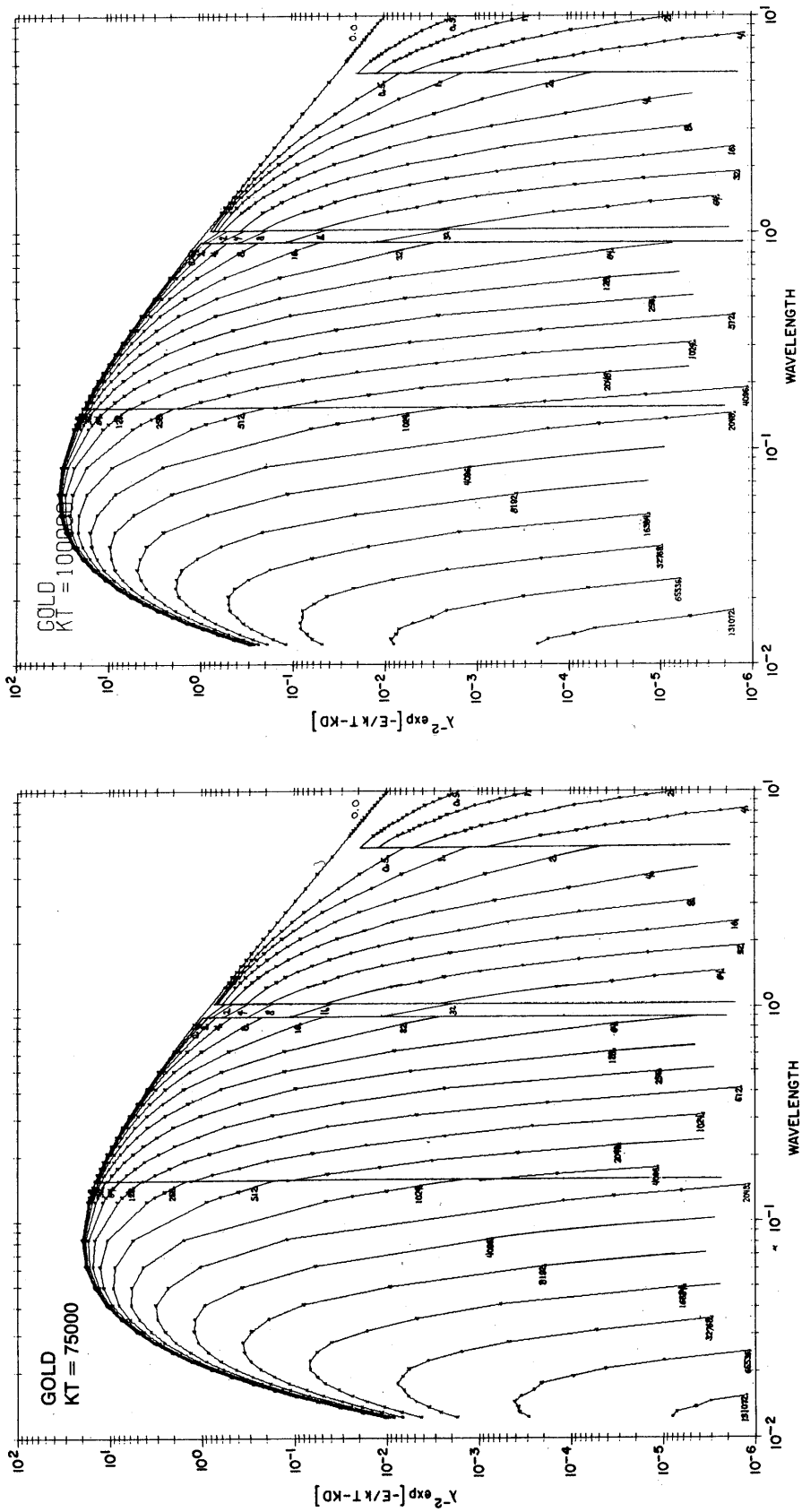

Fig. 23 - Relative bremsstrahlung emission at a temperature kT (in electron volts) transmitted through absorbing foils of thickness D (in mg/cm^2) versus wavelength (in Å) (Continued).

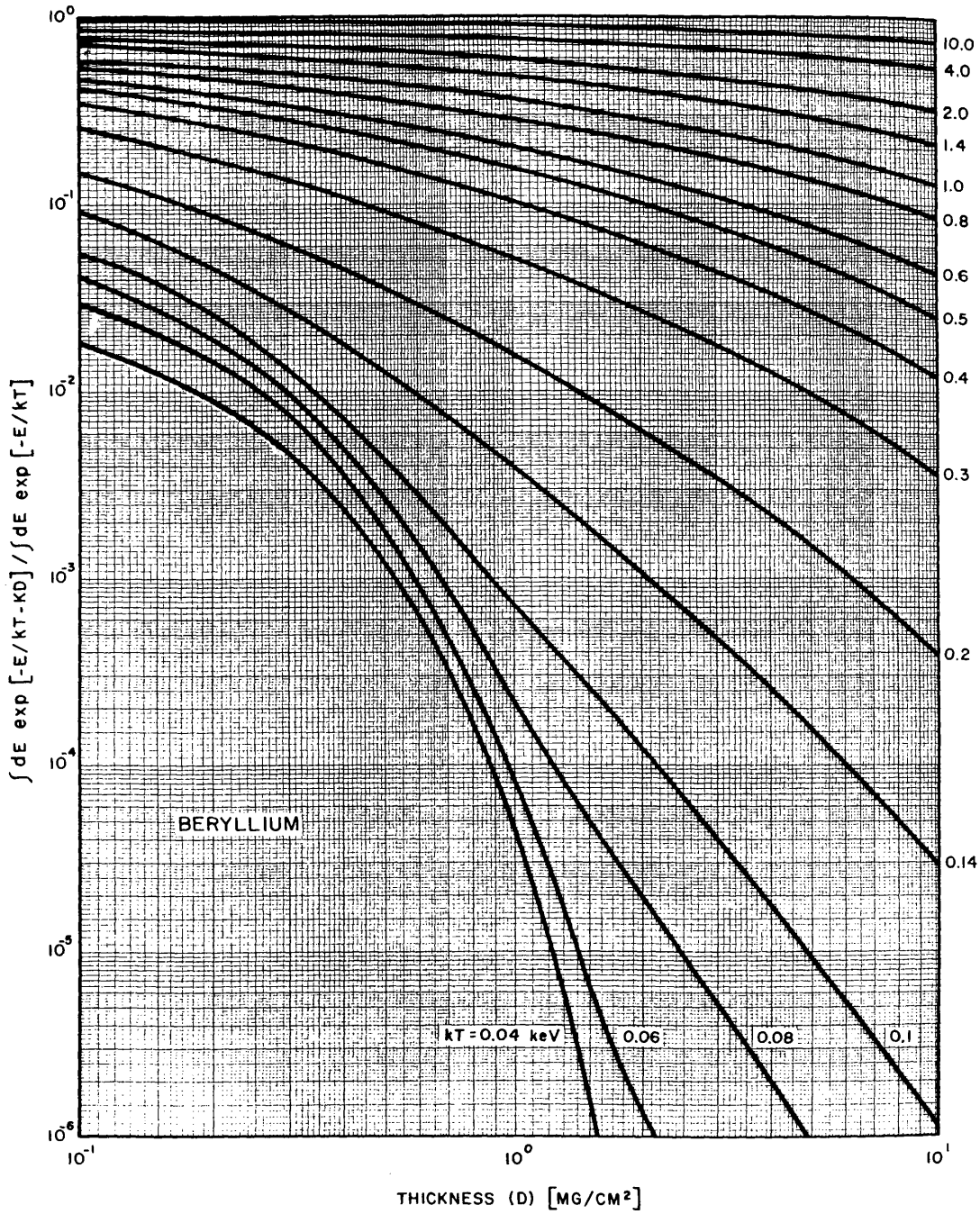

Fig. 24. Ratio of the integrated bremsstrahlung emission transmitted through foils of the designated material to the total incident flux versus foil thickness, D, for various temperatures. From this the ratio of ordinate values for two different thicknesses may be plotted versus temperature and used for plasma electron temperature determination; e.g., see Figs. 28 and 29 of Ref. 1.

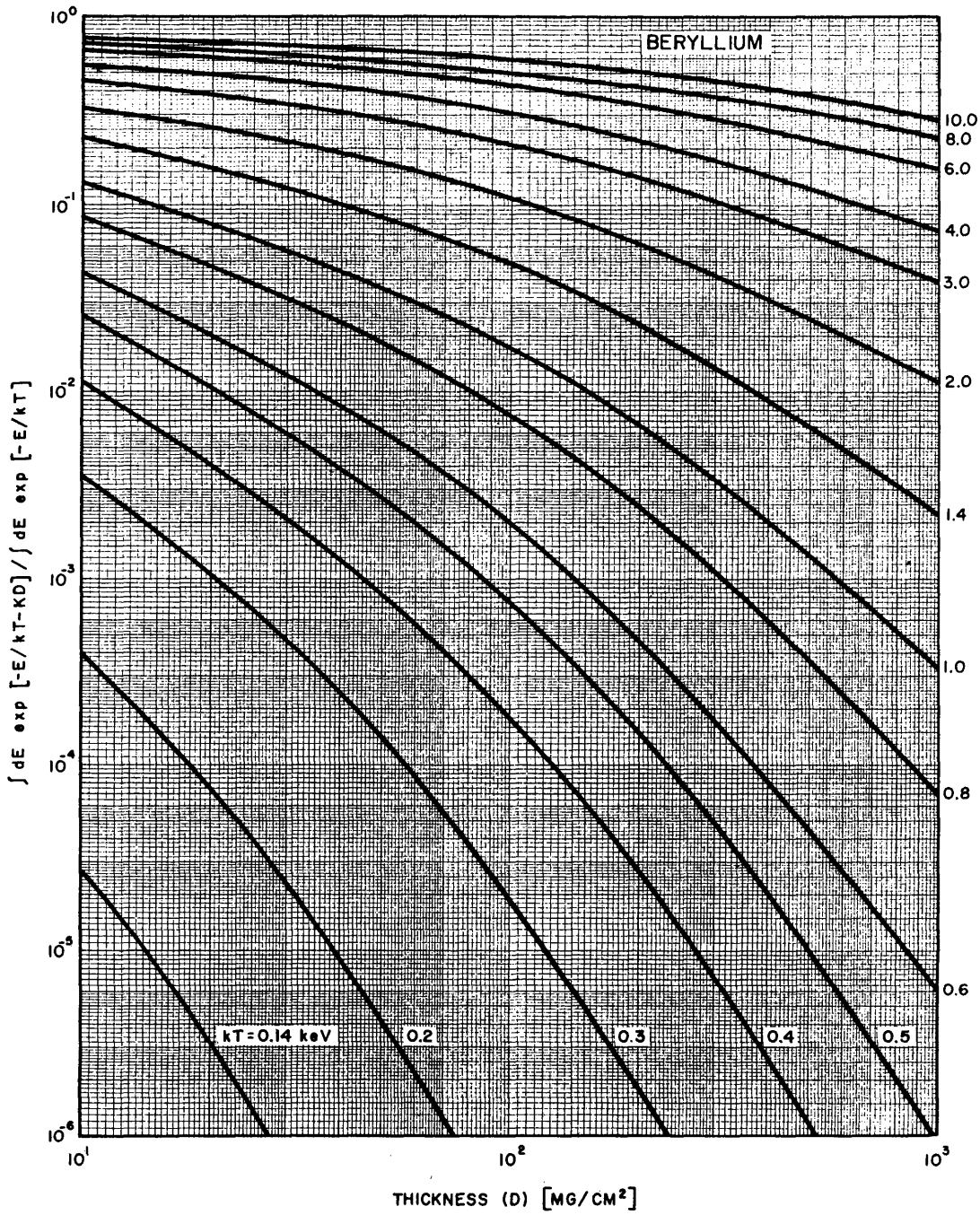

Fig. 25. Ratio of the integrated bremsstrahlung emission transmitted through foils of the designated material to the total incident flux versus foil thickness, D, for various temperatures. From this the ratio of ordinate values for two different thicknesses may be plotted versus temperature and used for plasma electron temperature determination; e.g., see Figs. 28 and 29 of Ref. 1.

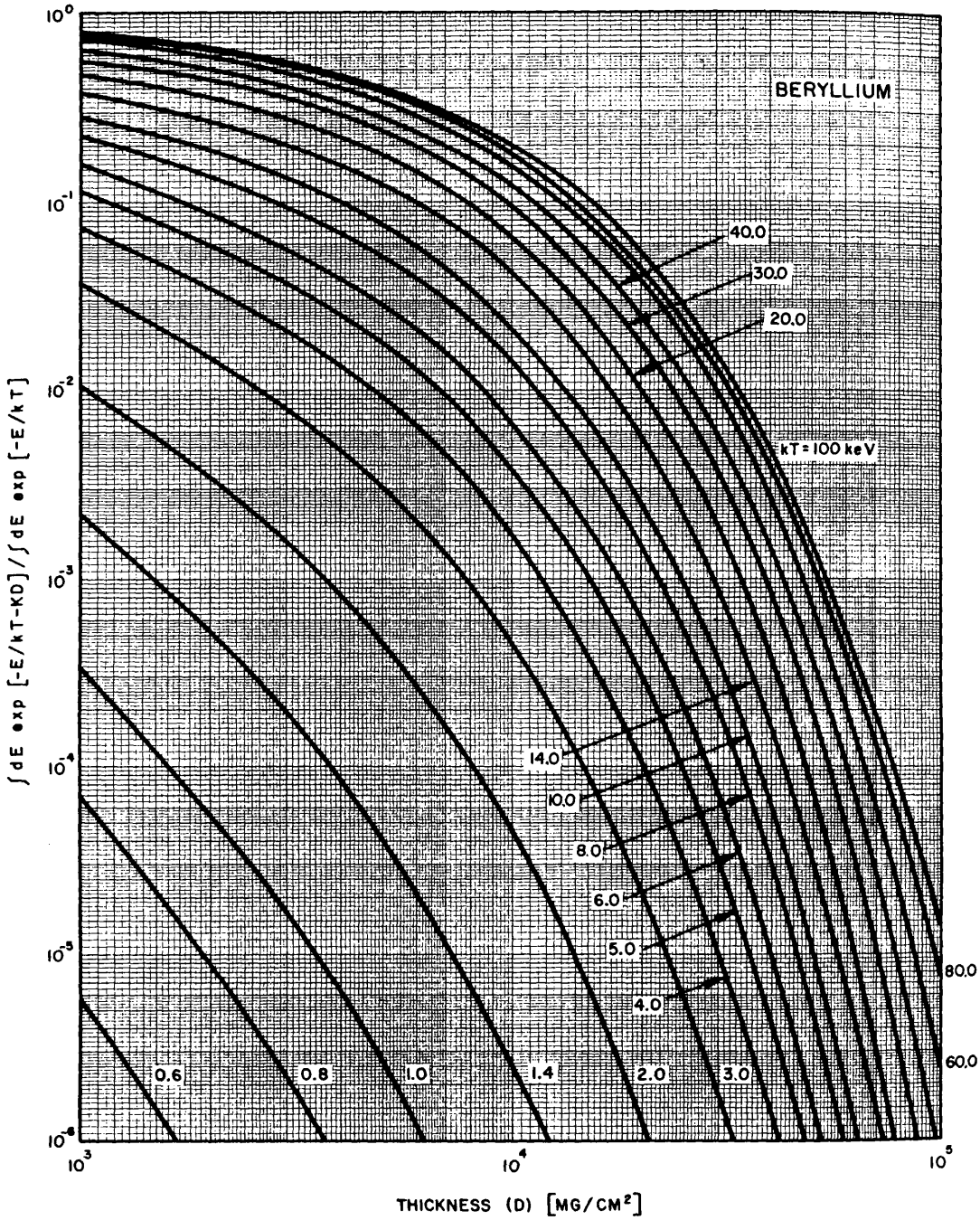

Fig. 26. Ratio of the integrated bremsstrahlung emission transmitted through foils of the designated material to the total incident flux versus foil thickness, D, for various temperatures. From this the ratio of ordinate values for two different thicknesses may be plotted versus temperature and used for plasma electron temperature determination; e.g., see Figs. 28 and 29 of Ref. 1.

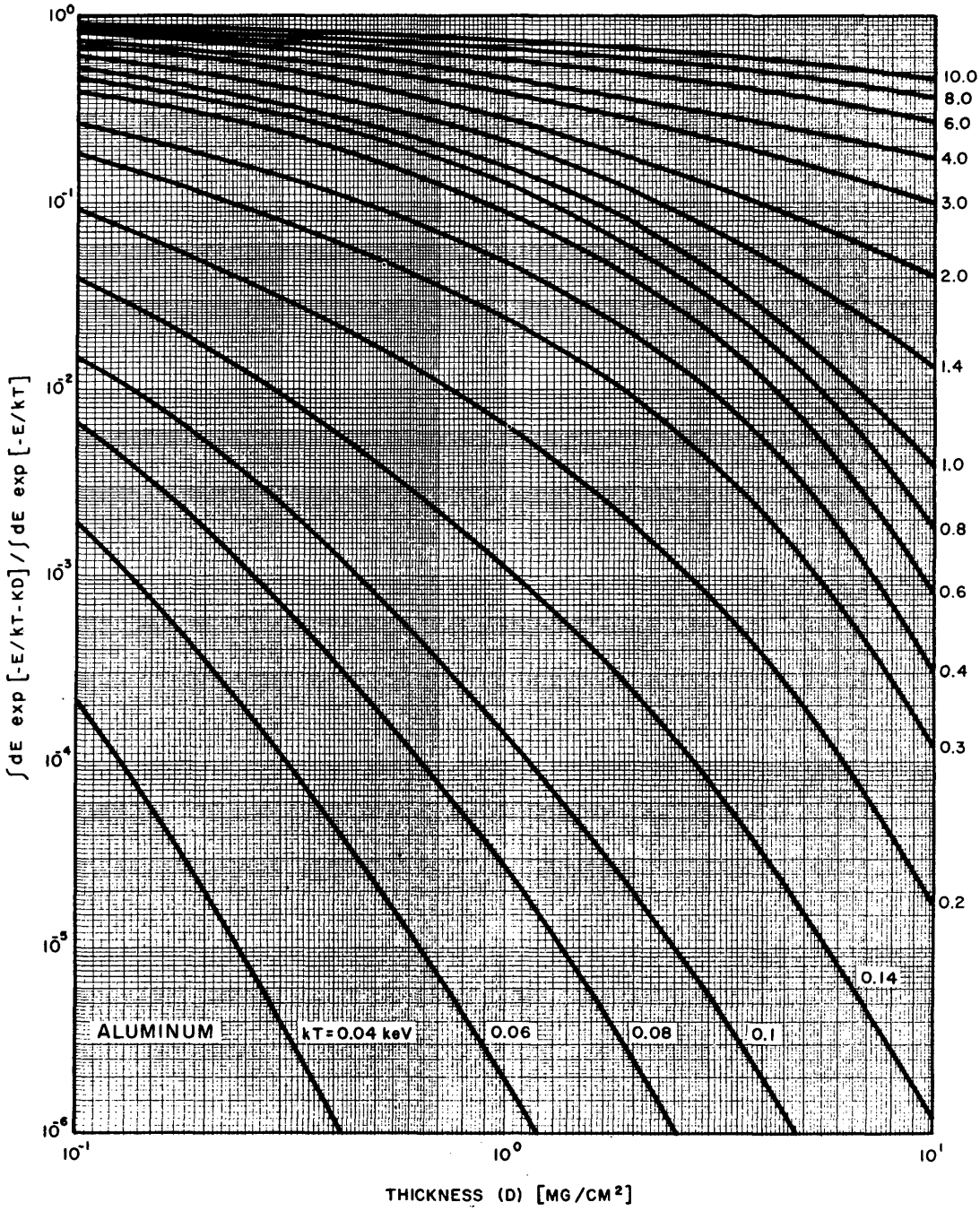

Fig. 27. Ratio of the integrated bremsstrahlung emission transmitted through foils of the designated material to the total incident flux versus foil thickness, D, for various temperatures. From this the ratio of ordinate values for two different thicknesses may be plotted versus temperature and used for plasma electron temperature determination; e.g., see Figs. 28 and 29 of Ref. 1.

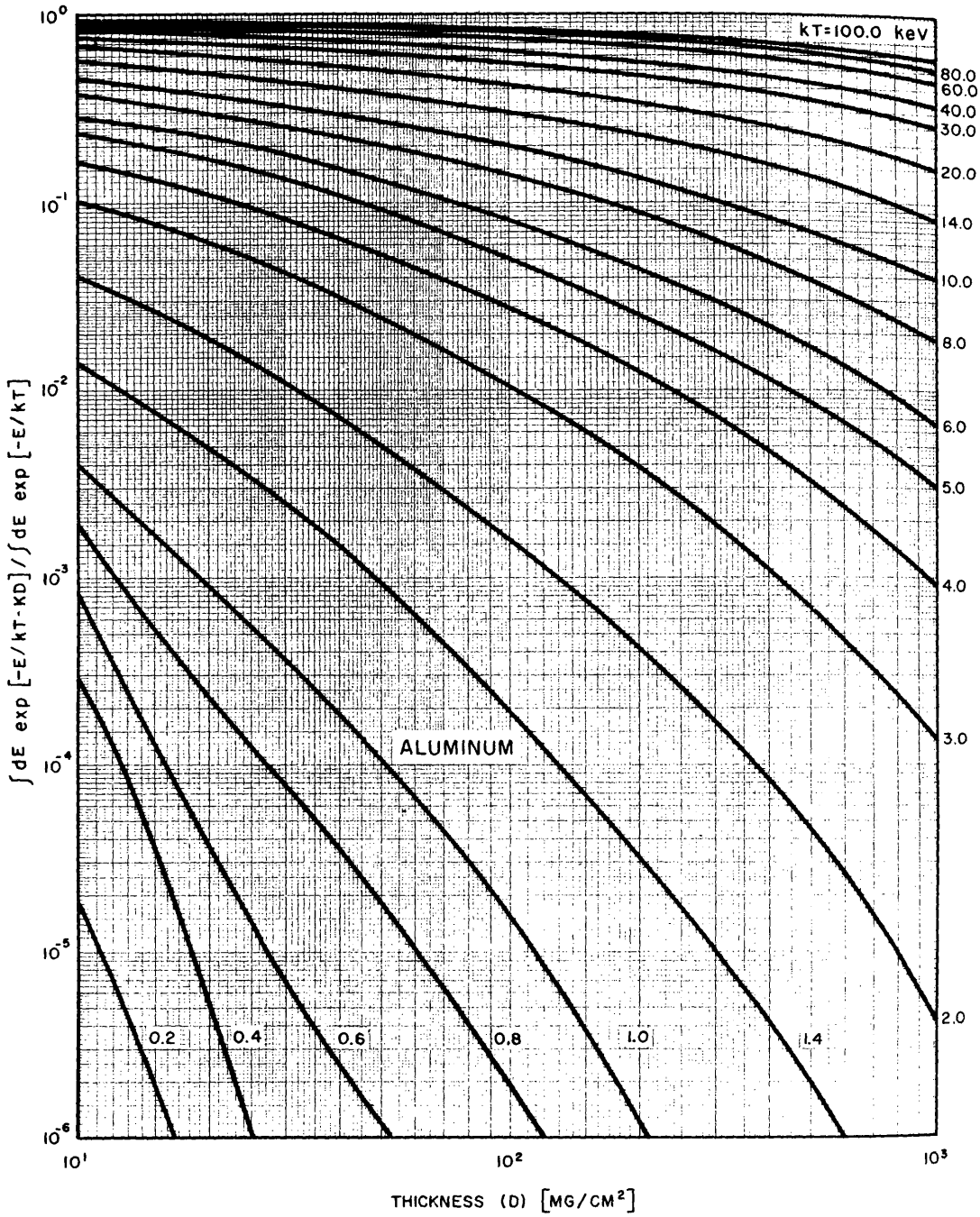

Fig. 28. Ratio of the integrated bremsstrahlung emission transmitted through foils of the designated material to the total incident flux versus foil thickness, D, for various temperatures. From this the ratio of ordinate values for two different thicknesses may be plotted versus temperature and used for plasma electron temperature determination; e.g., see Figs. 28 and 29 of Ref. 1.

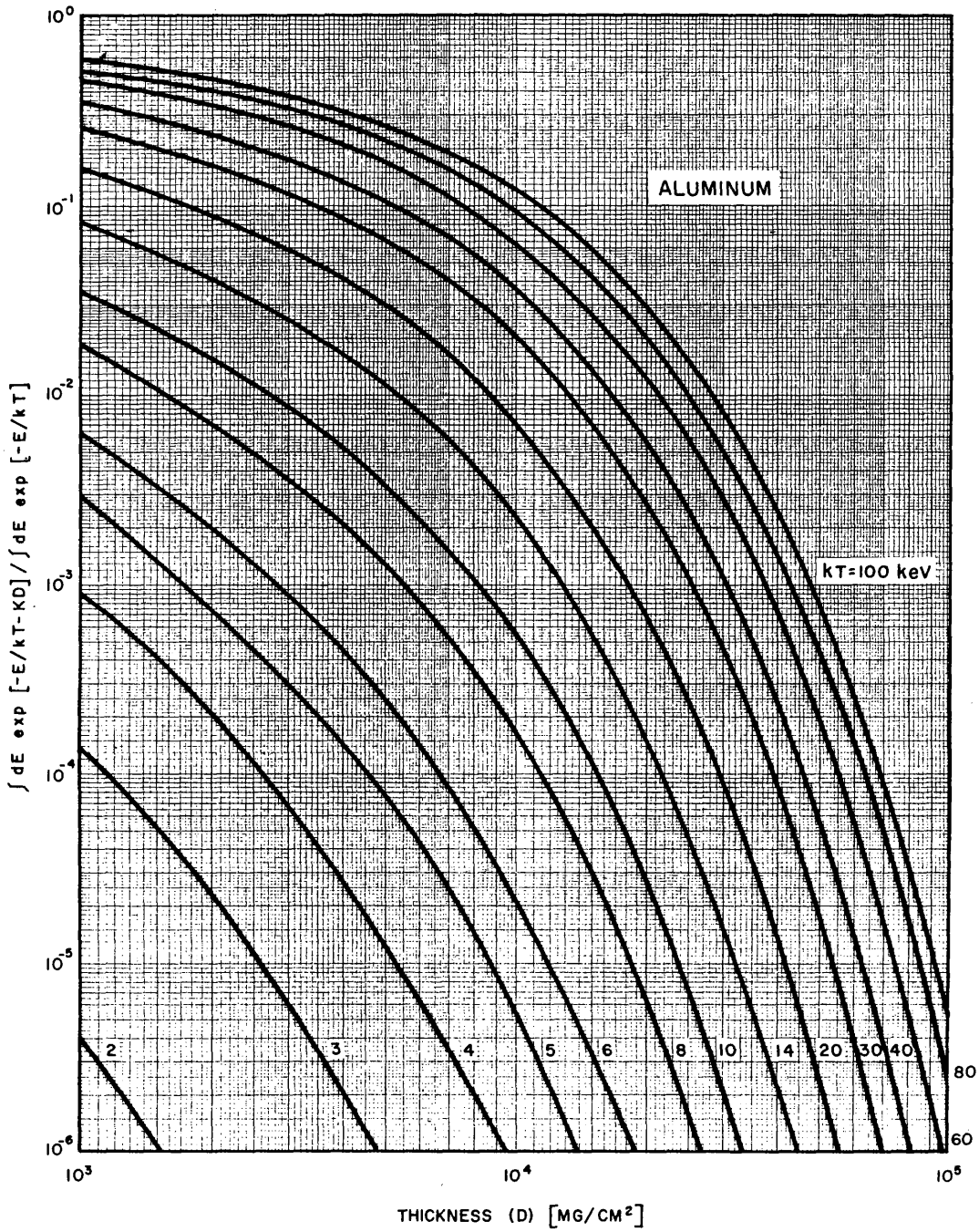

Fig. 29. Ratio of the integrated bremsstrahlung emission transmitted through foils of the designated material to the total incident flux versus foil thickness, D, for various temperatures. From this the ratio of ordinate values for two different thicknesses may be plotted versus temperature and used for plasma electron temperature determination; e.g., see Figs. 28 and 29 of Ref. 1.

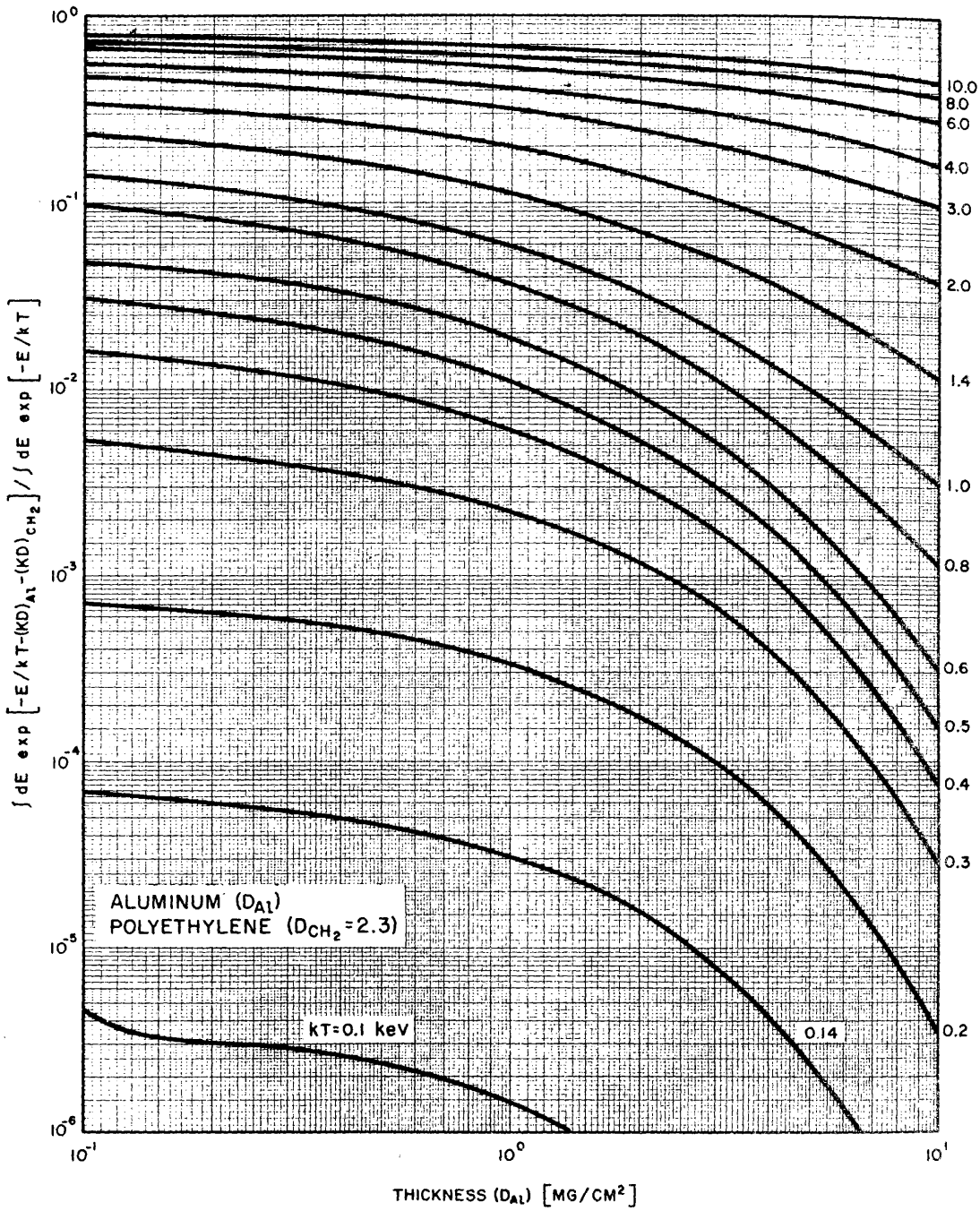

Fig. 30. Ratio of the integrated bremsstrahlung emission transmitted through a combination of absorbing aluminum and polyethylene foils to the total incident flux versus aluminum foil thickness, D_{Al}, for various temperatures. The polyethylene thickness D_{CH_2} is 0.001 in. (2.3 mg/cm^2). From these data, the ratio of ordinate values for two different thicknesses may be plotted versus temperature and used for plasma electron temperature determination; e.g., see Figs. 28 and 29 of Ref. 1.

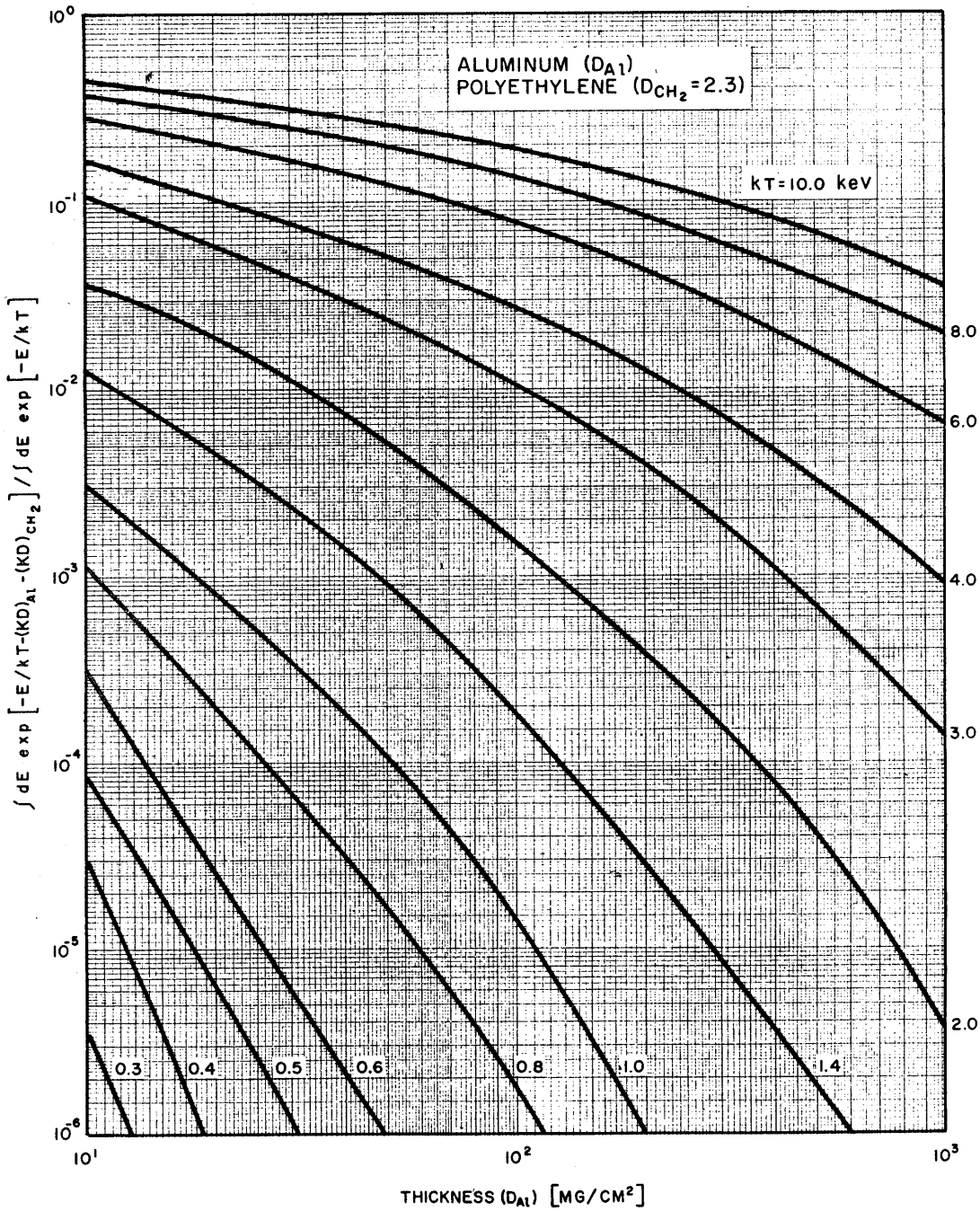

Fig. 31. Ratio of the integrated bremsstrahlung emission transmitted through a combination of absorbing aluminum and polyethylene foils to the total incident flux versus aluminum foil thickness, D_{Al}, for various temperatures. The polyethylene thickness D_{CH_2} is 0.001 in. (2.3 mg/cm^2). From these data, the ratio of ordinate values for two different thicknesses may be plotted versus temperature and used for plasma electron temperature determination; e.g., see Figs. 28 and 29 of Ref. 1.

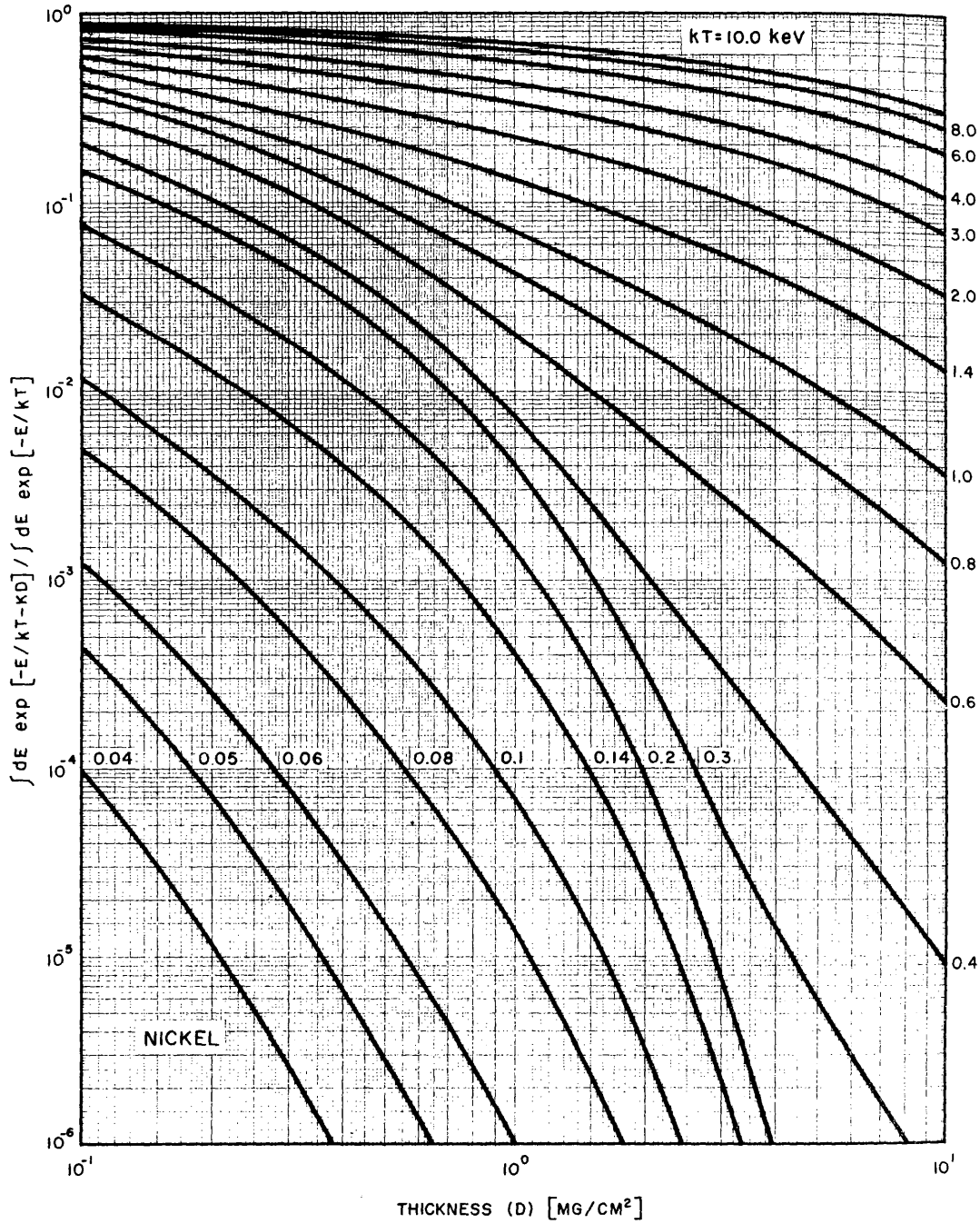

Fig. 32. Ratio of the integrated bremsstrahlung emission transmitted through foils of the designated material to the total incident flux versus foil thickness, D, for various temperatures. From this the ratio of ordinate values for two different thicknesses may be plotted versus temperature and used for plasma electron temperature determination; e.g., see Figs. 28 and 29 of Ref. 1.

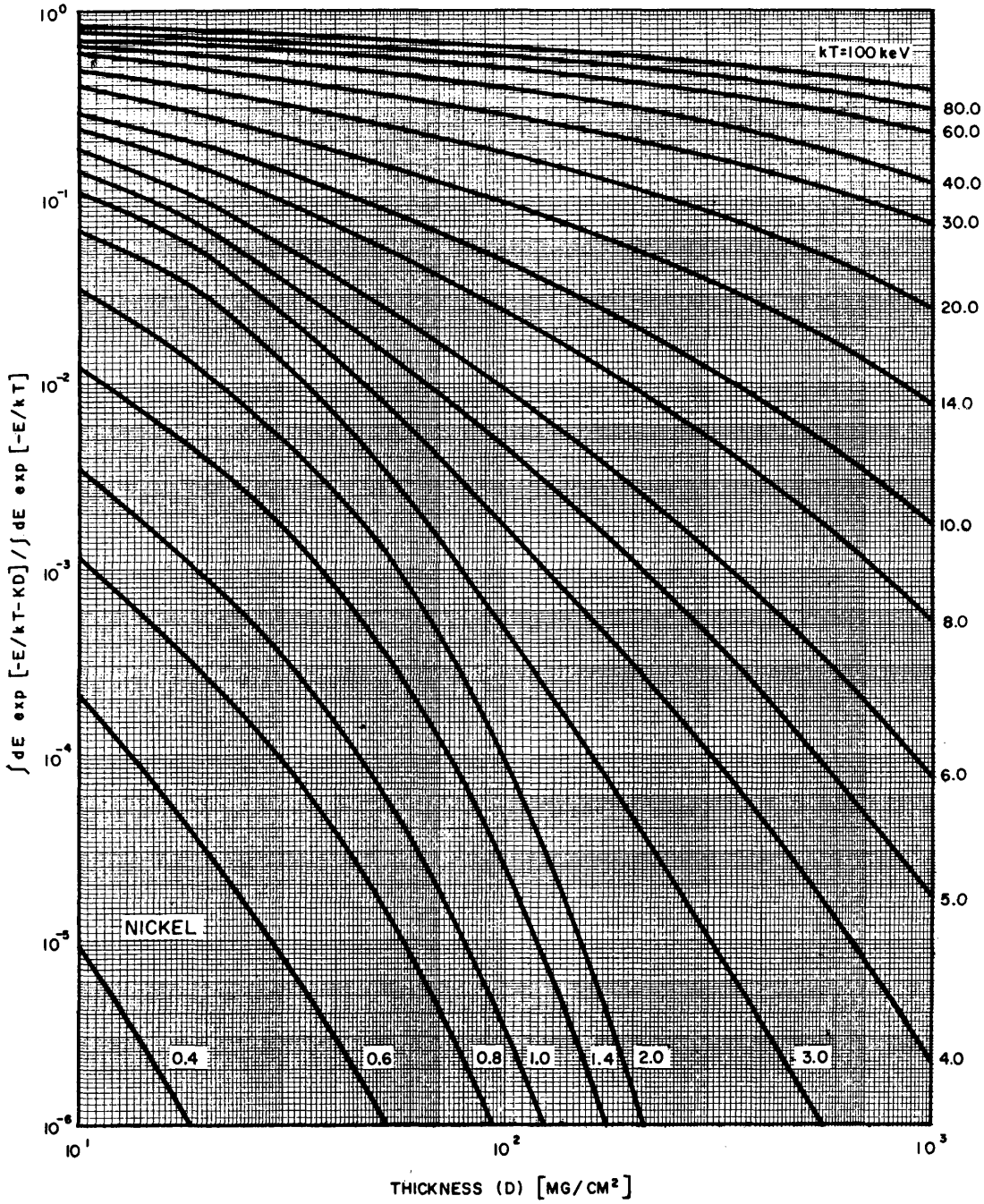

Fig. 33. Ratio of the integrated bremsstrahlung emission transmitted through foils of the designated material to the total incident flux versus foil thickness, D, for various temperatures. From this the ratio of ordinate values for two different thicknesses may be plotted versus temperature and used for plasma electron temperature determination; e.g., see Figs. 28 and 29 of Ref. 1.

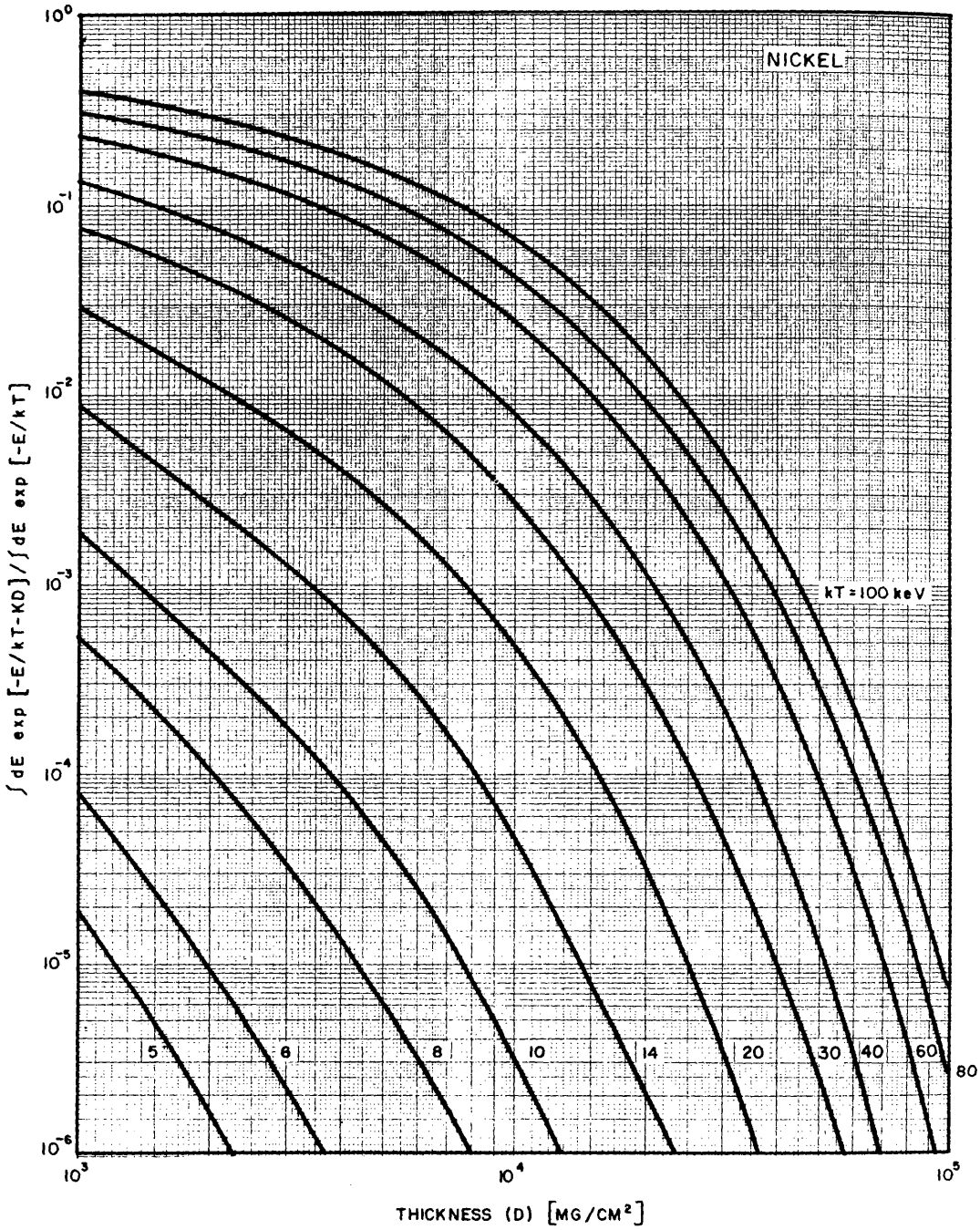

Fig. 34. Ratio of the integrated bremsstrahlung emission transmitted through foils of the designated material to the total incident flux versus foil thickness, D, for various temperatures. From this the ratio of ordinate values for two different thicknesses may be plotted versus temperature and used for plasma electron temperature determination; e.g., see Figs. 28 and 29 of Ref. 1.

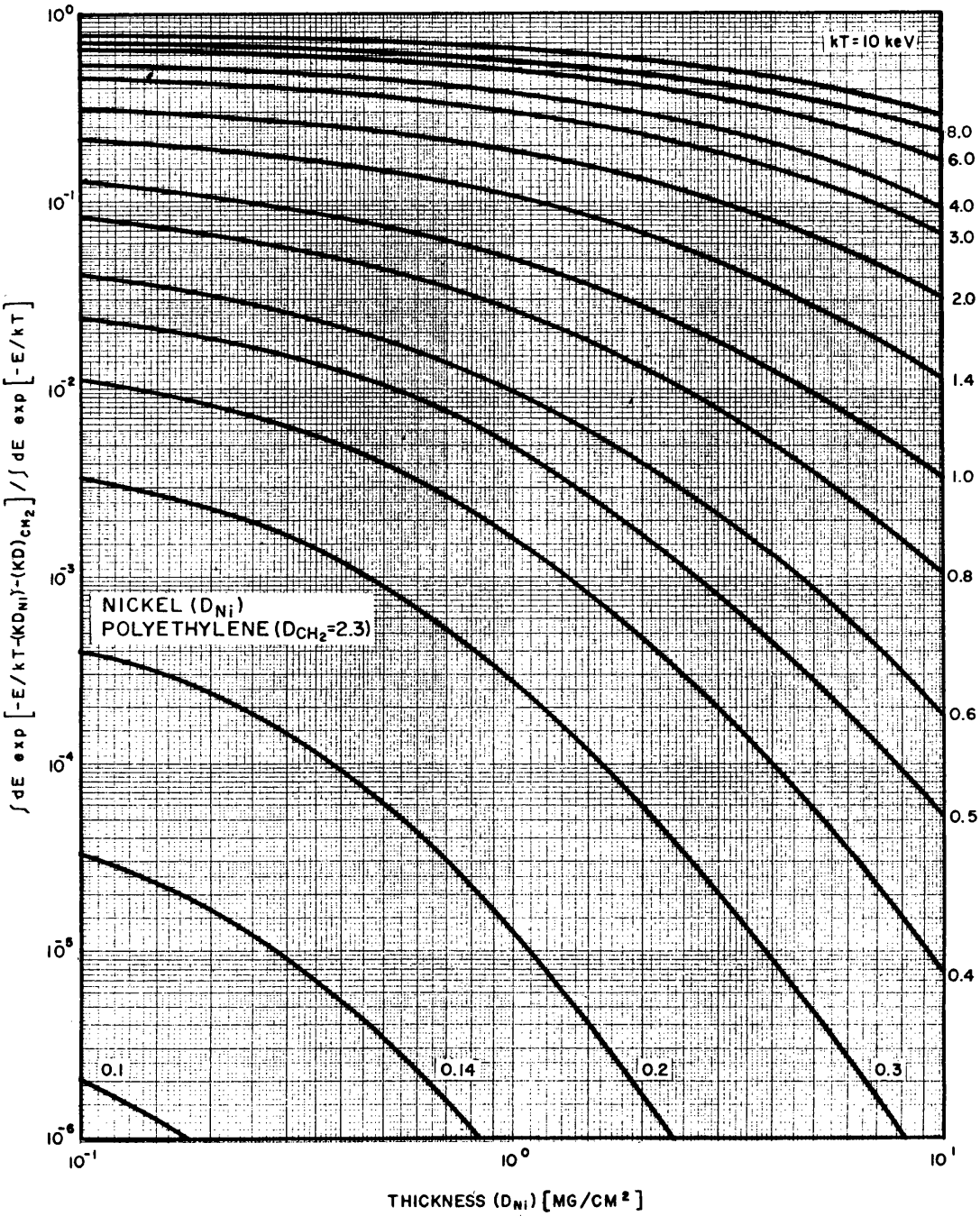

Fig. 35. Ratio of the integrated bremsstrahlung emission transmitted through a combination of absorbing nickel and polyethylene foils to the total incident flux versus nickel foil thickness, D_{Ni}, for various temperatures. The polyethylene thickness D_{CH_2} is 0.001 in. (2.3 mg/cm^2). From these data the ratio of ordinate values for two different thicknesses may be plotted versus temperature and used for plasma electron temperature determination; e.g., see Figs. 28 and 29 of Ref. 1.

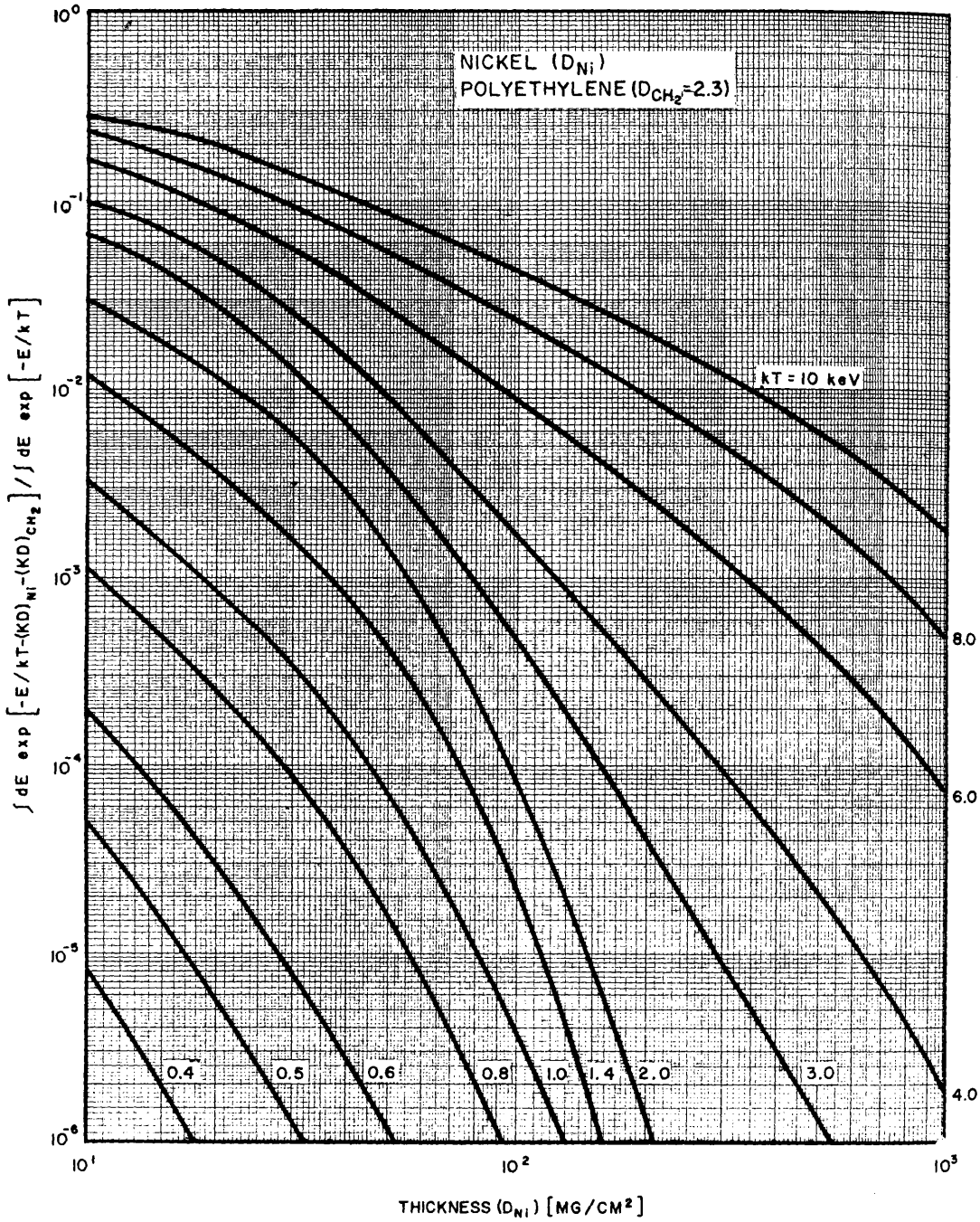

Fig. 36. Ratio of the integrated bremsstrahlung emission transmitted through a combination of absorbing nickel and polyethylene foils to the total incident flux versus nickel foil thickness, D_{Ni}, for various temperatures. The polyethylene thickness D_{CH_2} is 0.001 in. (2.3 mg/cm^2). From these data the ratio of ordinate values for two different thicknesses may be plotted versus temperature and used for plasma electron temperature determination; e.g., see Figs. 28 and 29 of Ref. 1.

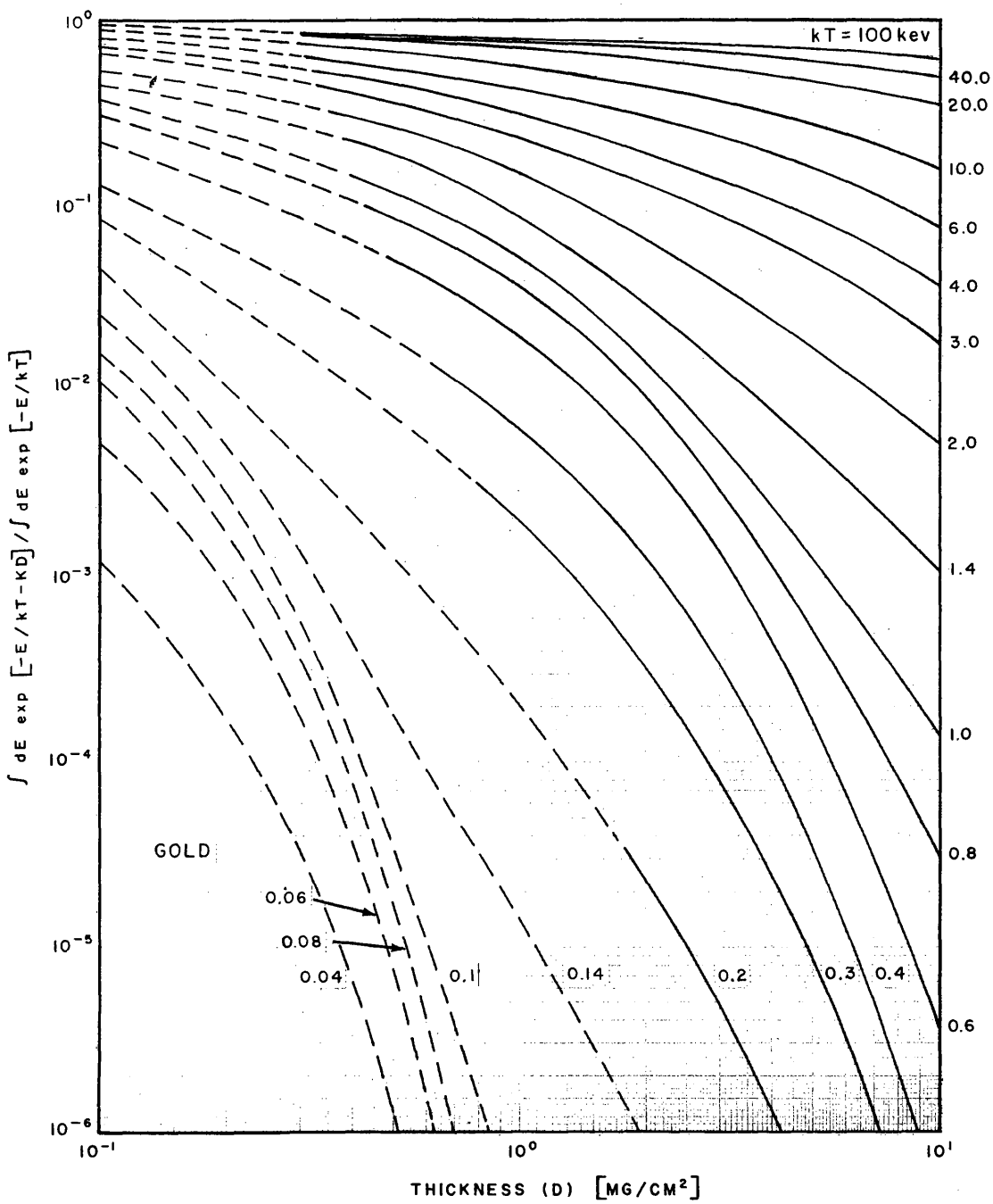

Fig. 37. Ratio of the integrated bremsstrahlung emission transmitted through foils of the designated material to the total incident flux versus foil thickness, D, for various temperatures. From this the ratio of ordinate values for two different thicknesses may be plotted versus temperature and used for plasma electron temperature determination; e.g., see Figs. 28 and 29 of Ref. 1.

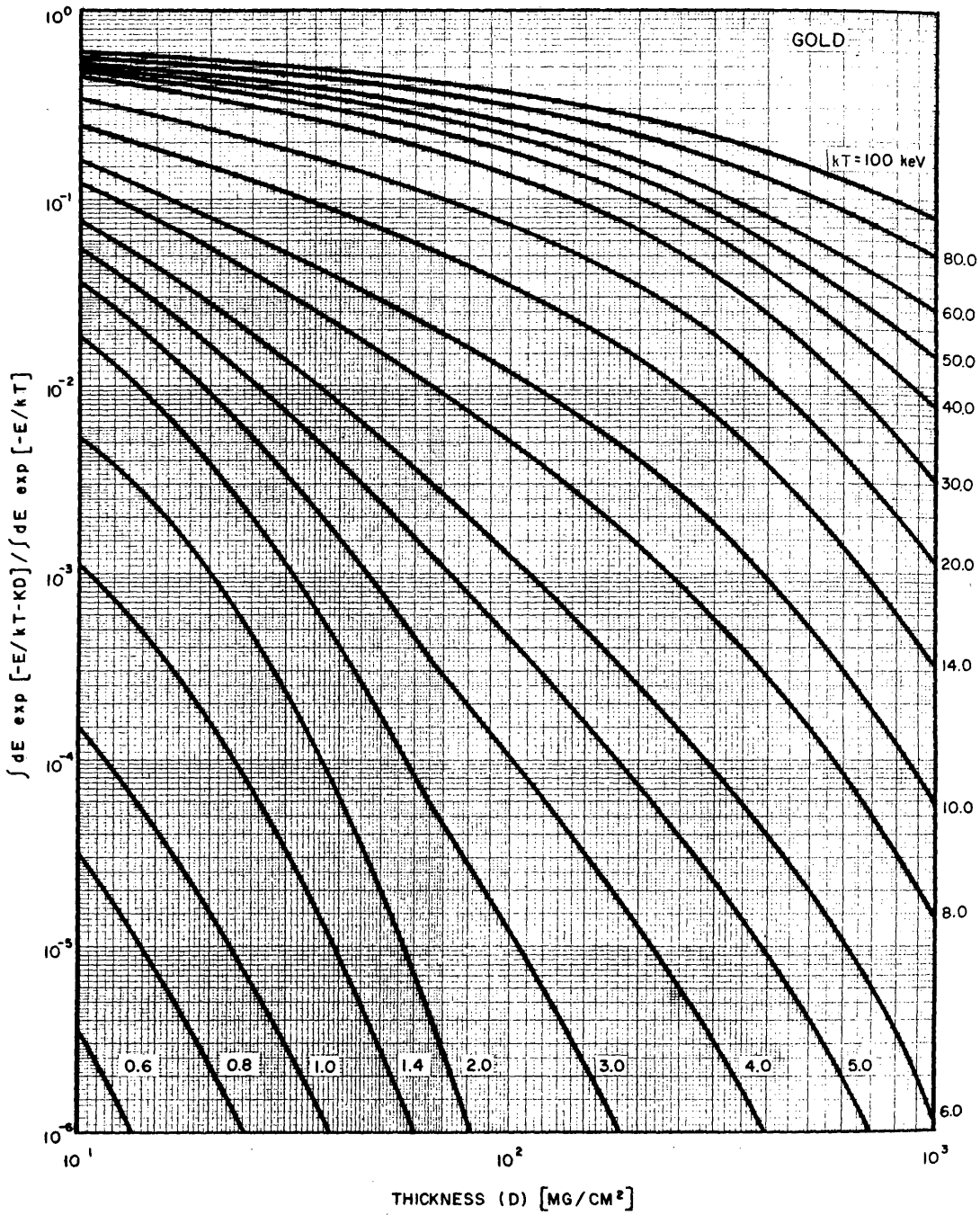

Fig. 38. Ratio of the integrated bremsstrahlung emission transmitted through foils of the designated material to the total incident flux versus foil thickness, D, for various temperatures. From this the ratio of ordinate values for two different thicknesses may be plotted versus temperature and used for plasma electron temperature determination; e.g., see Figs. 28 and 29 of Ref. 1.

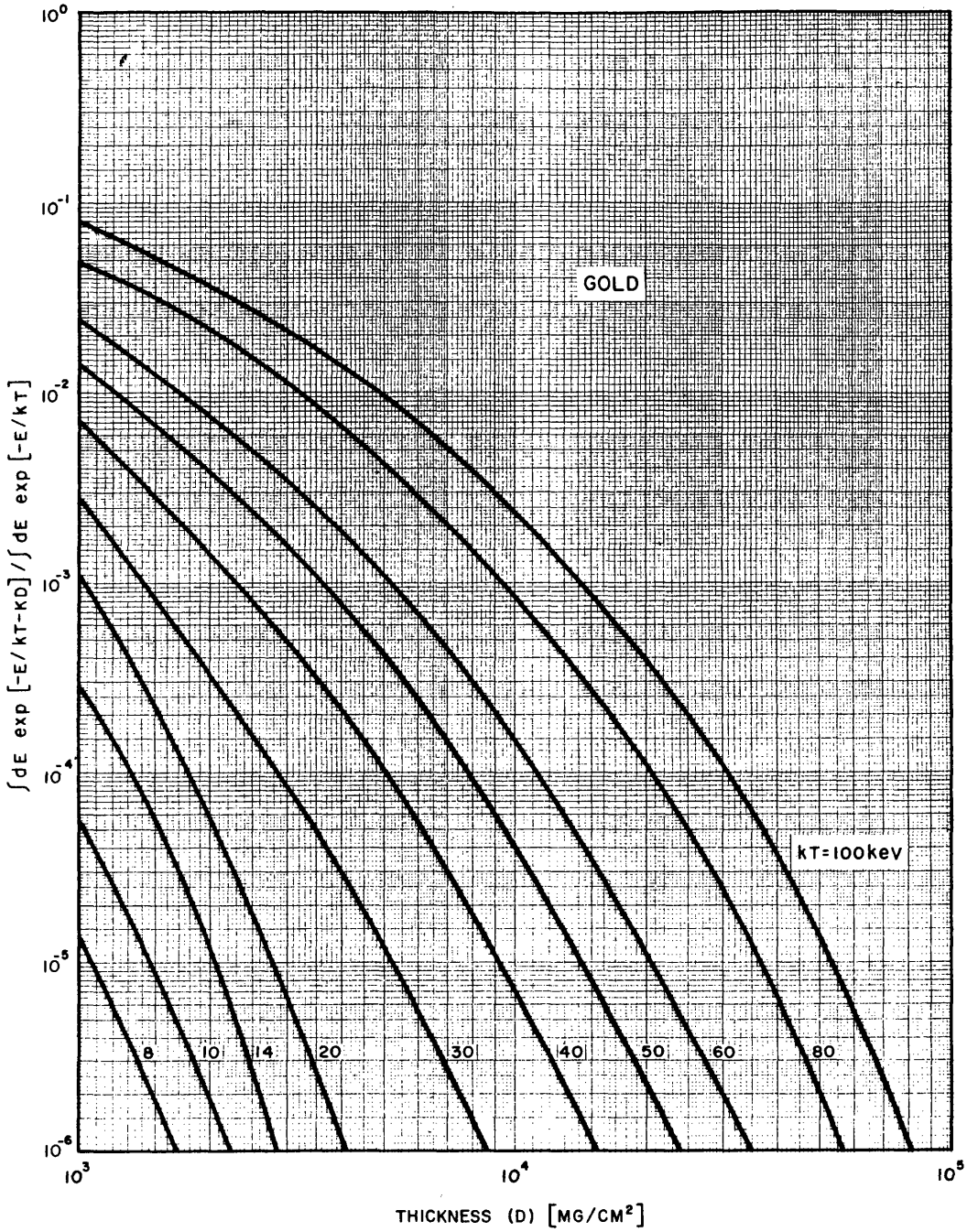

Fig. 39. Ratio of the integrated bremsstrahlung emission transmitted through foils of the designated material to the total incident flux versus foil thickness, D, for various temperatures. From this the ratio of ordinate values for two different thicknesses may be plotted versus temperature and used for plasma electron temperature determination; e.g., see Figs. 28 and 29 of Ref. 1.

Security Classification

DOCUMENT CONTROL DATA - R & D

(Security classification of title, body of abstract and indexing annotation must be entered when the overall report is classified)

1. ORIGINATING ACTIVITY *(Corporate author)*

Naval Research Laboratory
Washington, D.C. 20390

2a. REPORT SECURITY CLASSIFICATION

Unclassified

2b. GROUP

3. REPORT TITLE

DETERMINATION OF ELECTRON TEMPERATURES BETWEEN 50 eV and 100 keV FROM X-RAY CONTINUUM RADIATION IN PLASMAS

4. DESCRIPTIVE NOTES *(Type of report and inclusive dates)*

A final report on one phase of the problem.

5. AUTHOR(S) *(First name, middle initial, last name)*

R. C. Elton

6. REPORT DATE

December 11, 1968

7a. TOTAL NO. OF PAGES

70

7b. NO. OF REFS

18

8a. CONTRACT OR GRANT NO.

NRL Problem H02-24

b. PROJECT NO.

RR 002-09-41-5054

c.

d.

9a. ORIGINATOR'S REPORT NUMBER(S)

NRL Report 6738

9b. OTHER REPORT NO(S) *(Any other numbers that may be assigned this report)*

10. DISTRIBUTION STATEMENT

This document has been approved for public release and sale; its distribution is unlimited.

11. SUPPLEMENTARY NOTES

12. SPONSORING MILITARY ACTIVITY

Dept. of the Navy (Office of Naval Research), Washington, D.C. 20360

13. ABSTRACT

Previous calculations of the total integrated bremsstrahlung radiation passing through absorbing foils of beryllium, aluminum, and nickel (as well as aluminum and nickel in combination with carbon (polyethylene)) are included and extended to cover temperatures equivalent to an energy range from 50 eV to 100 keV and to include gold. Such information is necessary in obtaining values for the electron temperature in a plasma from measurements of the soft x-ray continuum emission. The spectral distribution of the transmitted continuum radiation is presented over the entire temperature range, for use in determining the most suitable spectral region.

DD FORM 1 NOV 65 1473 (PAGE 1)

S/N 0101-807-6801

Security Classification

Security Classification

14. KEY WORDS	LINK A ROLE	LINK A WT	LINK B ROLE	LINK B WT	LINK C ROLE	LINK C WT
Plasmas						
X-ray bremsstrahlung						
Recombination continuum radiation						
X-ray transmission curves						
Electron temperature						
Thin metallic foils						

DD FORM 1 NOV 65 1473 (BACK)
(PAGE 2)

Security Classification